5-2015

Physical Records of Impacts in the Early and Modern Solar System

Robert Ellis Beauford
University of Arkansas, Fayetteville

Physical Records of Impacts in the Early and Modern Solar System

Physical Records of Impacts in the Early and Modern Solar System

A dissertation submitted in partial fulfillment
of the requirements for the degree of
Doctor of Philosophy in Space and Planetary Sciences

by

Robert E. Beauford
Southern Methodist University, Dallas, TX
Bachelor of Science in Anthropology, 1993

May 2015
University of Arkansas

This dissertation is approved for recommendation to the Graduate Council.

_____
Dr. John C. Dixon
Dissertation Director

_____
Dr. Derek W. G. Sears
Committee Member

_____
Dr. William F. Oliver
Committee Member

_____
Dr. Vincent Chevrier
Committee Member

_____
Dr. Doy L. Zachry
Committee Member

ABSTRACT

The study of terrestrial meteorite impact craters and of impacted meteorites expands our understanding of cratered rocky surfaces throughout the solar system. Terrestrial craters uniquely expand upon data from remote imaging and planetary surface exploration by providing analogs for understanding the buried sub-surface portions of impact structures, while impacted meteorites provide examples of a much wider range of surface and subsurface impactite materials than we can directly sample thus far through solar system exploration.

This report examines three facets of the impact record preserved in terrestrial impact craters and in meteorites. First, it looks at the macroscopic structure of the Sutters Mill meteorite, a brecciated regolithic CM chondrite that preserves a three-dimensional record of the one of the most primitive known impact gardened surfaces in the solar system. The report details distinct lithologies preserved in the meteorite and the ways in which these lithologies reflect impact and alteration processes, with the intention of contextualizing and illuminating the wider body of recently published instrumental work on the stone by the current authors and others. Second, this dissertation presents a detailed analysis of the origin and nature of unique sub-spherical 'round rocks' commonly associated with the surface exposed sediments at the proposed Weaubleau impact structure, in west-central Missouri. Third, and finally, the dissertation looks at the nature of impact evidence for small impact pits and craters on earth. Unambiguously proving the impact origin of sub-kilometer terrestrial impact craters has presented significant historical challenges. A systematic analysis of field reports for all widely recognized sub-km terrestrial craters addresses both the nature of compelling evidence for impact origin for structures in this size range and the adequacy of the existing record of evidence for currently recognized structures.

ACKNOWLEDGEMENTS

Tremendous thanks to my advisor and colleague, Dr. Derek Sears, for advice, support, and encouragement, and to the members of my committee, Drs. John Dixon, Vincent Chevrier, William Oliver, and Doy Zachry, for their valuable support and comments.

Thanks to my parents, Judy and Ed Beauford for support and encouragement throughout, and to Jerri Stevens for endless patience and help in keeping my business and life running throughout this process.

A special thanks, also, to my fellow graduate students for their personal and professional advice and encouragement.

I am also grateful to Steve and Qynne Arnold for samples and for useful conversation, to Marlin Cilz for stone cutting, to Peter Jenniskens of SETI/NASA Ames Research Center for organizing the Sutter's Mill research consortium, to Dr. Mourad Benamara for SEM and EDS training, to Alex Ruzicka, Melinda Hutson, Knut Metzler, Linda Welzenbach and Hazel Sears for proofing and reviewing papers, and to NASA, the Lunar and Planetary Institute, and the University of Arkansas for travel support to conferences.

Thank you to Steve Arnold, Don McColl and Marvin Killgore for recounting personal observations at the Haviland, White Court, Odessa, Monteraqui, Wolfe Creek and Imilac craters and to the people of Vista, Missouri, for property access and for friendly support of research efforts.

DEDICATION

To Jerri Stevens: for endless support and encouragement in every facet of the process.

To my parents, Judy and Ed Beauford: for constant support and encouragement and for so much more I couldn't begin to list it.

To Dr. Derek Sears and the members of my dissertation committee: for encouraging me to begin it and for encouragement throughout.

To Robbie DeJhong, Patrick Crowley, Todd Hoeg, Charlie Snell, Richard and Dorothy Norton, Bevan French, Marvin Killgore, Rhian Jones, Steve and Qynne Arnold, and all of the other professionals in the meteorite, rock, fossil, and mineral communities who build bridges for future researchers by taking the time to write clearly, patiently answer questions, and identify meteorwrongs.

TABLE OF CONTENTS

Chapter 1 Introduction

1.1 Purpose and scope of study

Impact craters are among the most common geological features preserved on rocky surfaces in the solar system. On earth, however, they are scarce. Despite the fact that impact craters dominate or even define the surfaces of all but a few planetary or small body targets in the inner solar system, less than 200 well supported terrestrial crater locations comprise the entire body of readily accessible analogs by which we understand them. Impact altered meteorites provide further insights into the solar system's cratered surface. Though they cannot offer the large scale structural insights that might be gained from intact terrestrial impact craters, shock altered, brecciated and regolithic meteorites provide mineralogical and petrologic time capsules of some of the solar system's least accessible impact environments. Impacted meteorites and terrestrial impact craters become steadily more important, both as analogs and as direct records of distant events, as surface exploration of the inner solar system progresses.

The body of research presented here looks at three facets of the impact process and its physical record. The first section presents a focused investigation of the physical record of impacts preserved in the plowed, regolithic surface of a primitive outer solar system object, the Sutter's Mill CM chondrite meteorite. Next, it examines the nature and genesis of unusual concretions associated with the Weaubleau structure, a probable Mississippian impact crater located on Missouri's western Ozark Plateau. From these examinations, the report jumps forward in time to a very different group of impacts, Earth's suite of sub-kilometer impact craters. A systematic review of literature reveals limits on the effectiveness of popular lines of unambiguous impact evidence for the identification of the planet's youngest and smallest craters, and looks systematically at what types of evidence have proven useful in their identification.

1.2 The Sutter's Mill CM chondrite

The Sutter's Mill meteorite fell on April 22nd, 2012, in California, USA, producing a shower of gravel-sized pieces totaling less than 1 kg. It has been classified as a CM chondrite regolith breccia (Jenniskens et al., 2012).

CM chondrites are scarce, representing slightly less than 1% of all meteorite falls by number, and significantly less by mass. They are also scientifically important, comprising some of the most detailed time capsules we currently posses from the early solar system. Rapid recovery maximized the research potential of this fall (Fries et al., 2014; Jenniskens, 2014). The CM chondrites are characterized by elemental and isotopic ratios closer to the solar photosphere than any other class of meteorite except the CI chondrites (e.g. Sears, 2004). They are regolithic impact breccias (Bischoff et al., 2006; Bischoff and Schultz, 2004), meaning they are impactites composed of the shattered fragments of the repeatedly impacted surface of an asteroid. They contain one of the most varied assemblages of minerals of any of the meteorite groups, as well as the 2nd highest abundance of water and associated hydrated minerals, after CI1 chondrites. Their potential contribution to science is further enhanced by the highest abundances of organic carbon molecules of any meteorite group yet studied, and by the presence of a significant fraction of presolar grains older than the solar system itself.

Sutter's Mill has proven similar to other CM chondrites in major elemental abundance and in its origin as a regolith breccia (Jenniskens et al., 2012; Nishiizumi et al., 2014), but is somewhat atypical in several regards. Cosmic-ray exposure ages are young (Jenniskens et al., 2012; Nishiizumi et al., 2014), it contains unusual xenolithic inclusions (Jenniskens et al., 2012), and it records a complex history of both thermal and aqueous alteration (Zhao et al., 2014; Beck

et al., 2014; Burton et al., 2014). Several researchers have reported that the meteorite has been heated to higher temperatures than are typical of CM chondrites. Sears and Beauford (2014) ascribed this to heating in the atmosphere.

In chapter 2 of this dissertation, we examine 8 slices prepared from a complete individual from the Sutter's Mill meteorite fall, using microscopy and photomicrographs to observe and report variations in the preserved lithologies that make up the breccia, to describe relationships between the clasts and matrix, and to assess possible textural and structural indicators of regolith maturation in CM chondrites. We also present observations on the shape of the stone and its fusion crust and on the potential significance and origin of fractures in the stone. It is hoped that this work provides a macroscopic framework useful in placing detailed work on this meteorite in a larger context and that it may provide fresh insights into processes that occur on the CM chondrite parent body.

1.3 The Weaubleau impact structure

Since less than 200 known impact crater locations comprise our entire body of terrestrial analogs for understanding craters throughout the rest of the solar system, each newly discovered structure on Earth represents a substantial addition to the literature. The Weaubleau impact structure was first identified as an anomalous geological formation by Beveridge (1949, 1951), and was first identified as a possible impact crater in Rampino and Volk (1996). The first strongly suggestive evidence of impact origin, planar deformation features in quartz, was reported in abstract in Evans et al. (2003b) and described in detail in abstract in Morrow and Evans (2007). Compelling evidence of impact origin was described briefly in a peer reviewed publication in (Miller et al., 2008).

The Weaubleau Structure is centered at approximately 37°58'N 93°40'W (Finn et al., 2012) in west-central Missouri, USA. A circular topographic feature (Cox and Evans, 2007; Finn et al., 2012; Miller et al., 2008), roughly corresponding to a 7 to 8 km region of polymict breccias and clast bearing sediments (Dulin and Elmore, 2008; Miller et al., 2008) is incompletely surrounded by a lens of breccia and displaced and folded strata extending beyond the proposed crater to produce an overall region of disturbance with a maximum diameter of about 19km (Evans et al., 2003c; Dulin and Elmore, 2008; Miller et al., 2008; Finn et al., 2012). The outer portion of the disturbed region overlies intact strata to a depth of typically less than 60 meters, while drilling within the circular structure has indicated breccia to a substantially greater depth. The age of the structure has been constrained to the mid-Mississippian, latest Osagean or early Meramecian (Miller et al., 2008; Elmore and Dulin, 2007; Dulin and Elmore, 2008), or about 335 to 340 Ma.

The region of the Weaubleau structure is best known locally for the presence of 'round rocks.' These sub-spherical cherty concretions, averaging about the size of a baseball, are found in large numbers in the region of the disturbance. When broken, they typically reveal a loosely cemented to friable nucleus with the general appearance and texture of packed clay. The research reported in chapter 3 of this dissertation examines the round rocks for their own sake and as a potential window into understanding the Weaubleau structure as a whole. It specifically determines what they are and how they formed, and answers questions about if and how they are associated with impact processes and the genesis of the Weaubleau structure.

1.4 Small terrestrial impact craters

Even with close study, it can be difficult to distinguish meteorite impact craters from craters of terrestrial origin or from crater-like structures. Recognition of hypervelocity meteorite

impact craters hinges upon the recognition of changes to rocks and minerals that are uniquely produced by extremely high shock pressures. No naturally occurring process on Earth's surface duplicates impact related shock, so the resulting unique and permanent changes that are produced provide unambiguous criteria by which the structures can be distinguished from morphologically similar terrestrial structures. The most commonly employed lines of evidence include shattercones, planar deformation features (PDF) in quartz or other minerals, the formation of diaplectic glass, or the presence of high pressure mineral polymorphs, such as coesite or stishovite. In the absence of these or similar types of unambiguous evidence, researchers depend upon finding impactor fragments or their chemical traces (e.g. French, 2004; French and Koeberl, 2010).

Research on small terrestrial meteorite impact pits and craters is plagued by sparse evidence. Small hypervelocity impacts simply produce limited volumes of shock altered rock, while lower velocity impacts that produce simple pits may produce no such evidence at all. Even in the cases of the most energetic small crater-forming impacts, some types of evidence may not be produced at all due to inadequate pressure. The planet's smallest impact structures should be the most common group, significantly outnumbering larger craters, but they make up only about 10% of known craters (eg: Herd et al., 2008; Bland and Artemieva, 2006).

Chapter 4 of this dissertation summarizes the evidence that has been presented for all currently recognized terrestrial sub-kilometer impact craters and pits, and identifies trends within the literature in order to construct a generalizable description of the group and of the evidence that reveals their unambiguous impact origin. The intention of the work is to solve the 'small crater problem,' meaning a lack of useful criteria for their recognition, by clearly identifying what types of evidence past researchers have used, and to point to the locations and contexts in

which such evidence might reasonably be found in the field. An unexpected outcome of this work has been the observation that two of our most widely recognized sub-kilometer impact craters lack significant published evidence of impact origin, and that an additional two leave significant room for doubt.

1.5 Publications

In addition to the papers presented here, thirty-one published articles have directly or tangentially emerged from the related work performed during preparation of this dissertation, including seven extended conference abstracts, two peer reviewed papers to which I contributed as a subordinate author, and twenty-two public education and outreach papers.

For Jenniskens et al. (2012), *Radar-Enabled Recovery of the Sutter's Mill Meteorite, a Carbonaceous Chondrite Regolith Breccia*, I provided research team support with initial photographs, photomicrographs, and detailed descriptions of the macrostructure of a sample of the meteorite, as well as a figure included in the final paper published in Science. More detailed results of our specific work were presented as extended abstracts at the 44th Lunar and Planetary Science Conference (Beauford et al., 2013 and Beauford and Sears, 2013) and at the 75th Annual Meteoritical Society Meeting (Beauford et al., 2012). The thermal history of the Sutter's Mill meteorite was examined in depth in Sears and Beauford (2014), *The Sutter's Mill meteorite: Thermoluminescence data on thermal and metamorphic history*, for which I performed detailed measurements of thickness and layering characteristics of fusion crust and descriptions of orientation and character of flow features, along with associated supporting photomicrographs produced using a scanning electron microscope. The paper was published in Meteoritics and Planetary Science. In addition to these conference abstracts and peer reviewed papers, 9

education and public outreach articles have arisen directly from work on the Sutter's Mill meteorite. These included a series of 4 articles on meteorite fieldwork, including *Science of Fieldwork* (Beauford, 2014) and parts 1, 2, and 3 of *Introductory Meteorite Fieldwork* (Arnold and Beauford, 2014), a discussion of the overall significance of the meteorite to our understanding of solar system history titled *Sutter's Mill - What's so special about CM chondrites?* (Beauford, 2012), a brief examination of why and how meteorites such as Sutter's Mill break up in the atmosphere, *Chelyabinsk, Fireballs, and Fragmentation* (Beauford, 2012), and reports on two of the conferences at which the research was reported. Publication details regarding each of these publications are listed in following sections of this chapter.

In addition to the summary of work at the Weaubleau probable impact structure that is reported herein, related fieldwork on the Ozark Plateau of southern and central Missouri has resulted in 3 published extended abstracts and 2 education and public outreach articles. Extended abstracts include *Preliminary Reconnaissance of the Belton Structure, A Possible Impact Crater in Cass County, Missouri* (Beauford and Evans, 2014), *Ferrous Minerals and Impactite Mineralization at Missouri's Crooked Creek and Decaturville Impact Craters* (Beauford, 2012), and *Carbonate Melts and Sedimentary Impactite Variation at Crooked Creek and Decaturville Impact Craters, Missouri, USA* (Beauford, 2012), which were presented at the 43rd and 45th Lunar and Planetary Science Conferences. Two introductory level education and public outreach articles, *More Than Meets the Eye – Ancient Meteorite Impact Craters of the Ozark Plateau* (Beauford, 2012), and *Craters of the Ozarks – The Crooked Creek, Decaturville, and Weaubleau Impact Structures* (Beauford, 2012) were published in The Ozarks Mountaineer magazine and Meteorite magazine respectively.

In addition to the systematic analysis of suggestive and unambiguous evidence indicating impact origin for small terrestrial craters that is reported as Chapter 4 of this dissertation, research on the topic of impact evidentiation has supported three related education and public outreach articles on the subject. These include a March 2013 Meteorite magazine review of Gordon Osinski and Elisabetta Pierazzo's *Impact Cratering - Processes and Products*, as well as *A Short History and the Future of Impact Astrogeology* (Beauford, 2012) and *Impacts on Earth - How Are Craters Confirmed?* (Brachaniec and Beauford, 2014).

The chapters included in this volume represent 3 papers in preparation for future publication as follows. Chapter 2: Beauford R. E., Sears D. W. G., and Arnold S. K. 2014. *Observations on the Macrostructure of the Sutter's Mill CM Chondrite*. Submitted, in review. Chapter 3: Beauford R. E. and Evans K. R. 2014. *Origin of Concretions in the Proposed Weaubleau Impact Structure, Missouri, USA*. In submission. And Chapter 4: Beauford R. E. 2014. *Indicators of Impact Origin in Small Terrestrial Craters*. In preparation.

The works described above comprise only a partial listing of publications. Complete lists of publications that have emerged either directly from the work reported in this dissertation or that have been contributed to as a result of this work are listed in the following sections.

1.5.1 Published peer reviewed articles

Jenniskens P., Fries M. D., Yin Q., Zolensky M., Krot A. N., Sandford S. A., Sears D., Beauford R., Ebel D. S., Friedrich J. M., Nagashima K., Wimpenny J., Yamakawa A., Nishiizumi K., Hamajima Y., Caffee M. W., Welten K. C., Laubenstein M., Davis A. M., Simon S. B., Heck P. R., Young E. D., Kohl I. E., Thiemens M. H., Nunn M. H., Mikouchi T., Hagiya K., Ohsumi K., Cahill T. A., Lawton J. A., Barnes D., Steele A., Rochette P., Verosub K. L., Gattacceca J.,

Cooper G., Glavin D. P., Burton A. S., Dworkin J. P., Elsila J. E., Pizzarello S., Ogliore R., Schmitt-Kopplin P., Harir M., Hertkorn N., Verchovsky A., Grady M., Nagao K., Okazaki R., Takechi H., Hiroi T., Smith K., Silber E. A., Brown P. G., Albers J., Klotz D., Hankey M., Matson R., Fries J. A., Walker R. J., Puchtel I., Lee C-T. A., Erdman M. E., Eppich G. R., Roeske S., Gabelica Z., Lerche M., Nuevo M., Girten B., Worden S. P., and (the Sutter's Mill Meteorite Consortium). 2012. Radar-Enabled Recovery of the Sutter's Mill Meteorite, a Carbonaceous Chondrite Regolith Breccia. *Science* 21:338(6114):1583-1587.

Sears D. W. and Beauford R. 2014. The Sutter's Mill meteorite: Thermoluminescence data on thermal and metamorphic history. *Meteoritics & Planetary Science*. doi: 10.1111/maps.12259

1.5.2 Published extended abstracts

Beauford R. E. and Evans K. R. 2014. Preliminary Reconnaissance of the Belton Structure, A Possible Impact Crater in Cass County, Missouri (abstract #1217), 45th Lunar and Planetary Science Conference

Beauford R. E., Arnold S. K., and Sears D. 2013. The Macrostructure of the Sutter's Mill CM Chondrite Regolith Breccia (abstract #1683), 44th Lunar and Planetary Science Conference

Beauford R. E. and Sears D. 2013. Timing of Fine-grained Rim Formation in the Sutter's Mill CM Chondrite (abstract #1692), 44th Lunar and Planetary Science Conference

Beauford R. E., Arnold S. K., Sears D. 2012. The Macrostructure of the Sutter's Mill Meteorite (abstract #5091), 75th Annual Meteoritical Society Meeting

Beauford, R. E. 2012. Ferrous Minerals and Impactite Mineralization at Missouri's Crooked Creek and Decaturville Impact Craters (abstract #1710), 43rd Lunar and Planetary Science Conference.

Beauford, R. E. 2012. Carbonate Melts and Sedimentary Impactite Variation at Crooked Creek and Decaturville Impact Craters, Missouri, USA (abstract #1705), 43rd Lunar and Planetary Science Conference.

Beauford, R. E. 2011. Meteorwrongs Received by the Arkansas Center for Space and Planetary Sciences. Program Results and Potentials (abstract #1100), 42nd Lunar and Planetary Science Conference.

1.5.3 Education and public outreach articles, first author

Beauford R. E. 2014. Science of Fieldwork. *Meteorite*. June 2014. Volume 20, No. 2.

Beauford R. E. 2013. Chelyabinsk, Fireballs, and Fragmentation. *Meteorite* magazine. June 2013. Volume 19, No. 2.

Beauford R. E. 2013. "*Impact Cratering - Processes and Products" by Gordon R. Osinski and Elisabetta Pierazzo* [book review]. *Meteorite* magazine. March 2013. Volume 19, No. 1.

Beauford R. E. 2012. The Meteoritical Society Meeting, 2012. *Meteorite* magazine. November 2012. Volume 18, No. 4.

Beauford R. E. 2012. Sutter's Mill - What's so special about CM chondrites? *Meteorite* magazine. November 2012. Volume 18, No. 4.

Beauford R. E. 2012. Ensisheim to L'Aigle – Meteorites and Meteoritics from 1492 to 1803. *Meteorite* magazine. August 2012. Volume 18, No. 3.

Beauford R. E. 2012. The Springs of Eureka Springs. *The Ozarks Mountaineer*. July/August 2012. Volume 60, No. 4

Beauford R. E. 2012 More Than Meets the Eye – Ancient Meteorite Impact Craters of the Ozark Plateau. *The Ozarks Mountaineer*. May/June 2012. Volume 60, No. 3

Beauford R. E. 2012 The 43rd LPSC, Conference Abstracts, and Bridges to Knowledge. *Meteorite* magazine. May 2012. Volume 18, No. 2

Beauford R. E. 2012. From the Editors, A Short History and the Future of Impact Astrogeology. *Meteorite* magazine. Feb 2012. Volume 18, No. 1

Beauford R. E. 2012. Craters of the Ozarks – The Crooked Creek, Decaturville, and Weaubleau Impact Structures. *Meteorite* magazine. Feb 2012. Volume 18, No. 1

Beauford R. E. 2011. From the Editors, No End to Discovery. *Meteorite* magazine. Nov 2011. Volume 17, No. 4

Beauford R. E. 2011. From the Editors, Still the Most Amazing Thing I've Ever Seen. *Meteorite* magazine. August 2011. Volume 17, No. 3

Beauford R. E. 2011. From the Editors, Dream Big and The World Will Dream With You. *Meteorite* magazine. May 2011. Volume 17, No. 2

Beauford R. E. 2010. Meteorwrongs and Why They Matter More Than We Think. *Meteorite* magazine. November 2010. Volume 16, No. 4

Beauford R. E. 2010. “Meteorites.” The Encyclopedia of Arkansas History and Culture. 21 September 2010. http://encyclopediaofarkansas.net/encyclopedia/entry-detail.aspx?entryID=6236

1.5.4 Education and public outreach articles, subordinate author

Arnold S. and Beauford R. E. 2014. Introductory Meteorite Fieldwork - Part 3: Chasing Witnessed Falls and Fireballs. *Meteorit*e magazine. Fall 2014. Volume 20, No. 3.

Arnold S. and Beauford R. E. 2014. Introductory Meteorite Fieldwork - Part 2: Where to Hunt and Why to Hunt There. *Meteorite* magazine. Summer 2014. Volume 20, No. 2.

Arnold S. and Beauford R. E. 2014. Introductory Meteorite Fieldwork - Part 1: An Overview of Meteorite Hunting. *Meteorite* magazine. February 2014. Volume 20, No. 1.

Brachaniec T. and Beauford R. E. 2014. Impacts on Earth - How Are Craters Confirmed? *Meteorite* magazine. February 2014. Volume 20, No. 1.

Brachaniec T. and Beauford R. E. 2012. Search for a Meteorite Driven Extinction in the Late Devonian. *Meteorite* magazine. August 2012. Volume 18, No. 3.

Kohler E. and Beauford R. E. 2011. Planetary atmospheres and meteorite impacts in the inner solar system. *Meteorite* magazine. May 2011. Volume 17, No. 2

1.6 References

Beck P., Quirico E., Garenne A., Yin Q.-Z., Bonal L., Schmitt B., Montes-Hernandez G., Montagnac G., Chiriac R. and Toche F. 2014. The secondary history of Sutter's Mill CM carbonaceous chondrite based on water abundance and the structure of its organic matter from two clasts. *Meteoritics & Planetary Science*. doi: 10.1111/maps.12273

Beveridge T. A. 1949. The geology of the Weaubleau quadrangle, Missouri. Ph.D. thesis, State University of Iowa, Iowa City, Iowa.

Beveridge T. R. 1951. The Geology of the Weaubleau Creek Area, Missouri. *Missouri Geological Survey and Water Resources Report, Second Series*. 32.

Bischoff A., Scott E. R. D., Metzler K., Goodrich C. A. 2006. Nature and origins of meteoritic breccias. In *Meteorites and the Early Solar System II*, edited by Lauretta D. S., McSween H. Y. Tucson, AZ: University of Arizona Press. pp. 679-712.

Bischoff A. and Schultz L. 2004. Abundance and meaning of regolith breccias among meteorites (abstract). *Meteoritics & Planetary Science* 39:A15.

Bland P. A. and Artemieva N. A. 2006. The rate of small impacts on Earth. *Meteoritics & Planetary Science* 41:607–631.

Burton A. S., Glavin D. P., Elsila J. E., Dworkin J. P., Jenniskens P. and Yin Q.-Z. 2014. The amino acid composition of the Sutter's Mill CM2 carbonaceous chondrite. *Meteoritics & Planetary Science*. doi: 10.1111/maps.12281

Cox M. R. and Evans K. R. 2007. Geologic map of the Vista 7.5' Quadrangle, St. Clair county, Missouri: Missouri Department of Natural Resources Division of Geology and Land Survey Open-File Report OFM-07-101-GS.

Dulin S. and Elmore R. D. 2008. Paleomagnetism of the Weaubleau structure, southwestern Missouri. In The sedimentary record of meteorite impacts, edited by Evans K. R., Horton J. W. Jr., King D. T. Jr., and Morrow J. R. *Geological Society of America Special Paper 437*. pp. 55-64.

Elmore R. D. and Dulin S. 2007. New paleomagnetic age constraints on the Decaturville impact structure and Weaubleau structure along the 38th parallel in Missouri (North America). *Geophysical Research Letters* 34(13).

Evans K. R., Rovey C. W. II, Mickus K. L., Miller J. F., Plymate T., and Thomson K. C. 2003b. Weaubleau-Osceola structure, Missouri: deformation, event stratification, and shock metamorphism of a mid-Carboniferous impact site (abstract #4111). Third International Conference on Large Meteorite Impacts, Nordlingen, Germany.

Evans K. R., Mickus K. L., Rovey C. W. II, and Davis G. H. 2003c. The Weaubleau-Osceola Structure: Evidence of a Mississippian Meteorite Impact in Southwestern Missouri, in A*ssociation of Missouri Geologists Fieldtrip Guidebook*. 50th Annual Meeting. Report of Investigation No. 75. Guidebook No. 26:1-30.

Finn M. P., Krizanich G. W., Evans K. R., Cox M. R., Yamamoto K. H. 2012. Visualizing Impact Structures Using High-Resolution LiDAR-Derived DEMs: A Case Study of Two Structures in Missouri. *Surveying and Land Information Science* 72(2):87-97.

French B. M. 2004. The importance of being cratered: The new role of meteorite impact as a normal geological process. *Meteoritics & Planetary Science* 39(2):169–197.

French B. M. and Koeberl C. 2010. The convincing identification of terrestrial meteorite impact structures: What works, what doesn't, and why. *Earth-Science Reviews* 98(1–2):123-170.

Fries M., Le Corre L., Hankey M., Fries J., Matson R., Schaefer J. and Reddy V. 2014. Detection and rapid recovery of the Sutter's Mill meteorite fall as a model for future recoveries worldwide. *Meteoritics & Planetary Science*. doi: 10.1111/maps.12249

Herd C. D., Froese D. G., Walton E. L., Kofman R. S., Herd E. P., and Duke M. J. 2008. Anatomy of a young impact event in central Alberta: Prospects for the ‘‘missing’’ Holocene impact record. *Geology* 36:955–958.

Jenniskens P., Fries M. D., Yin Q., Zolensky M., Krot A. N., Sandford S. A., Sears D., Beauford R., Ebel D. S., Friedrich J. M., Nagashima K., Wimpenny J., Yamakawa A., Nishiizumi K., Hamajima Y., Caffee M. W., Welten K. C., Laubenstein M., Davis A. M., Simon S. B., Heck P. R., Young E. D., Kohl I. E., Thiemens M. H., Nunn M. H., Mikouchi T., Hagiya K., Ohsumi K., Cahill T. A., Lawton J. A., Barnes D., Steele A., Rochette P., Verosub K. L., Gattacceca J., Cooper G., Glavin D. P., Burton A. S., Dworkin J. P., Elsila J. E., Pizzarello S., Ogliore R., Schmitt-Kopplin P., Harir M., Hertkorn N., Verchovsky A., Grady M., Nagao K., Okazaki R., Takechi H., Hiroi T., Smith K., Silber E. A., Brown P. G., Albers J., Klotz D., Hankey M., Matson R., Fries J. A., Walker R. J., Puchtel I., Lee C-T. A., Erdman M. E., Eppich G. R., Roeske S., Gabelica Z., Lerche M., Nuevo M., Girten B., Worden S. P., and (the Sutter’s Mill Meteorite Consortium). 2012. Radar-Enabled Recovery of the Sutter’s Mill Meteorite, a Carbonaceous Chondrite Regolith Breccia. *Science* 21:338(6114):1583-1587.

Jenniskens P. 2014. The Sutter's Mill Fall. *Meteoritics & Planetary Science*. doi: 10.1111/maps.12343

Morrow J. R. and Evans K. R. 2007. Preliminary shocked-quartz petrography, upper Weaubleau breccia, Missouri, USA (abstract #5237). *Meteoritics and Planetary Science* 42 (Suppl.):5237.pdf.

Miller J. F., Evans K. R., Ausich W. I., Bolyard S. E., Davis G. H., Ethington R. L., Rovey C. W. II., Sandberg C. A., Thompson T. L., and Waters J. A. 2008. Mixed-age echinoderms, conodonts, and other fossils used to date a meteorite impact, and implications for missing strata in the type Osagean (Mississippian) in Missouri, USA. In *Echinoderm Paleobiology*, edited by Ausich W. I. and Webster G. D. University of Indiana Press, Bloomington. p. 246-288.

Nishiizumi K., Caffee M. W., Hamajima Y., Reedy R. C. and Welten K. C. 2014. Exposure history of the Sutter's Mill carbonaceous chondrite. *Meteoritics & Planetary Science*. doi: 10.1111/maps.12297

Rampino M. R. and Volk T. 1996. Multiple impact event in the Paleozoic: Collision with a string of comets or asteroids? *Geophysical Research Letters* 23(1):49-52.

Sears D. 2004. The Origin of Chondrules and Chondrites: Cambridge Planetary Science Series. Cambridge University Press.

Zhao X., Lin Y., Yin Q.-Z., Zhang J., Hao J., Zolensky M. and Jenniskens P. 2014. Presolar grains in the CM2 chondrite Sutter's Mill. *Meteoritics & Planetary Science*. doi: 10.1111/maps.12289

Chapter 2 Observations on the macrostructure of the Sutter's Mill CM chondrite

2.1 Abstract

A 5.1 gram individual of the Sutter's Mill meteorite (SM48) was cut to expose eight faces. There are considerable face-to-face differences, but four distinct lithologies and an internal structure consistent with regolith breccia can be identified under a low-power binocular microscope. The first and most abundant lithology is finely comminuted matrix composed of fine particles, submillimeter clasts, and breccia-within-breccia clasts. The second lithology, dark clasts rich in chondrules and inclusions, shows little evidence of regolith working. The third lithology is light clasts that are chondrule-poor, with a homogenous color and texture suggesting substantial alteration. The fourth lithology is a 'dark inclusion' that appears similar to those seen in Allende. Though textural and structural indicators of regolith maturation are apparent in the macrostructure of the stone, neither lightening nor darkening provides a reliable proxy for regolith maturity. The shape and fusion crust properties, similar to other Sutter's Mill stones, indicate orientation during atmospheric passage. Cracks along clast boundaries may represent incomplete cementation of fractures formed during comminution or later impacts, and may have contributed to reported early atmospheric breakup, as well as to the size and number of recovered stones. Observations of thick crust and the presence of deep surface cracks, along with drainage of thermoluminescence, reported elsewhere, suggest considerable heating occurred throughout the stone, and may explain low abundances of volatile organics and water. This investigation provides a macroscopic framework that we hope will help place work on this and other CM asteroidal regoliths within a whole-rock context.

2.2 Introduction

The Sutter's Mill meteorite was probably about 70 metric tons when it entered the atmosphere on April 22nd, 2012, but while it produced considerable commotion, it only produced a small shower of gravel-sized pieces. At the time of writing, the total recovered mass of the 78 fragments was slightly less than 1 kg. The largest fragment is 205.2 g while the smallest is 0.3 g. The meteorite was classified as a CM chondrite regolith breccia based on elemental and isotopic abundances (Jenniskens et al., 2012) but shows unusual evidence of heating and certain matrix regions contain oldhamite (Jenniskens et al., 2012; Beck et al., 2014). Very fast recovery, made possible in part by the use of weather radar data, substantially increased the scientific potential of the fall (Fries et al., 2014; Jenniskens, 2014). A consortium of over seventy researchers was established to examine the meteorite (Jenniskens et al., 2012).

One of the present authors (Steve Arnold) obtained a 5.1 g fully crusted stone, measuring approximately 1.5 cm x 1.5 cm x 1.5 cm, through his activities as a meteorite dealer. He arranged for it to be cut into as many slices as the friability of the stone would permit, but before selling them he offered the slices to his coauthors for photographic documentation and description. This article is the result. We used low-powered binocular microscopy and photography under various illumination conditions with, in view of the practical constraints, minimal application of other techniques. While this study lacks the insights provided by higher order microscopy and analysis, which are covered by several other research groups in the Sutter's Mill consortium (Jilly et al., 2014; Nuevo et al., 2014; Zhao et al., 2014; Beck et al., 2014), examination of the macrostructure of eight slices taken from a single stone does provide a larger scale context and, we suggest, fresh insights into previously discussed processes that occur on the parent body of these meteorites. Our study is somewhat analogous to the study of Zezin

and Bazilevskiy (1972) of lunar regolith breccia clasts and CT scans of meteorites by more recent authors (e.g. Ebel and Hill, 2012).

The CM chondrite class is defined by unique elemental and isotopic abundances which place it closer to the solar photosphere than any other class but the CI chondrites (e.g. Sears, 2004). They are impact breccias (Bischoff et al., 2006) with a regolithic history (Bischoff and Schultz, 2004) as suggested by sparsely observed breccia-in-breccia structures (Metzler, 2004), the abundances of volatile elements emplaced from the solar wind (Schultz and Kruse, 1989; Bischoff and Schultz, 2004), the selective distribution of solar gas enrichment in comminuted matrix as opposed to clasts of primary accretionary material (Nakamura et al., 1999a,b), and in similar distribution of pre-irradiated grains (Metzler, 2004).

All CM chondrites show aqueous alteration. The extent of aqueous alteration varies significantly, from less altered examples such as Murchison that preserve significant amounts of mafic silicates, to nearly completely altered meteorites in which oxidation and hydrolysis have completely converted the anhydrous silicates to phyllosilicates (Rubin et al., 2007). The specific mineralogical and textural changes associated with aqueous alteration have been well described (e.g., Browning et al., 1996; Hanowski and Brearley, 2001; Rubin et al., 2005, 2007; Lee et al., 2012).

Previous investigation of CM chondrites has found primary accretionary precursor lithologies to be present as clasts in most CM chondrite breccias, though the proportion and visibility of these clasts varies (Bischoff et al., 2006). That these clasts are the probable parent material for the fine grained matrix of the breccias, through comminution, has been demonstrated for at least eleven CM chondrites by Bischoff et al. (2006) and Metzler et al. (1992). For clarity, we use the term ‘matrix’ here, and in several other places in this paper, to refer to the fine

grained material produced between clasts in a breccia rather than in the more specific sense of fine-grained material between chondrules in an unbrecciated chondrite.

Variation among primary lithic clasts in brecciated CM chondrites has been described in terms of a light-dark dichotomy by previous authors (e.g. Heymann and Mazor, 1967; Metzler, 2004). Greenwood et al. (1993) identified lithic clasts in Cold Bokkeveld that were both lighter and darker than their surrounding matrix. Metzler (2004) made similar observations for Nogoya. Variation in extent of aqueous alteration between clasts within individual CM chondrites has been reported by Rubin et al. (2007), Rubin and Wasson (1986), Metzler et al. (1992), and others.

Other issues that have been discussed in the literature are resolving parent body and pre-accretionary processes, the timing of various apparent processes, and the relationship between fine-grained rims on clasts and the matrix (Metzler et al. 1992; Metzler 1987, 2004; Zega and Buseck 2003; Lauretta et al. 2000; Nakamura et al., 1999a and b; Sears et al., 1992, 1993; Chizmadia et al., 2003; Trigo-Rodriguez et al., 2006; Browning et al., 2000; Hanowski and Brearley, 2001). Similar studies have been reported for Tagish Lake and other carbonaceous chondrite groups (Tomeoka and Tanimura, 2000; Takayama and Tomeoka, 2012; Greshake et al., 2005; Bischoff, 1998; Brearley, 1993; Krot et al., 2000; Tomeoka and Ohnishi, 2010; Bland et al., 2011; Zolensky et al., 1993).

Sutter's Mill is very similar to other CM chondrites in major elemental composition and in its origin as a regolith breccia exhibiting aqueous alteration (Jenniskens et al., 2012; Nishiizumi et al., 2014). It falls among minority groupings of CM chondrites in several ways, however; cosmic-ray exposure ages are short compared to most CM chondrites (Jenniskens et al., 2012; Nishiizumi et al., 2014), it contains reduced xenolithic inclusions (Jenniskens et al.,

2012), shows both thermal metamorphism and aqueous alteration, with extent of alteration varying between clasts (Zhao et al., 2014; Beck et al., 2014; Burton et al., 2014), and exhibits thermal metamorphism subsequent to aqueous alteration (Beck et al., 2014).

Sutter's Mill has been altered by heating to 300° C, most likely within last 10^5 years (Sears and Beauford, 2014), resulting in lower abundances of organic compounds (Burton et al., 2014; Pizzarello and Garvie, 2014), reduction in water content of phyllosilicates (Beck et al., 2014; Pizzarello and Garvie, 2014) and in recrystallization of phyllosilicates (Beck et al., 2014). There are also hints that the thermal history of the stone may be more complex than a single heating event accounts for. Differences in thermal history are evident between adjacent clasts (Beck et al., 2014), with some clasts indicating heating up to 500° C (Jenniskens et al., 2012) and examination of fusion crust (Sears and Beauford, 2014) suggests relatively deep alteration of the small stones by heating during atmospheric passage. Cumulatively, these indications suggest that individual samples may have been affected by impact induced heating (Beck et al., 2014) as well as ablative heating (Sears and Beauford, 2014), both compounding possible overall heating of the meteorite by recent proximity to the sun during orbit (Beck et al., 2014; Nuevo et al., 2014; Sears and Beauford, 2014). Discussion of previously identified examples of heated CM chondrites is found in Beck et al. (2014) and more detailed discussions concerning aqueous alteration in CM chondrites are found in Rubin et al. (2007), Rubin and Wasson (1986), and Metzler et al. (1992).

Here we describe the slices mentioned above and we discuss our observations in the context of previous work on CM chondrites and on Sutter's Mill. Progress reports have been made at conferences (Beauford et al., 2012; 2013; Beauford and Sears 2013), but the present paper supersedes those. We report variations among the clasts and relationships observed

between the clasts and the matrix, and speculate on the relative timing of their formation. We describe possible textural and structural indicators of regolith maturation that are apparent in the macrostructure. We also describe some observations on the shape of the stone and its fusion crust. This work provides a macroscopic framework that we hope will be useful in placing work on this meteorite in a whole-rock context.

2.3 Sample preparation

The 5.1 gram individual designated SM48 was found on May 5th, 2012 (Jenniskens et al. 2012), by Kelly Heavin, subsequent to rainfall in the collection area. Slices were prepared by Marlin Cilz at Montana Meteorite Laboratory using a 0.1 mm wire on a Well Precision Diamond Wire Saw, resulting in no fluid exposure and generating a total combined curf loss of approximately 1 mm. A single attempt at polishing did not improve resolvability of detail, and a standard thin section prepared from a representative section proved largely opaque. The meteorite was extremely friable, but eight slices, some cracked in two, were obtained. Their surfaces were recorded as a series of macro photographs with a Canon SD1300 IS digital camera and photomicrographs were prepared under reflected light with a Spencer binocular microscope fitted with a 3.5MP digital camera.

2.4 Results

We distinguished, by microscopic examination, what appear to be four distinct and readily observable lithologies (Fig. 2.1). The most abundant of the four is a finely comminuted matrix composed of fine particles, submillimeter clasts, and breccia-in-breccia clasts. Within this matrix are relatively large clasts of a second and third lithology. These appear as dark clasts that are rich in chondrules and inclusions and light clasts that are chondrule-poor with a

homogenous color and texture suggesting substantial alteration. A single example of a fourth lithology occurs as a 'dark inclusion' that appears similar to those seen in Allende.

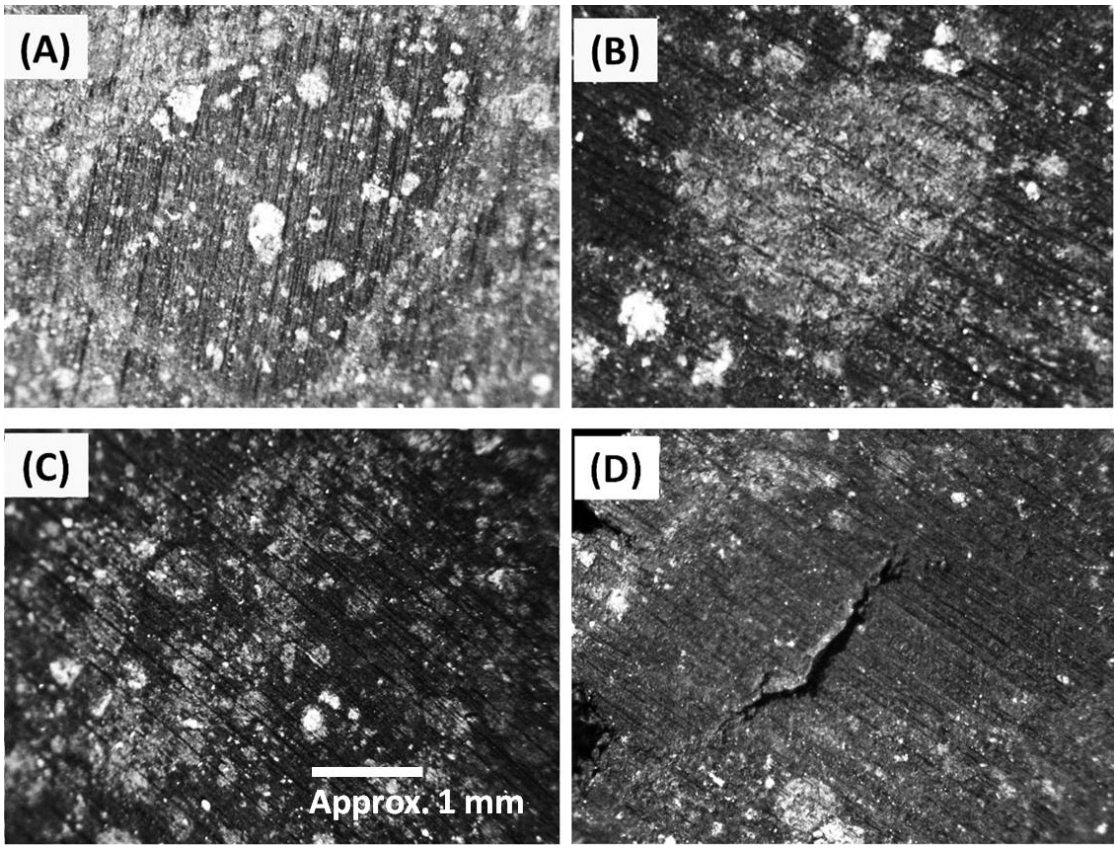

Figure 2.1 *Close up views of the four lithologies seen in the macrostructure of Sutter's Mill. A. Dark clast. B. Light clast. C. Matrix. D. The dark inclusion (from slice 8) has an internal crack in the same location as the large curved crack in slice 7.*

Figures 2.1a through 1.1d illustrate the four visually distinguishable lithologies. An example of a dark clast is shown in Fig. 2.1a. Larger examples of dark clasts reveal sharp outlines, are angular to sub-angular in shape, and have textures typical of unbrecciated chondrites. They do not contain clasts of other lithologies, are rich in chondrules and inclusions and contain sparse CAIs which tend to be small. The chondrules have sharp outlines and are typically less than 0.4 mm in size. The groundmass in the dark clasts is fine-grained, and darker fine grained rims are clearly visible as dark haloes around some chondrules. Where fine-grained rims occur around chondrules near the edge of dark lithology clasts, they are cross-cut by clast

boundaries and do not continue in adjacent matrix. Fine-grained rims in dark clasts are consistently intact, reveal well defined boundaries, and show no notable damage or separation from the chondrules or other inclusions around which they are formed. In contrast, fine-grained rims are frequently lacking or incomplete around chondrules in the matrix and light lithology clasts.

Clasts composed of the light lithology (Fig. 2.1b) range in size from more than 0.5 cm to less than 1.0 mm, below which they become impossible to distinguish from the comminuted matrix. The clasts have irregular, angular, fragmentary edges. Chondrules and a few inclusions are indistinct. In fact, the light clasts can best be distinguished by their homogenous appearance, the lack of contrasting CAI or aggregates, very sparse to non-visible chondrules, and an even, grey groundmass.

We refer to the interclast material as the matrix. An example of matrix is shown in Fig. 2.1c. It is composed of fine particles and sub-mm clasts of dark and light lithologies and of breccia-in-breccia clasts. Because the matrix appears to be composed of the remnants of the clasts it contains, the distinction between matrix and clasts may primarily be a matter of size and distinguishability. The matrix becomes difficult or impossible to visually resolve in regions where clasts are ground smaller than 1 to 2 mm. Chondrules and fragments of chondrules are occasionally found preserved within the matrix.

A single dark inclusion, resembling those in the Allende CV3 (eg: Varela et al., 2012), was observed in one of our slices (Fig. 2.1d), but was not examined in great detail. The object has a smooth outline and is larger than the chondrules and aggregates. It is fine grained, dark, and nearly featureless at magnification less than 100x. A large crack is observed in this inclusion and, like the larger crack in slice 7, it does not connect to the exterior of the stone.

Figues 2.2-2.5 show the eight slices to approximately the same scale, in the order they were removed from the stone, and with sketches to highlight the major features. Since this stone was initially fully crusted, all of the perimeters of the slices in our study consist of fusion crust, although in several cases the crust has chipped during slicing. These instances of crust chipping away demonstrate the ease with which the crust spalls off, as well as revealing the thickness of the crust. The overall shape of the stone, reflected in the slices, was rounded with an asymmetry commonly observed in oriented meteorites.

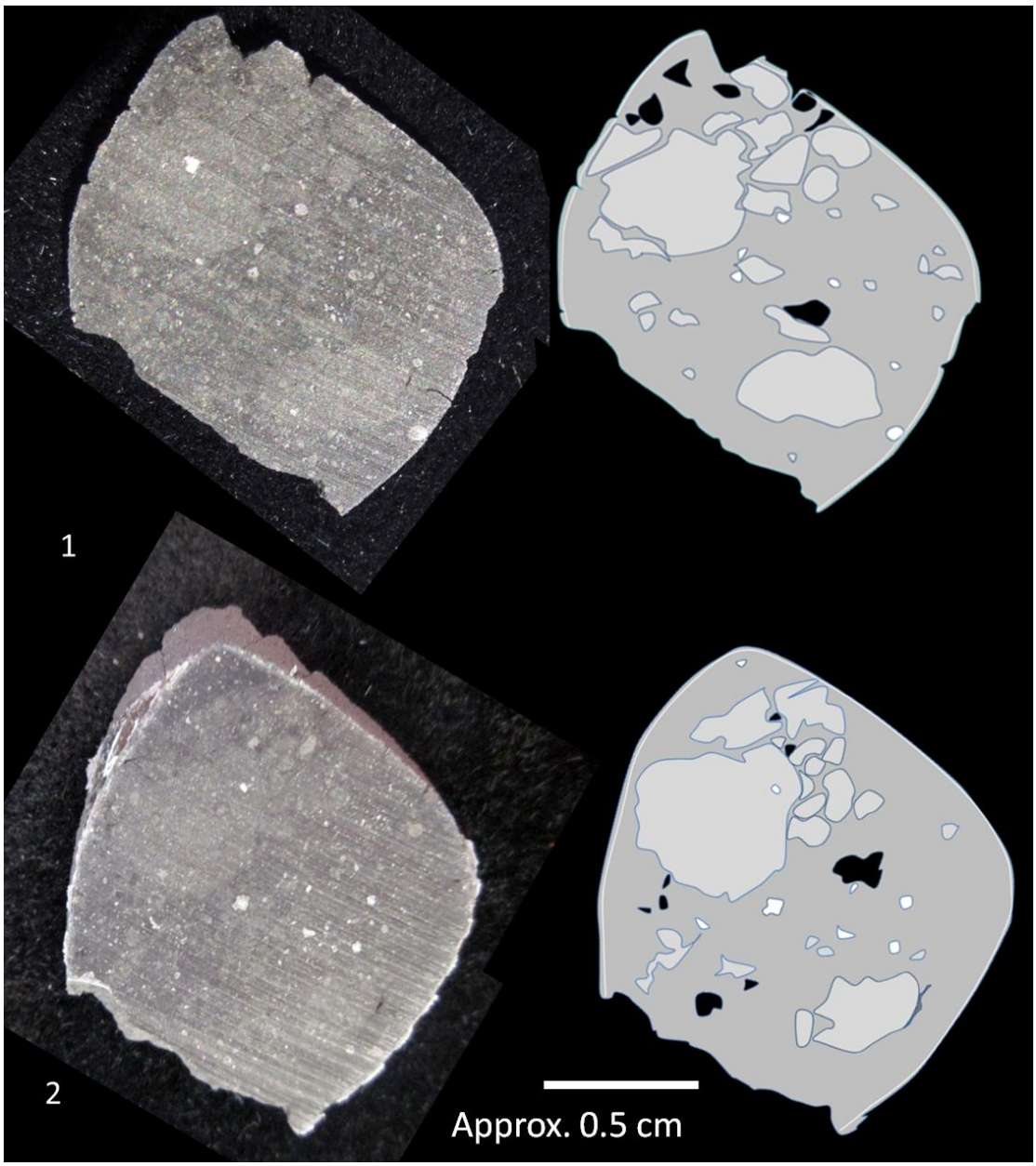

Figure 2.2. *Sutter's Mill (SM-48) slices 1 and 2 at same scale. The sketches highlight many of the major features in the slices; black = dark clasts, mid-grey = matrix, light grey = light clasts, white = chondrules and refractory inclusions. A white line indicates the inner boundary of the fusion crust. The slice is 1.5 cm in maximum dimension. Matrix predominates in these slices, followed by light clasts and thirdly, dark clasts.*

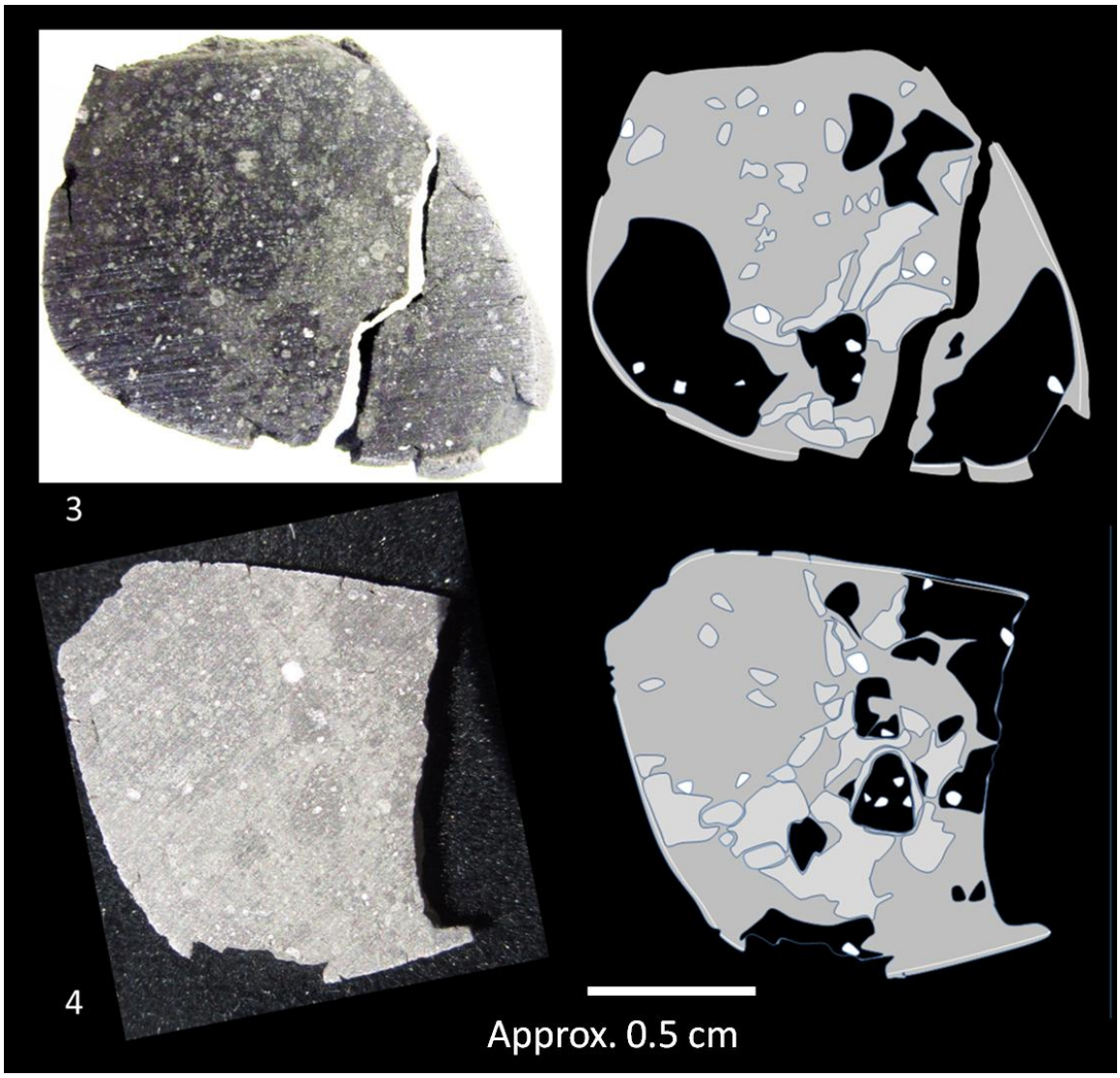

Figure 2.3. *Sutter's Mill (SM-48) slices 3 and 4 at same scale, and sketches with the same shading as in Fig. 2.1. Matrix again predominates, but there are a considerable number of dark clasts and a large number of complex shaped light clasts. About a third of slice 4 was lost in cutting and fusion crust chipped from the bottom of both slices. These instances of chipped crust demonstrate the thickness the crust can have on these stones.*

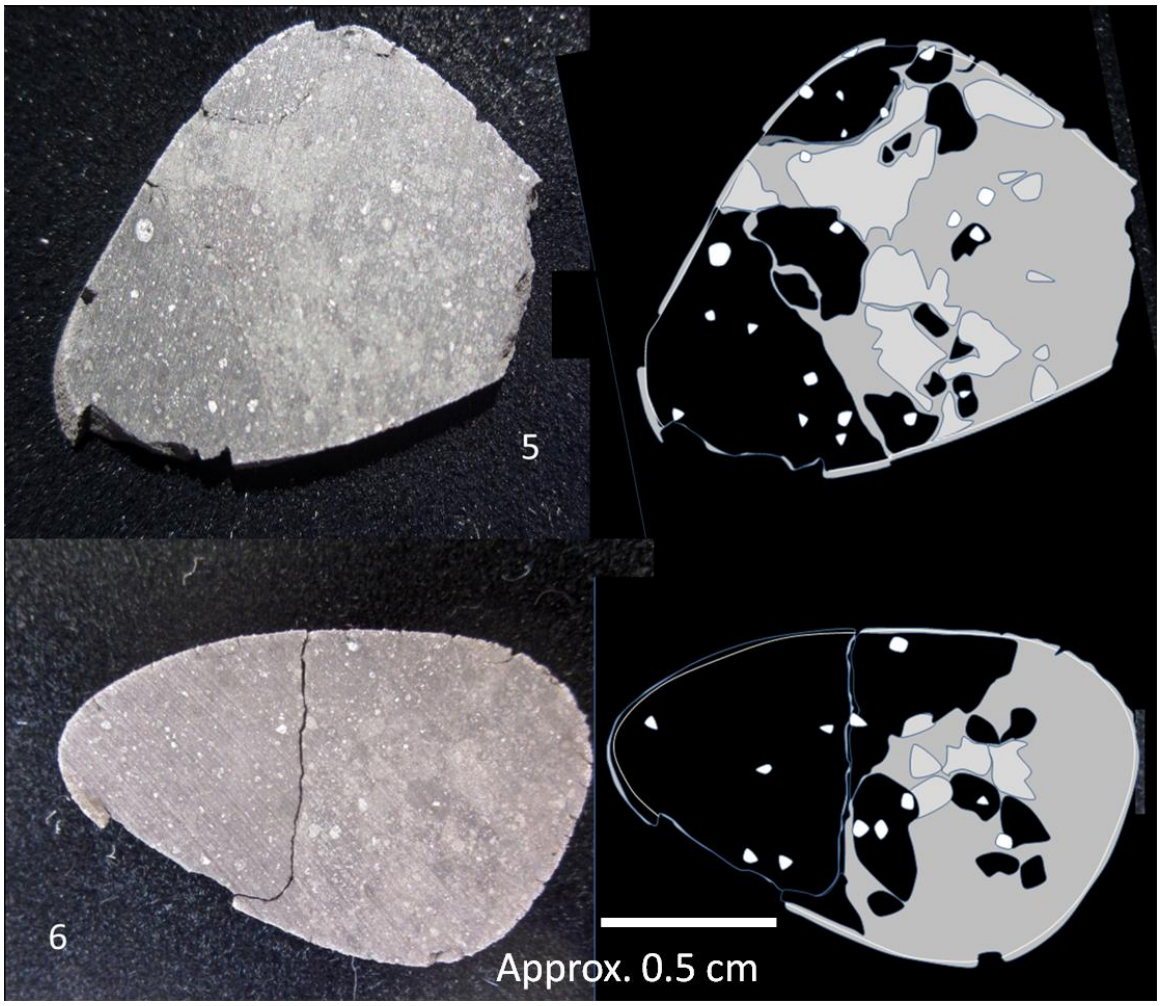

Figure 2.4. *Sutter's Mill (SM-48) slices 5 and 6 at same scale, and sketches with the same shading as in Fig. 2.1. Matrix and dark clast are approximately equally present in these slices and light clasts are relatively rare. Both slices show cracks between clast and matrix, demonstrating the ease with which the meteorite can fragment along clast boundaries. Again, the instances of chipped crust illustrate its thickness and the overall shape suggests orientation during atmospheric passage.*

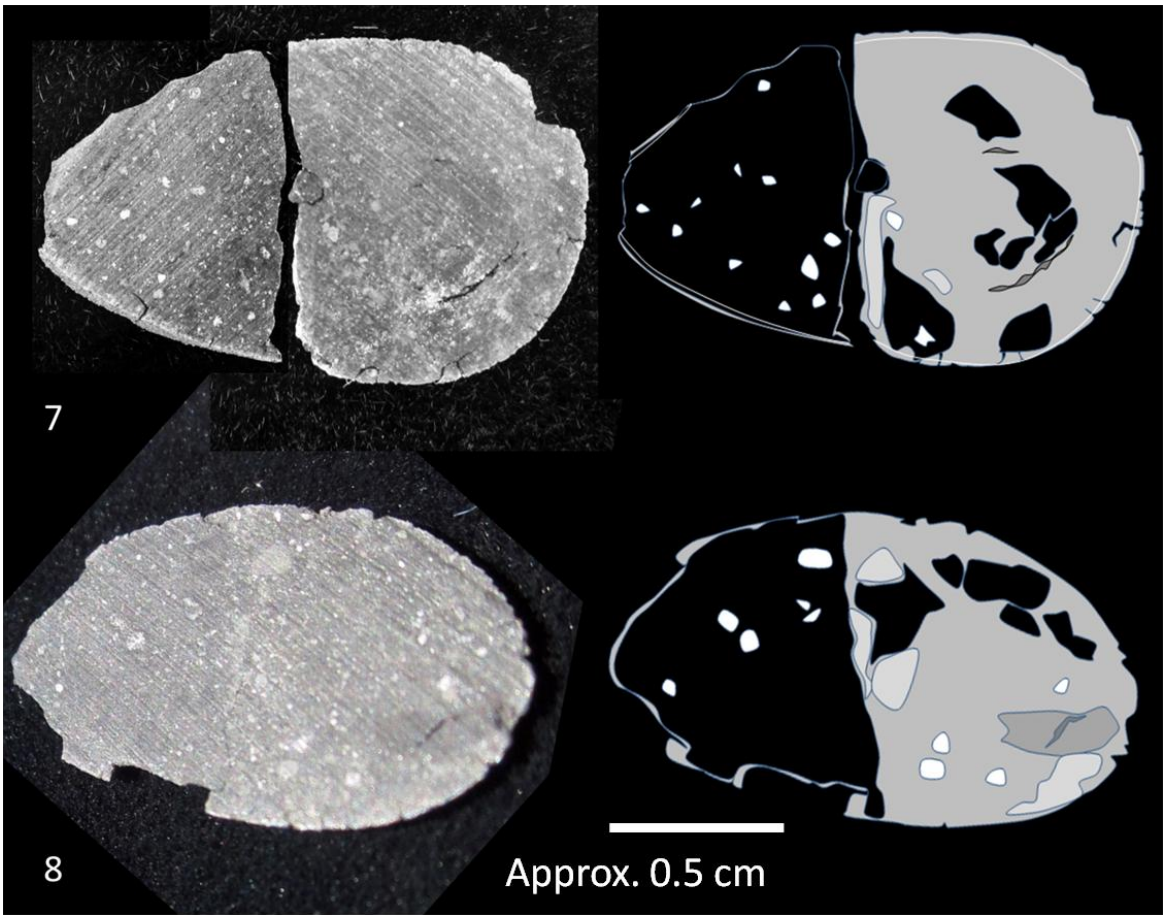

Figure 2.5. *Sutter's Mill (SM-48) slices 7 and 8 at same scale, and sketches with the same shading as in Fig. 2.1. Two egg shaped pieces, one with thick, chipped fusion crust and the other cracked in two. In addition to dark clasts, matrix, and light clasts, slice 8 contains a large dark inclusion indicated in mid grey. It contains a crack which is more conspicuous in slice 7 and appears curved in a concentric pattern around the dark clast.*

Figure 2.2 shows slices 1 and 2 which are quite similar. The slices mostly show matrix. Edges of light clasts up to 0.5 cm in diameter are visibly fragmented. The resulting smaller clasts, entrained into the surrounding matrix, become visually indistinguishable from the matrix at smaller scales. The larger light clasts are visible in both faces. There are also a few small dark clasts in these faces, which are difficult to resolve in the photos shown here, but which reveal distinct boundaries in microscopic examination. We can readily identify three out of the four different lithologies observed in SM48 in these slices: light clasts, matrix and dark clasts, where the matrix has intermediate darkness. Small, bright objects are chondrules and refractory

inclusions which can occasionally be several millimeters in size. About three-quarters of the perimeters of these two slices consist of fusion crust, and the opposite side (not shown) of slice 1 is largely fusion crusted.

Figure 2.3 shows slices 3 and 4. These slices have considerably more of the dark clast material; in fact, most of the smaller chip of slice 3 is composed of a dark clast. Light clasts are also present, but are small, irregular and scattered within the matrix. Chondrules and refractory inclusions are again present, visible as small, bright inclusions. Except for regions of chipping, the outer perimeter is smooth and has fusion crust, although the thickness varies considerably, being especially thick in the bottom right corner of slice 3. In several places, fusion crust has chipped off so that its thickness is readily seen. A large breccia-in-breccia clast, composed of finely comminuted material, is resolved in the upper left quadrant of slice 4.

Figure 2.4 shows slices 5 and 6. These two slices are also approximately equal mixtures of dark clasts and matrix, with a few light clasts and a sprinkling of small, bright chondrules and refractory inclusions. A crack separates the two halves of slice 6 and runs along a clast boundary. A large clast of the dark lithology, showing no sign of brecciation and exhibiting an accretionary texture, dominates to the left of the crack. Fine grained rims are clearly visible around many of the chondrules and refractory inclusions within the dark lithology, and close inspection reveals that these rims are truncated with chondrules at clast boundaries. A second crack partially surrounds a dark clast near the top of slice 5. Again the overall shape is a smoothed triangular/egg shape characteristic of oriented stones and the fusion crust is highly variable in thickness, being especially thick in the lower right edge of slice 5. Again, chipping of the fusion crust indicates its thickness.

Figure 2.5 shows slices 7 and 8. In both of these slices, dark clasts constitute just under half the surface, with matrix dominating the remainder. There are a few small light clasts in both faces. A scattering of small, bright chondrules and refractory inclusions are both more abundant and more distinct in the dark lithology. In slice 7, three of the four lithologies are present, while in slice 8, all four lithologies are observed. This is the only slice in which the fourth lithology, a rather large dark inclusion similar to those found in Allende, is found. Both slices are egg shaped, with fusion crust on the unchipped perimeter and the chips revealing the thickness of the fusion crust at that point. There is a large curved crack within slice 7 which does not extend to the apparent surface but extends to visibly cross-cut the dark inclusion in slice 8. The other side of slice 8 is the fusion crusted exterior of the stone.

In summary of figures 2.1 to 2.5, there are four major lithologies present in the Sutter's Mill meteorite based on observation of discrete clasts with differing visible and textural properties. Three of these are key structural elements of the Sutter's Mill meteorite. These are dark clasts, light clasts, and the interclast material we term "matrix," which appears in all slices. The matrix is intermediate in darkness between the light and dark clasts. The fourth distinct lithology is represented by a single dark inclusion in slice 8 and figure 2.1d. There is considerable variation in clast size, from ~1 cm across downwards. As the clasts get smaller, they seem to cluster and it becomes more difficult to distinguish individual clasts. It is immediately clear from Figs. 2.2-2.5 that Sutter's Mill is a complex polymict breccia with considerable diversity at the mm to cm scales as observed in these 8 slices.

While some slices are very similar, some are quite dissimilar. It is therefore not clear which, if any, is really typical of the meteorite as a whole. Of course, the Sutter's Mill

consortium has already experienced this, since only one sample, the first to be examined, contains oldhamite in its matrix.

Though slight differences in saw angle or cut position would rather evidently have produced a somewhat different outcome, we have approximated the percentage of the sawn surfaces that reveal each lithology in order to give some quantitative sense of their relative abundance. Totaled over all of the surfaces studied, the dark clasts represent ~32.3% of the faces exposed by cutting, while the light clasts make up ~16% of the surfaces, and the matrix comprises ~51.4%. The fourth lithology, represented by a dark inclusion on one face (face 8) represents a relative area of less than 1%. Percentages were approximated by carefully cutting up printed maps of the surfaces and weighing the portions represented by each lithology as well as the weight of the whole map. While limits on precision are obvious, this does give some sense of relative abundance of lithologies, at least in this stone. The variability in lithologic abundance from face-to-face was particularly noteworthy, as it reveals that a small sample might be very misleading if assumed to represent the entirety of the Sutter's Mill meteorite fall. To what extent this stone may be representative of the fall as a whole is also not revealed by examination at this scale.

2.5 Discussion

We will discuss what we observed in the dissected stone in terms of the following topics; (1) the four lithologies we observed, (2) comparison of the slices with previously published CT scans, (3) what the 3-dimensional structure of the stone might reveal about regolith evolution, (4) the numerous cracks and their possible significances, and (5) the shape of the stone and its fusion crust. Our examination of the fusion crust is discussed in somewhat greater detail in Sears and Beauford (2014).

2.5.1 The four lithologies

We interpret the dark clasts as primary material relatively unaltered by regolithic comminution. They have sharp outlines, are usually angular to sub-angular in shape, are unbrecciated and are rich in chondrules which also have sharp outlines. These are commonly referred to as primary accretionary rocks (Metzler et al., 1992). Beck et al. (2014) observe clasts with very low degrees of aqueous alteration in SM 51 that may be analogous. That fine-grained rims around chondrules and refractory inclusions in these clasts are severed, with chondrules, at clast boundaries indicates that fine-grained rims must have formed prior to disruption of the associated dark lithology and entrainment of the associated clasts in the currently observed regolithic assemblage.

The light clasts, on the other hand, we interpret as highly altered regolith samples that are either finely ground or secondarily altered to produce what appears macroscopically to be a homogenous grey mass. Light clasts have irregular, fragmentary edges and very few distinguishable chondrules or other inclusions. Explaining these clasts as simply highly aqueously altered materials may be too simplistic, as the meteorite exhibits both zones of highly comminuted material and evidence of recrystallization in some clasts due to heating subsequent to significant aqueous alteration, as Beck et al. (2014) observed in SM18. Clasts showing significant evolution of phyllosilicates associated with aqueous alteration have been reported in (Beck et al., 2014; Jenniskens et al. 2012; Jilly et al., 2014). To what extent the loss of internal visual distinctions in the light lithology clasts we see here results from comminution versus aqueous alteration or thermal metamorphism cannot be distinguished by simple microscopy, though this study may give some sense of distribution of highly altered materials relative to unaltered materials and comminuted matrix, contextualizing prior and subsequent studies.

The third lithology, the matrix, is a comminuted mixture of dark and light clasts and thus has intermediate darkness. Greenwood et al. (1993) and Metzler (2004) observed that, for Cold Bokkeveld and Nogoya, the clasts were sometimes darker and sometimes lighter than the matrix, and now we observe this is also true of Sutter's Mill. Thus this lithology consists of fine particles and sub-mm clasts of dark and light lithologies and of breccia-in-breccia clasts. The presence of chondrules and fragments of chondrules suggests a less thorough regolith working or less complete aqueous alteration than the light clasts. The fourth lithology, the single dark inclusion, we will not discuss further other than to note its presence in Sutter's Mill.

2.5.2 The present slices and previously published observations

A method of documenting the interior of a meteorite stone, besides taking slices as we have done, is to perform x-ray computed tomography (CT) scanning. Ebel and Hill (2012) performed CT scans on SM-3 and SM-9 and found a situation similar to that which we have observed here. Both meteorites contained a dominant lithology characterized by abundant clasts (with chondrules or CAI) in the range of 200 to 400 μm diameter, and they also found metal oxide or sulfide grains in the 0.05 - 0.15 μm range. A second lithology, with matrix exhibiting higher atomic mass (Z), and with more abundant clasts, appears as irregular, angular lithic fragments many mm in size. Several large clasts > 1 mm include a low-Z spherical object that appears to be concentrically zoned, and a similar object with zoned high-Z (metal) and low-Z (silicate) layers. Other large clasts are irregular, blocky objects. We somewhat tentatively suggest that the dominant lithology observed in the CT scans was equivalent to what we describe as matrix, and that the secondary lithology was a mixture of our observed light and dark clasts. The Ebel and Hill (2012) CT scans also revealed frequent cracks similar to those we discuss below.

2.5.3 Regolith development and maturation in Sutter's Mill

All prior CM chondrites that have been investigated have proven to be regolithic impact breccias (Bischoff et al., 2006; Bischoff and Schultz, 2004) as suggested by breccia-in-breccia structures (Metzler, 2004), abundances of volatile elements (Schultz and Kruse, 1989; Bischoff and Schultz, 2004), distribution of solar gas enrichment (Nakamura et al., 1999a,b), and distribution of pre-irradiated grains (Metzler, 2004). Primary accretionary precursor lithologies have been observed in CM chondrite breccias (Bischoff et al., 2006), and it has been demonstrated that these clasts are the probable parent material for the comminuted inter-clastic matrix of these breccias (Bischoff et al., 2006; Metzler et al., 1992.) Variation among primary lithic clasts in CM chondrite regolith breccias has been described in terms of a light-dark dichotomy by previous authors (e.g. Heymann and Mazor, 1967; Metzler, 2004), and in at least two instances (Greenwood et al., 1993; Metzler, 2004) it has been observed that such clasts were both lighter and darker than their surrounding matrix.

Like previous CM chondrites, Sutter's Mill is a regolith breccia (Jenniskens et al., 2012). We observe the physical signatures of the meteorites regolithic history preserved in its lithologic structure and composition. Multiple generations of impacts are evidenced by breccia-in-breccia clasts distributed within a finely comminuted matrix amongst discrete clasts with varying histories of thermal and aqueous alteration (Jenniskens et al., 2012; Beck et al., 2014).

There has been considerable discussion of methods to determine the maturity of the regoliths on airless bodies. For the Moon, there are several quantitative measurements that reflect the time-evolution of the regolith, i.e. maturity. These are trapped solar wind, charged-particle tracks, agglutinate abundance, thermoluminescence sensitivity and cathodoluminescence (Benoit et al., 1996; Akridge et al., 2004). The process can also be followed spectroscopically

since the evolved matrix is darker than the unaltered material that remains as clasts, giving these meteorites the familiar light-dark structure (Britt and Pieters, 1994; Pieters and Fischer, 1993). For the ordinary chondrites, trapped solar wind, charged-particle tracks, and thermoluminescence sensitivity are effective indicators of regolith maturity (Haq et al., 1989).

It has long been known that CM chondrites are extremely heterogeneous (McSween, 1979; Kerridge and Bunch, 1979; Hanowski and Brearley, 2001). Because of their mineralogy and the complexity of their regolith histories, it is difficult to find a single quantitative parameter to track regolith maturity in CM chondrites. Like ordinary chondrites, the matrix of CMs is enriched in solar wind noble gases relative to the dark clasts and might be used as an index of regolith maturity (Nakamura et al., 1999a,b). With increasing time in the active regolith, we might also expect a progressive reduction in clast size, the matrix to lighten or darken visibly, the appearance of recycled breccia-in-breccia clasts, and an increase in the ratio of fine grained matrix to clasts. The challenge, in the case of the CM chondrites, is that there has been uneven aqueous alteration and multiple recycling of regolith material. We find that lightness and darkness of clasts does not appear to be a proxy for regolith maturity. While the dark lithology clasts show the least evidence of physical comminution, the visibly shattered and recycled matrix is intermediate in darkness between these apparently least-altered clasts and the more visually homogenous light clasts, which have a less certain and possibly more complex alteration history.

At a minimum, we can suggest that we observe four degrees of regolith maturation as follows. First, the dark clasts appear to represent primary material. They show few signs of comminution within the regolith. Second, we observe the light clasts that we interpret to represent advanced regolith working and/or aqueous alteration, as evidenced by the loss of most visibly distinguishable inclusions. Third, we have the matrix of the present stone, which we

interpret to represent mixing of light and dark clasts. And finally, we have the overall accumulation we now observe, a complex mix of materials with varying regolith histories.

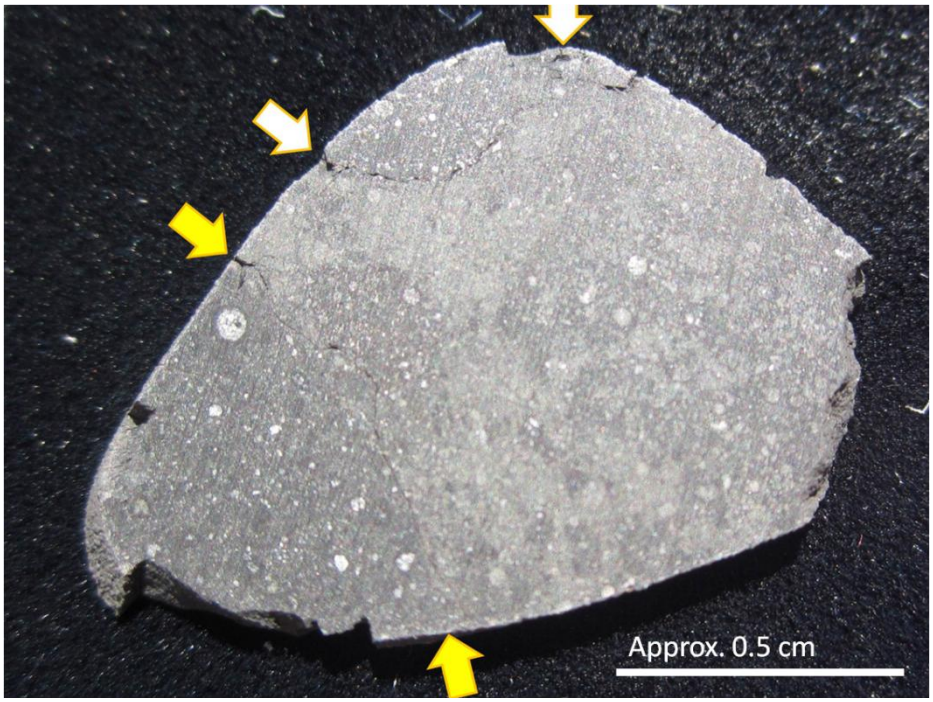

Figure 2.6. *Slice 5, with the two major cracks along clast boundaries indicated by the pairs of arrows. The slice readily parted along the larger fracture. It is possible that these clasts represent late stage entrainment of bedrock lithologies in a regolith that had become too cold and dry to accomplish thorough cementation. Weak boundaries along lithologies may have contributed to high altitude disruption of the stone, diminished atmospheric survival, and the small size of individual recovered samples (Popova et al., 2011).*

2.5.4 Significance of cracks

Cutting revealed at least 3 types of fractures in SM48: (1) cracks associated with fusion crust, which result in the crust spalling or peeling, (2) cracks along significant lithologic boundaries, which produce spontaneous parting of the samples, and (3) small cracks within the stone that do not reach the surface and do not appear to follow lithologic boundaries.

Fractures along clast boundaries seem to represent incomplete cementation in a late stage of comminution. They appear to be simple crumbling interfaces; uncemented rock surfaces in a poorly consolidated and partially cemented regolith. Apparently, available fluids or heat were

not sufficient to cement clast/clast and clast/matrix boundaries (Fig. 2.6). It seems highly likely that since this meteorite is a sample of regolith, with a history of prolonged reworking, that these preexisting interfaces were opened by shock during the fall to earth. This poorly consolidated breccia resulted in the early atmospheric breakup reported in Jenniskens et al. (2012) and Jenniskens (2014). Pervasive internal fractures were also observed in CT scans reported by Ebel and Hill (2012). They also suggested that these may explain the small size and number of recovered specimens. The lack of higher average atomic mass (high-Z) veins observed by Ebel and Hill (2012) is consistent with our study since we did not observe any metal and sulfide-rich shock veins associated with the cracks. We speculate that some internal cracks that do not reach the surface may result from volume reduction during water loss from phyllosilicates with reheating, reported in Pizzarello and Garvie (2014) and Beck et al. (2014).

An incompletely cemented regolithic breccia may also represent a transition between unconsolidated surface material and consolidated breccia. Such a situation has been observed in polymict eucrites (Delaney, 1984) and lunar materials (Rode and Lindstrom, 1994). The friability of such materials explains their rarity in the meteorite record (Britt et al., 2002; Popova et al., 2011) and may help us understand physical properties of regoliths (eg: Clark et al., 2002).

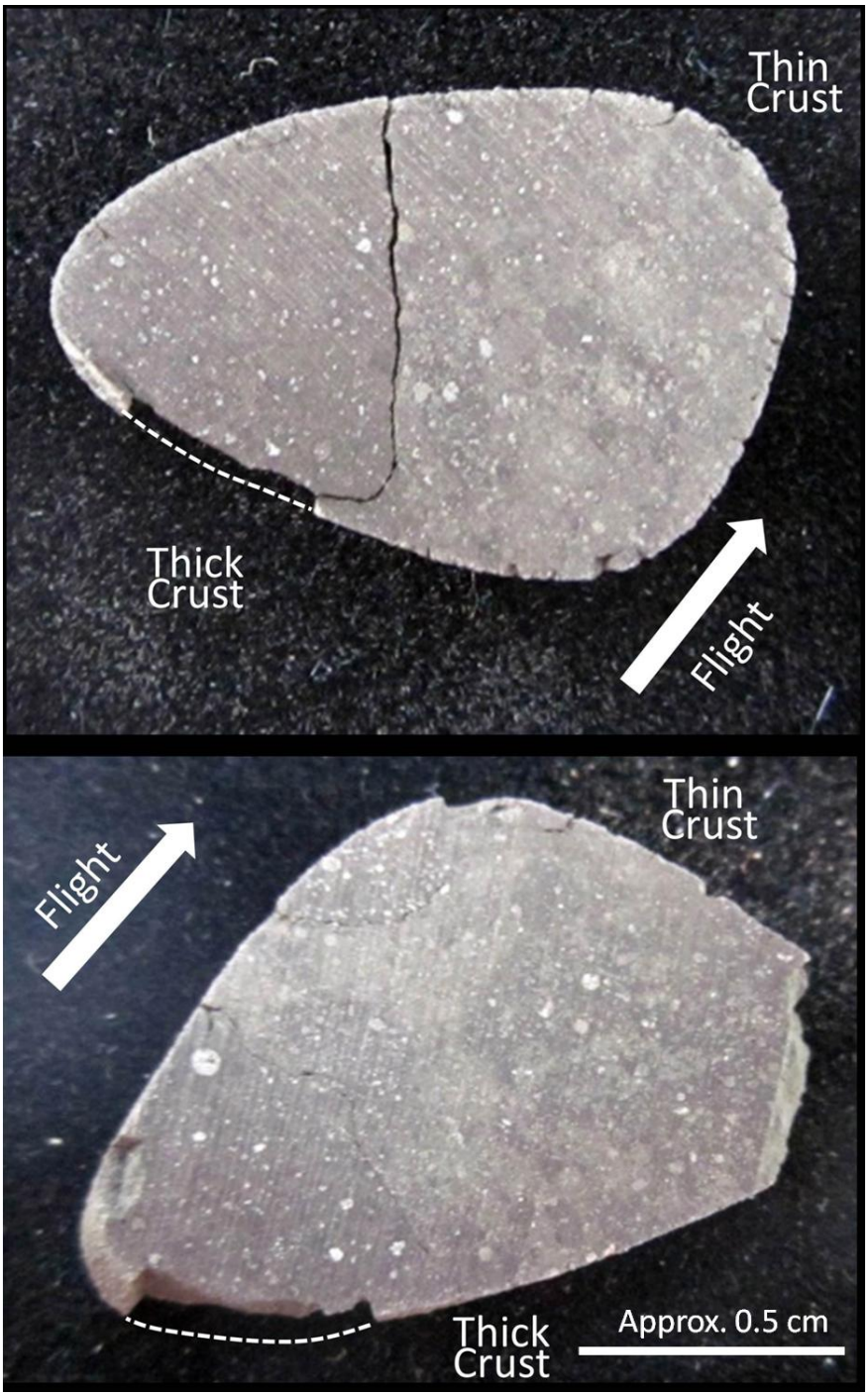

Figure 2.7. *Two of the present slices showing the overall shape of the meteorite and how the thickness of fusion crust varies from the front of the oriented stone, where the crust is thin, to the back, where it is quite thick. The thickness can be readily judged from the locations in which it spalled off during handling.*

2.5.5 Meteorite shape and fusion crust.

Evidence of orientation during final stages of flight is common among Sutter's Mill stones. Orientation is a well-known phenomenon in meteorite fall and is a consequence of the stone adopting a maximum drag configuration during flight, after which it ablates into a characteristic, almost conical form, as a consequence of plasma flowing around the stone. The present stone was oriented in the manner indicated in Fig. 2.7. In addition to producing a recognizable overall shape for the stone, passage through the atmosphere causes the fusion crust to have a certain texture reflecting the orientation during flight. The textures associated with orientation of meteorites can be quite dramatic. Oriented stones are typically smooth on the frontal face, striated on the lateral faces, and scoriaceous on the rear faces. There are clear signs of fluid flow on the surface of the Sutter's Mill stones, especially when flow encounters a ridge. The most dramatic instance of flow textures in the Sutter's Mill fusion crust known to the present authors is stone SM-64 recovered by Kieth Jenkerson. The rear face of the oriented stone is shown in Fig. 2.8b. The melt crust has flowed sluggishly around the edges but frozen before it could go far across the face.

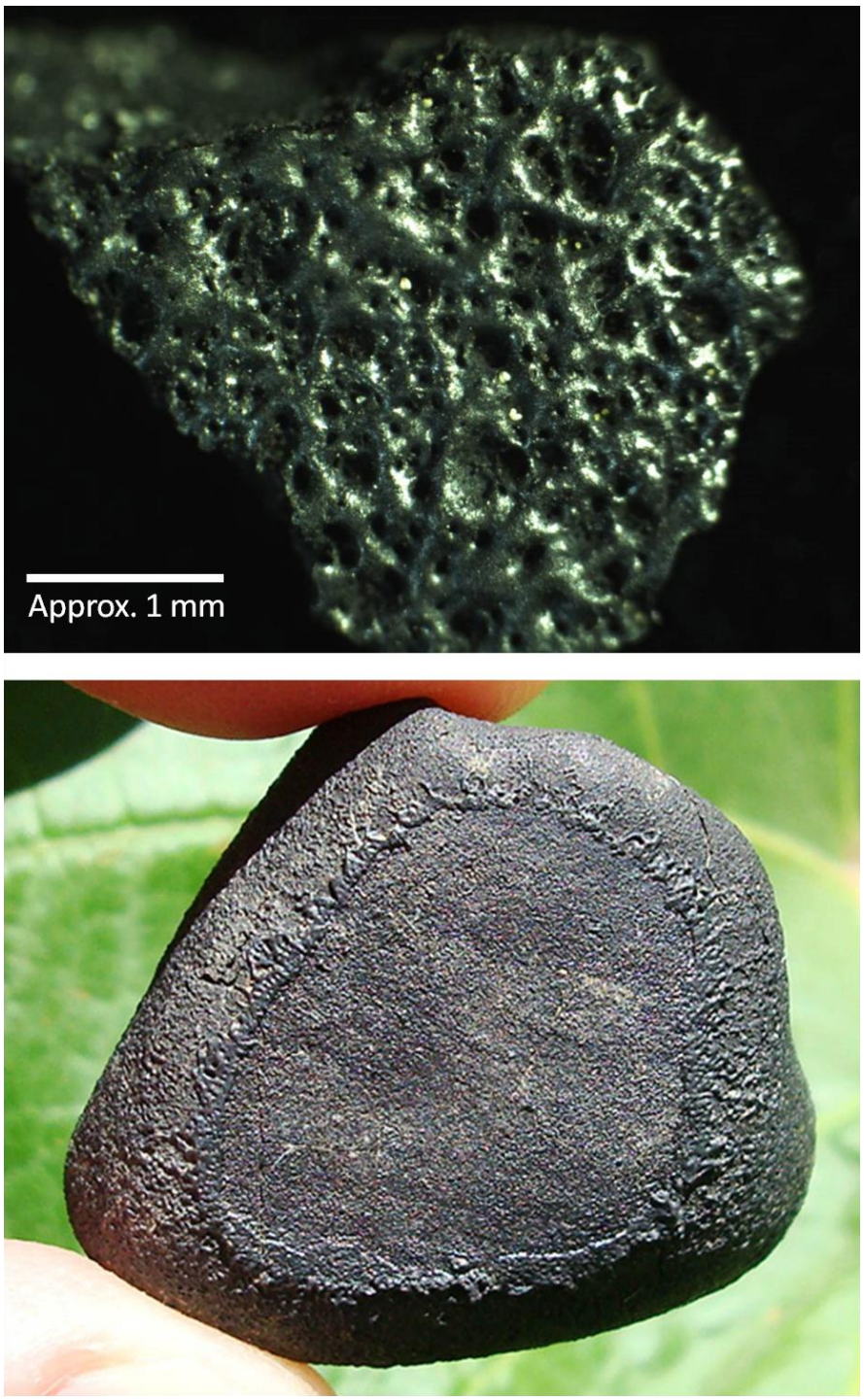

Figure 2.8. (a, above) *The fusion crust of the present stone showing a volatile-rich, viscous, melted surface that has frozen to produce a glassy coating.* ***(b, below)*** *Flow structures in the fusion crust of Sutter's Mill are generally minimal and poorly developed. Arguably the best flow structures identified to date are on this stone (SM64) found by Kieth Jenkerson (of KD meteorites). Apparently the stone was oriented during flight and the melted crust flowed around the sides where it froze before being able to move far onto the rear surface. Other images of this stone appear in color in Meteorite magazine for March 2013.*

2.6 Conclusions

Eight slices of the Sutter's Mill stone SM48 showed four distinct lithologies and an internal structure consistent with regolith breccia. These lithologies were light clasts, dark clast, matrix of intermediate darkness, and a single dark inclusion. The dark clasts appeared to be primary (unbrecciated) material, the visually homogenous light clasts were interpreted as heavily altered by comminution and/or aqueous alteration, while the matrix was a visibly comminuted mixture of the light and dark clasts with breccias-within-breccias. CT scans performed on other Sutter's Mill stones (Ebel and Hill, 2012) revealed a similar structure. In such a complicated mixture, involving considerable recycling and secondary alteration of components, neither lightening nor darkening may be considered a significant proxy for regolith maturity. We also note that cross-cutting of fine-grained rims at dark lithology clast boundaries constrains the timing of formation of these structures to the period prior to the fragmentation and entrainment of this lithology in the regolith environment.

We observe that SM48, like all Sutter's Mills stones, was oriented during flight and thick fusion crusts were produced on trailing faces of the stones. Numerous cracks in the stone, often along clast boundaries, illustrate the friability of this meteorite and were undoubtedly responsible for the fall consisting of a large number of small (centimeter-sized) stones. The thick fusion crust and contraction (dehydration) cracks suggest that the stones were heated enough for the loss of volatile organics and water during fall.

2.7 Acknowledgments

We are grateful to Jerri Stevens and Qynne Arnold for support with this work, Marlin Cilz (Montana Meteorite Laboratory) for cutting the stone, Peter Jenniskens SETI/NASA Ames Research Center) for organizing the Sutter's Mill research consortium, Alex Ruzicka, Melinda

Hutson, Knut Metzler, Linda Welzenbach and Hazel Sears for reviewing earlier versions of this paper, Hazel Sears also for proofing, and NASA and the University of Arkansas for conference travel support to communicate preliminary results.

2.8 References

Akridge D. G., Akridge J. M. C., Batchelor J. D., Benoit P. H., Brewer J., DeHart J. M., Keck B. D., Jie L., Meier A., Penrose M., Schneider D. M., Sears D. W. G., Symes S. J. K., Yanhong Z. 2004. Photomosaics of the cathodoluminescence of 60 sections of meteorites and lunar samples, *Journal of Geophysical Research* 109:E7.

Beauford R. E., Sears D. 2013. Timing of Fine-Grained Rim Formation in the Sutter's Mill CM Chondrite (abstract #1692) 44th Lunar and Planetary Science Conference.

Beauford R. E., Arnold S. K., Sears D. 2012. The Macrostructure of the Sutter's Mill Meteorite (abstract). *Meteoritics and Planetary Science* 48 (Suppl.):5091.pdf.

Beauford R. E., Arnold S. K., Sears D. 2013. The Macrostructure of the Sutter's Mill CM Chondrite Regolith Breccia (abstract #1683) 44th Lunar and Planetary Science Conference.

Beck P., Quirico E., Garenne A., Yin Q.-Z., Bonal L., Schmitt B., Montes-Hernandez G., Montagnac G., Chiriac R. and Toche F. 2014. The secondary history of Sutter's Mill CM carbonaceous chondrite based on water abundance and the structure of its organic matter from two clasts. *Meteoritics & Planetary Science*. doi: 10.1111/maps.12273

Benoit P. H., Sears D. W. G., Symes S. J. K. 1996. The thermal and radiation exposure history of lunar meteorites. *Meteoritics and Planetary Science* 31:869-875.

Bischoff A. 1998. Aqueous alteration of carbonaceous chondrites: Evidence for preaccretionary alteration — A review. *Meteoritics & Planetary Science* 33:1113–1122.

Bischoff A., Scott E. R. D., Metzler K., Goodrich C. A. 2006. Nature and origins of meteoritic breccias. In *Meteorites and the Early Solar System II*, edited by Lauretta D. S., McSween H. Y. Tucson, AZ: University of Arizona Press. pp. 679-712.

Bischoff A. and Schultz L. 2004. Abundance and meaning of regolith breccias among meteorites (abstract). *Meteoritics & Planetary Science* 39:A15.

Bland P. A., Howard L. E., Prior D. J., Wheeler J., Hough R. M. & Dyl K. A. 2011. Earliest rock fabric formed in the Solar System preserved in a chondrule rim. *Nature Geoscience* 4:244–247. doi:10.1038/ngeo1120.

Brearley A. J. 1993. Matrix and fine-grained rims in the unequilibrated CO3 chondrite, ALH A77307: Origins and evidence for diverse, primitive nebular dust components. *Geochimica et Cosmochimica Acta* 57:1521–1550.

Britt D. T., Yeomans D., Housen K., Consomagno G. 2002. Asteroid Density, Porosity, and Structure. In *Asteroids III*, edited by Bottke Jr. W. F., Cellino A., Paolicchi P., and Binzel R. P., Tucson, AZ: University of Arizona Press. pp. 485-500.

Britt D. T., Pieters C. M. 1994. Darkening in black and gas-rich ordinary chondrites: The spectral effects of opaque morphology and distribution. *Geochimica et Cosmochimica Act*a 58(18):3905-3919.

Browning L., McSween H., and Zolensky M. 1996. Correlated alteration effects in CM carbonaceous chondrites. *Geochimica et Cosmochimica Acta* 60:2621–2633.

Browning L., McSween H. Y. and Zolensky M. E. 2000. On the origin of rim textures surrounding anhydrous silicate grains in CM carbonaceous chondrites. *Meteoritics & Planetary Science* 35: 1015–1023. doi: 10.1111/j.1945-5100.2000.tb01489.x.

Burton A. S., Glavin D. P., Elsila J. E., Dworkin J. P., Jenniskens P. and Yin Q.-Z. 2014. The amino acid composition of the Sutter's Mill CM2 carbonaceous chondrite. *Meteoritics & Planetary Science*. doi: 10.1111/maps.12281

Chizmadia L. J., Xu Y., Schwappach C., and Brearley A. J. 2003. Insights into Fe,Ni metal survival in the hydrated fine-grained rims in the Y-791198 CM2 carbonaceous chondrite (abstract). *Meteoritics & Planetary Science* 38:A137.

Clark B.C., Hapke B., Pieters C., and Britt D. 2002. Asteroid space weathering and regolith evolution. In *Asteroids III* edited by Bottke W. F., Cellino A., Paolicchi P., and Binzel R. P., Tucson, Arizona, University of Arizona Press. pp. 585-599.

Delaney J. S. 1984. Why did so Many Polymict Eucrites Land and Survive Only in Antarctica? (abstract). 25th Lunar and Planetary Science.

Ebel D. S. and Hill M. 2012. Computed Tomography (CT) of five samples of the Sutter's Mill CM2 chondrite. American Museum of Natural History Research Library Supplemental Text for Jenniskens, P. and 69 coauthors. 2012. Radar-Enabled Recovery of the Sutter's Mill Meteorite, a Carbonaceous Chondrite Regolith Breccia. Science 21:338(6114):1583-1587.

Fries M., Le Corre L., Hankey M., Fries J., Matson R., Schaefer J. and Reddy V. 2014. Detection and rapid recovery of the Sutter's Mill meteorite fall as a model for future recoveries worldwide. *Meteoritics & Planetary Science*. doi: 10.1111/maps.12249

Greenwood R. C., Hutchison R., and Jones C. G. 1993. The Structure and Evolution of a CM2 Regolith: A Three-dimensional Study of Cold Bokkeveld. *Meteoritics* 28(3):357-358.

Greshake A., Krot A. N., Flynn G. J., and Keil K.. 2005. Fine-grained dust rims in the Tagish Lake carbonaceous chondrite: Evidence for parent body alteration. *Meteoritics & Planetary Science* 40:9:1413-1431

Hanowski N. P., Brearley A. J. 2001. Aqueous alteration of chondrules in the CM carbonaceous chondrite, Allan Hills 81002: implications for parent body alteration. *Geochimica et Cosmochimica Acta* 65:495-518.

Haq M., Hasan F. A., Sears D. W. G., Moore C. B., Lewis C. F. 1989. Thermoluminescence and the origin of the dark matrix of Fayetteville and similar meteorites. *Geochimica et Cosmochimica Acta* 53(6):1435-1440.

Heymann D. and Mazor E. 1967. Light-dark structure and rare gas content of the carbonaceous chondrite Nogoya. *Journal of Geophysical Research* 72:2704–2707.

Jenniskens P., Fries M. D., Yin Q., Zolensky M., Krot A. N., Sandford S. A., Sears D., Beauford R., Ebel D. S., Friedrich J. M., Nagashima K., Wimpenny J., Yamakawa A., Nishiizumi K., Hamajima Y., Caffee M. W., Welten K. C., Laubenstein M., Davis A. M., Simon S. B., Heck P. R., Young E. D., Kohl I. E., Thiemens M. H., Nunn M. H., Mikouchi T., Hagiya K., Ohsumi K., Cahill T. A., Lawton J. A., Barnes D., Steele A., Rochette P., Verosub K. L., Gattacceca J., Cooper G., Glavin D. P., Burton A. S., Dworkin J. P., Elsila J. E., Pizzarello S., Ogliore R., Schmitt-Kopplin P., Harir M., Hertkorn N., Verchovsky A., Grady M., Nagao K., Okazaki R., Takechi H., Hiroi T., Smith K., Silber E. A., Brown P. G., Albers J., Klotz D., Hankey M., Matson R., Fries J. A., Walker R. J., Puchtel I., Lee C-T. A., Erdman M. E., Eppich G. R., Roeske S., Gabelica Z., Lerche M., Nuevo M., Girten B., Worden S. P., and (the Sutter's Mill Meteorite Consortium). 2012. Radar-Enabled Recovery of the Sutter's Mill Meteorite, a Carbonaceous Chondrite Regolith Breccia. *Science* 21:338(6114):1583-1587.

Jenniskens P. 2014. The Sutter's Mill Fall. *Meteoritics & Planetary Science*. doi: 10.1111/maps.12343

Jilly C. E., Huss G. R., Krot A. N., Nagashima K., Yin Q.-Z. and Sugiura N. 2014. ^{53}Mn-^{53}Cr dating of aqueously formed carbonates in the CM2 lithology of the Sutter's Mill carbonaceous chondrite. *Meteoritics & Planetary Science*. doi: 10.1111/maps.12305

Kerridge J. F. and Bunch T. E. 1979. Aqueous alteration on asteroids: evidence from carbonaceous meteorites. In *Asteroids*, edited by Gehrels T. Tucson, AZ: University of Arizona Press. pp. 745-764.

Krot A. N., Petaev M. I., Meibom A. and Keil K. 2000. In situ growth of Ca-rich rims around Allende dark inclusions. *Geochemistry International* 38:S351–S368.

Lauretta D. S., Hua X., and Buseck P. R. 2000. Mineralogy of fine-grained rims in the ALH81002 CM chondrite. *Geochimica et Cosmochimica Acta* 64:3263–3273.

Lee M., Lindgren P., Sofe M., Alexander C., and Wang J. 2012 Extended chronologies of aqueous alteration in the CM2 carbonaceous chondrites: evidence from carbonates in Queen Alexandra Range 93005. *Geochimica et Cosmochimica Acta* 92:148-169.

McSween H. Y. 1979. Alteration in CM carbonaceous chondrites inferred from modal and chemical variations in matrix. *Geochimica et Cosmochimica Acta* 43(11):1761-1770.

Metzler K. & Bischoff A. 1987. Accretionary Dark Rims in CM Chondrites. *Meteoritics* 22:458.

Metzler K. Bischoff A. and Stöffler D. 1992. Accretionary dust mantles in CM chondrites: Evidence for solar nebula processes. *Geochimica et Cosmochimica Acta* 56:2873–2897.

Metzler K. 2004. Formation of accretionary dust mantles in the solar nebula: Evidence from preirradiated olivines in CM chondrites. *Meteoritics & Planetary Science* 39, 1307–1319.

Nakamura T., Nagao K., and Takaoka N. 1999a. Microdistribution of primordial noble gases in CM chondrites determined by in situ laser microprobe analysis: Decipherment of nebular processes. *Geochimica et Cosmochimica Acta* 63:241–255.

Nakamura T., Nagao K., Metzler K. and Takaoka N. 1999b. Heterogeneous distribution of solar and cosmogenic noble gases in CM chondrites and implications for the formation of CM parent bodies. *Geochimica et Cosmochimica Acta* 63:257–273.

Nishiizumi K., Caffee M. W., Hamajima Y., Reedy R. C. and Welten K. C. 2014. Exposure history of the Sutter's Mill carbonaceous chondrite. *Meteoritics & Planetary Science*. doi: 10.1111/maps.12297

Nuevo M., Sandford S. A., Flynn G. J. and Wirick S. 2014. Mid-infrared study of stones from the Sutter's Mill meteorite. *Meteoritics & Planetary Science*. doi: 10.1111/maps.12269

Pieters C. M. and Fischer E. M. 1993. Optical Effects of Space Weathering: The Role of the Finest Fraction. *Journal of Geophysical Research* 98:20,817-20,824.

Pizzarello S. and Garvie L. A. J. 2014. Sutter's Mill dicarboxylic acids as possible tracers of parent-body alteration processes. *Meteoritics & Planetary Science*. doi: 10.1111/maps.12264

Popova O., Borovicka J., Hartmann W. K., Spurny P., Gnos E., Nemtchinov I. and Trigo-Rodriguez J. M. 2011. Very low strengths of interplanetary meteoroids and small asteroids. *Meteoritics & Planetary Science* 46:1525–1550.

Rode O. D. and Lindstrom M. M. 1994. Luna 24 regolith breccias: A possible source of the fine size material of the Luna 24 regolith. 25th Lunar and Planetary Science Conference.

Rubin A. E., Trigo-Rodriguez J. M., Wasson J. T. 2005. A new aqueous alteration index for CM carbonaceous chondrites (abstract). *Meteoritics and Planetary Science* 40.

Rubin A. E., Trigo-Rodríguez J. M., Huber H., Wasson J. T. 2007. Progressive aqueous alteration of CM carbonaceous chondrites. *Geochimica et Cosmochimica Acta* 71(9):2361-2382.

Rubin A. E. and Wasson J. T. 1986. Chondrules in the Murray CM2 meteorite and compositional differences between CM-CO and ordinary chondrite chondrules. *Geochimica et Cosmochimica Acta* 50:307–315.

Schultz L. and Kruse H. 1989. Helium, neon, and argon in meteorites – a data compilation. *Meteoritics* 24:155–172.

Sears D. 2004. The Origin of Chondrules and Chondrites: Cambridge Planetary Science Series. Cambridge University Press.

Sears D. W. G., Jie L., and Benoit P. H. 1992. Chondrule rims in Murchison, cathodoluminescence evidence for in situ formation by aqueous alteration. *Meteoritics* 27:288.

Sears D. W. G., Benoit P. H., and Jie L. 1993. Two chondrule groups each with distinctive rims in Murchison recognized by cathodoluminescence. *Meteoritics* 28:669–675.

Sears D. W. and Beauford R. 2014. The Sutter's Mill meteorite: Thermoluminescence data on thermal and metamorphic history. *Meteoritics & Planetary Science*. doi: 10.1111/maps.12259

Takayama A. and Tomeoka K. 2012. Fine-grained rims surrounding chondrules in the Tagish Lake carbonaceous chondrite: Verification of their formation through parent-body processes. *Geochimica et Cosmochimica Acta* 98:1-18.

Tomeoka K. and Tanimura I. 2000. Phyllosilicate-rich chondrule rims in the Vigarano CV3 chondrite: Evidence for parent-body processes. *Geochimica et Cosmochimica Acta* 64:1971–1988.

Tomeoka K. and Ohnishi I. 2010. Indicators of parent-body processes: Hydrated chondrules and fine-grained rims in the Mokoia CV3 carbonaceous chondrite. *Geochimica et Cosmochimica Acta* 74:4438-4453.

Trigo-Rodriguez J. M., Rubin A. E., Wasson, J. T. 2006. Non-nebular origin of dark mantles around chondrules and inclusions in CM chondrites, *Geochimica et Cosmochimica Acta* 70(5):1271-1290.

Varela M. E., Zinner E., Kurat G., Chu H.-T., and Hoppe P. 2012. New insights into the formation of fayalitic olivine from Allende dark inclusions. *Meteoritics & Planetary Science* 47:832–852.

Zezin R. B. and Bazilevskiy A. T. 1972. Morphology of Lunar Rocks in the Region Transversed by Lunokhod I. *NASA Technical Translation F-14* 179 from *Priroda* 11:7-9.

Zega T. J. and Buseck P. R. 2003. Fine-grained-rim mineralogy of the Cold Bokkeveld CM chondrite. *Geochimica et Cosmochimica Acta* 67:1711–1721.

Zhao X., Lin Y., Yin Q.-Z., Zhang J., Hao J., Zolensky M. and Jenniskens P. 2014. Presolar grains in the CM2 chondrite Sutter's Mill. *Meteoritics & Planetary Science*. doi: 10.1111/maps.12289

Zolensky M., Barrett R., Browning L. 1993. Mineralogy and composition of matrix and chondrule rims in carbonaceous chondrites. *Geochimica et Cosmochimica Acta* 57(13):3123-3148.

Chapter 3 Origin of concretions in the proposed Weaubleau impact structure, Missouri, USA

3.1 Abstract

The Weaubleau structure is a partially exposed, latest Osagean or early Meramecian (about 340 to 335 Ma), 7-8 km shallow-marine probable impact crater located beneath and south of the town of Vista, in southeastern St. Clair County, Missouri. Evidence supporting an impact origin includes abundant planar fractures (PFs) and planar deformation features (PDFs) common in quartz grains in localized deposits interpreted as resurge breccias. Weaubleau 'round rocks' are unusually spherical nucleated nodular concretions formed by silicification of carbonates surrounding nuclei composed of well-rounded pebble to cobble sized friable masses of extremely fine-grained silica. These locally popular concretions are uniquely formed in, and weather from, breccia associated with the Weaubleau structure. They accumulate in significant numbers on the surface due to substantially lower vulnerability to mechanical and chemical weathering than the surrounding carbonate matrix. This paper reviews the history of research at this location to date in some depth, in order to clarify and resolve past confusion regarding the name and scale of the structure, summarizes evidence for an impact origin, and looks in some detail at the petrology and origin of the unusual spherical concretions associated with the structure.

3.2 Introduction

3.2.1 Weaubleau round rocks

In simplest terms, Weaubleau round rocks (or eggs) are nearly spherical rocks that typically range from less than 5 cm to a little over 20 cm in diameter, or from about the size of a

golf ball to that of a bowling ball. Typical examples are about the size and shape of a baseball, or about 7-8 cm in diameter. (see Fig. 3.1) They are found in great abundance in the fields, along the dirt roads, and in streambeds extending north and south of the community of Vista, Missouri, and unevenly outward in the area between the nearby towns of Weaubleau and Osceola. The round rocks are comparatively resistant to chemical and mechanical weathering, and are found in great abundance in areas where localized erosion and sorting processes concentrate them. This study has aimed at describing Weaubleau round rocks, determining what they are, why they exist, and establishing if and how they are associated with impact processes and the Weaubleau structure.

Figure 3.1. *'Weaubleau round rocks' are nearly spherical concretions, ranging from less than 5 cm to a little over 20 cm in diameter. Most examples are about the size and shape of a baseball or about 7-8 cm in diameter. The concretions are comparatively resistant to mechanical and chemical weathering, and are concentrated in large numbers on eroded surfaces. The ones shown here were gathered within one minute, with little effort, in a creek bed.*

3.2.2 The Weaubleau structure, summary of previous literature

The Weaubleau Structure is an approximately 7 to 8 km in diameter disturbance showing significant evidence of a marine impact origin (Dulin and Elmore, 2008; Miller et al., 2008). It is roughly centered at approximately 37°58'N 93°40'W (Finn et al., 2012). A lobe of structurally disturbed terrain extends unevenly to a radius possibly as great as 11 km beyond the probable crater rim towards the east and northeast, producing an overall region of intense disturbance spanning as much as 19km (Evans et al., 2003c; Dulin and Elmore, 2008; Miller et al., 2008; Finn et al., 2012). The adjacent disturbance is expressed and preserved to a lesser extent in other directions as well (Evans et al., 2003c; Miller et al., 2008). An impact producing a 7 to 8 km structure in sedimentary rock should form a complex crater with a central uplift. Though the boundary of a solid central uplift has not yet been clearly delineated, Precambrian granite clasts were encountered in shallow drilling within the structure, reported in Miller et al. (2008) (MoDOT-SMSU-Vista 1 core) and the bottom 6.5 meters of drilling stopped in an aggregated granite mass beginning 69 meters below the surface. This mass was located 350 to 400 meters above its ordinary stratigraphic setting. Miller et al. (2008) also report Ordovician and Late Devonian conodonts from deeper deposits mixed in the surface breccia in addition to lower and middle Mississippian forms.

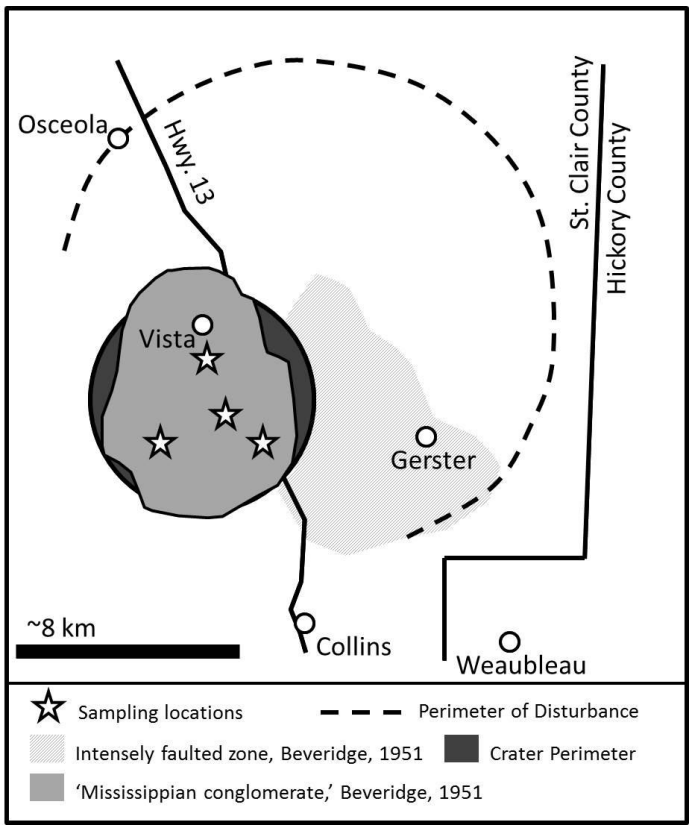

Figure 3.2. *This map relates early descriptions of 'Mississippian conglomerate' and adjacent folding and faulting as mapped by Beveridge, (1951) with a general current understanding of the probable perimeter of the structure and adjacent region of disturbance based on Evans et al. (2003c), Miller et al. (2008), Finn et al. (2012), and others.*

The directional lobe of displaced material can be very generally characterized as a sporadically preserved and sporadically exposed region of megabreccias and abruptly displaced and folded strata, typically less than 50 meters thick, overlain by a lens of polymict breccia less than 10 meters thick. The top of the latter is heavily weathered, and likely does not reflect an accurate thickness. This disturbed area has been visually described by some researchers as a 'train wreck,' when viewed in cut walls, due to the appearance of massive colliding blocks which are folded, tilted, skewed, and overridden by adjacent blocks as if they were pushed laterally, one into the next. This region is interpreted as proximal ejecta and deformation defining a zone of contiguously mobilized rocks on the crater perimeter. The region has presented difficulties in interpreting a boundary for the structure. Figure 3.2 illustrates the zones of breccia and structural

disturbance originally mapped by Beveridge (1951) in context with an approximation of the structure's possible perimeter based on current best evidence, and the general extent of the adjacent irregularly preserved zone of disturbance (Finn et al., 2012; Miller et al., 2008).

A hypervelocity impact origin for the structure is strongly suggested by multiple sets of planar fractures (PFs) and apparent planar deformation features (PDFs) in quartz grains. Both types of structure are relatively common in associated breccias and are readily observable in thin section, making up, in some instances, substantially greater than 1% of quartz grains. (see Fig. 3.3) Miller et al. (2008), report shock features in up to 10% of quartz grains in insoluble residues. The 7-8 km roughly circular region in which shocked quartz-bearing polymict breccias and clast bearing sediments are found roughly corresponds to the original published report of disturbance in the region, an area of 'Mississippian conglomerate,' mapped by Beveridge in 1951 (see Fig. 3.2). This region is known to later authors as the resurge facies of the Weaubleau Breccia (Miller et al., 2008). Drilling within the crater has produced polymict breccia to substantial depth. The age of the structure has been exceptionally well constrained stratigraphically and biostratigraphically (Miller et al., 2008) and through paleomagnetism (Elmore and Dulin, 2007; Dulin and Elmore, 2008) to the mid-Mississippian, latest Osagean or early Meramecian, or about 335 to 340 Ma.

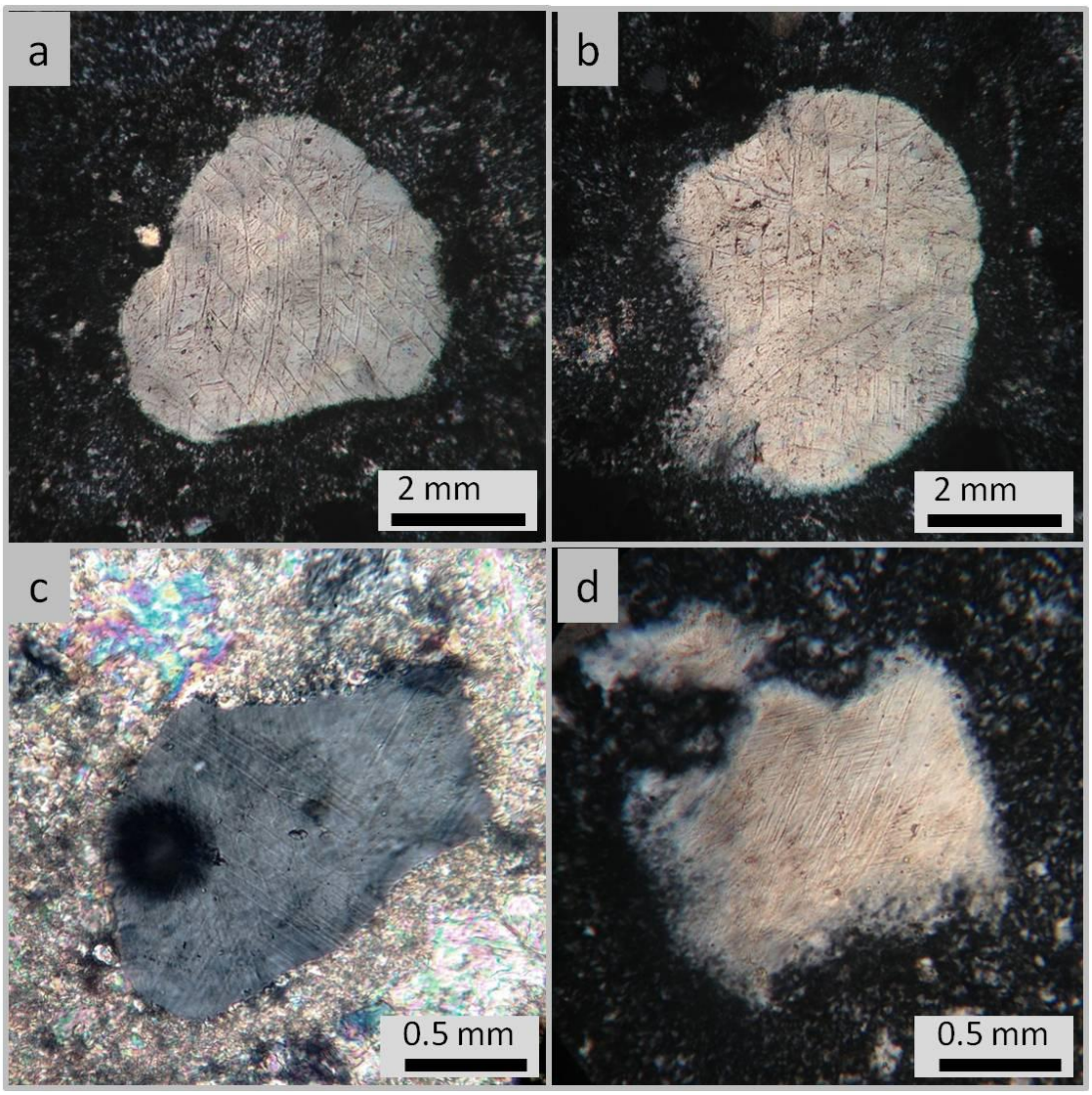

Figure 3.3. *PFs and PDF examples within quartz grains in thin sections produced for this study. 3.3a and 3.3b show at least three sets of planar fractures in quartz. 3.3c and 3.3d show two to three sets of planar deformation features in quartz. The large, dark circle in c is a bubble.*

3.2.3 History of research on the Weaubleau impact structure

An unusual 'Mississippian conglomerate,' associated with a substantial stratigraphic disturbance in the area of the Weaubleau Creek, Missouri, was first noted in the literature in the work of Beveridge (1949, 1951). Abruptly faulted, folded and displaced rock units, "unresolvably" complex stratigraphic disruptions and enormous quantities of breccia and clast bearing sediment have lingered unresolved. Tentative explanations for the disturbance have

included, among many others, intensive and chaotic localized thrust faulting (Beveridge, 1951), cryptovolcanism (Snyder and Gerdemann, 1965), a chain meteorite impact (Rampino and Volk, 1996), and more recently, a specific, increasingly well constrained crater forming impact event, addressed in many abstracts and articles as summarized below. The Rampino and Volk (1996) article, mentioned above, seems to be the first time that an impact origin was proposed for the structure, but the speculation involved no fieldwork at the location, and diagnostic indicators of hypervelocity impact were not discussed. A 'Weaubleau Structure' mentioned in Bretz (1950) is unrelated.

The Weaubleau Crater is not, at this writing, listed as a recognized impact crater in the Earth Impact Database (2014) or in the Meteoritical Bulletin Database. It is listed in the Impact Database (Rajmon, 2009) as a class 2, or 'probable' impact structure. Detailed treatment of both suggestive and unambiguous evidence of impact origin, though presented in abstract, is needed in peer reviewed context. Existing mention in peer reviewed literature is sparse; Beveridge (1951) described the geology of the Weaubleau 7.5-minute quadrangle and adjoining swaths to the west and north, and he noted chaotic faulting and associated breccia. Cox and Evans (2007a; Cox 2008) mapped the geology of the Vista 7.5-minute quadrangle. Elmore and Dulin (2007) and Dulin and Elmore (2008) addressed timing of the disturbance event, and Finn et al. (2012) examine digital elevation models of the location within a regional context. Miller et al. (2008) provides the most detailed description yet published, addressing biostratigraphic evidence of timing and briefly discussing the structure in general. Snyder and Gerdeman (1965) and Rampino and Volk (1996) also mention the location in journal articles, but only obliquely to the topic of their inquiry. In addition to these primary publications, the impact structure has been the subject of, at minimum, 38 published posters or conference abstracts, summarized below, and

four conference-related field trip guidebooks (Evans et al., 2003c; Evans et al., 2005a; Miller and Evans, 2007; Evans and Miller, 2010).

3.2.4 Abstracts relating to the structure

The impact hypothesis presented by Rampino and Volk (1996) began gaining substance with a series of abstracts published in 2003 (Evans et al, 2003a,b and Rovey et al., 2003). Subsequent abstracts have clarified the structure's size, morphology and location (Stockdell et al., 2004; Davis, 2005; Mickus et al., 2005; Cox et al., 2006, 2007; Evans, 2007; Finn et al., 2007; Shoberg and Stoddard, 2007; Evans and Mickus, 2008; Evans et al., 2012), the paleoenvironments of impact (Evans 2005b; Evans et al., 2006a) impact angle (Rovey et al., 2003) (Evans et al., 2004) (Evans and Mickus, 2008), the age of the structure (Dulin et al., 2004a and 2004b; Davis et al., 2005; Dulin et al., 2005a,b; Dulin and Elmore, 2005,2006; Miller et al. 2005a,b, 2006, 2007, 2010; Evans et al., 2011), its relationship to other regional structures (Miao et al., 2007; Evans et al., 2008) and its petrographic and lithologic record and context (Evans et al., 2006b; Steadman, 2007; Morrow and Evans, 2007; Lemons, 2008; Evans et al., 2010; Moon et al., 2010). The earliest unambiguous evidence of a hypervelocity impact was presented in an abstract by Evans et al., (2003b), which described and included photographs of planar deformation features (PDFs) in quartz. These were indexed in an abstract and poster by Morrow and Evans (2007). The numerous abstracts are listed above in order to provide a clearer foothold on the literature for future investigators and summarized in Table 3.1 in order to prevent confusion that could result from changes in understanding of the crater's dimensions and resulting changes in naming that occurred as research progressed. The table traces the evolution of understanding of the crater boundary and age, along with associated changes in naming, as

reflected in descriptions in both abstracts and peer-reviewed papers in the many decades since the structure's first description.

Table 3.1 Abstracts and juried publications concerning the Weaubleau structure.

Publication	Name	Size	Age
Beveridge, 1951	**unspecified**	**~4x5km conglomerate with adjacent faulting**	**Up to end of Osagean**
Snyder and Gerdeman, 1965	**Weaubleau structure/ Weaubleau fault zone**	**~4x5 km with adjacent faulting**	**Pre-Pennsylvanian**
McCracken, 1966	Weaubleau Creek Structure	-	-
Rampino and Volk, 1996	**Weaubleau Structure**	**-**	**Late Mississippian to Early Pennsylvanian**
Evans et al., 2003a	Weaubleau Structure	19 km	Osagean to Atokan
Evans et al., 2003b	Weaubleau-Osceola Structure	19 km	Terminal Osagean
Evans et al., 2003c	Weaubleau-Osceola Structure	19 km	Osagean to Atokan
Rovey et al., 2003	Weaubleau-Osceola Structure	27 km	Latest Osagean to Atokan
Stockdell et al., 2004	Weaubleau-Osceola Impact Structure	7 km eccentric to larger	-
Dulin et al., 2004a	Weaubleau-Osceola Impact Structure	19 km	Post-Osagean and pre-Desmoinesian
Evans et al., 2004	Weaubleau-Osceola Structure	7 km eccentric to 19 km	Middle to Late Mississippian
Dulin et al., 2004b	Weaubleau-Osceola Structure	19 km	Post-Osagean to pre-Desmoinesian
Evans et al., 2005a	Weaubleau-Osceola Structure	~8 km eccentric to 19 km	Latest Osagean or Earliest Meramecian
Davis et al., 2005	Weaubleau-Osceola Structure	-	Latest Osagean
Evans et al., 2005b	Weaubleau-Osceola Structure	9km eccentric to 19km	-
Mickus et al., 2005	Weaubleau-Osceola Structure	-	Late-Paleozoic
Miller et al., 2005a	Weaubleau-Osceola Structure	-	Latest Osagean to early Meramecian
Dulin and Elmore, 2005	Weaubleau-Osceola Impact Structure	-	Post-Osagean Mississippian
Dulin et al., 2005a	Weaubleau-Osceola	-	-
Dulin et al., 2005b	Weaubleau-Osceola Structure	-	Mississippian
Davis, 2005	Weaubleau-Osceola Impact Structure	-	-
Miller et al., 2005b	Weaubleau Structure	8 km	Latest Osagean to early Meramecian
Cox et al., 2006	Weaubleau Structure	11 km	Unspecified
Evans et al., 2006	Weaubleau Structure	8 km	Pre-Meramecian
Miller et al., 2006	Weaubleau Structure	-	Late Osagean to lower Meramecian
Dulin and Elmore, 2006	Weaubleau-Osceola Structure	-	-
Elmore and Dulin, 2007	**Weaubleau Structure / Weaubleau Feature**	**19 km**	**Late Mississippian**
Cox et al., 2007	Weaubleau Structure	-	-
Evans, 2007	Weaubleau Structure	-	-
Finn et al., 2007	Weaubleau Disturbance	-	-
Dulin and Elmore, 2008	**Weaubleau Structure**	**8 km eccentric to 19 km**	**Late Mississippian**
Shoberg and Stoddard, 2007	Weaubleau-Osceola Structure	19 km	-
Steadman, 2007	Weaubleau-Osceola Impact Structure	-	-
Miller et al., 2007	Weaubleau structure	-	Latest Osagean to earliest Meramecian
Morrow and Evans, 2007	Weaubleau Structure	9 km eccentric to 18 km	Late Osagean to early Meramecian
Miao et al., 2007	Weaubleau Structure	-	-
Evans and Mickus, 2008	Weaubleau Structure	-	-
Miller et al., 2008	**Weaubleau Structure**	**11 km eccentric to 19km**	**Latest Osagean to Earliest Meramecian**
Evans et al., 2008	Weaubleau Structure	-	Latest Osagean to earliest Meramecian
Lemons, 2008	Weaubleau-Osceola Structure	-	-
Evans et al., 2010	Weaubleau Structure	-	Latest Osagean to Earliest Meramecian
Miller et al., 2010	Weaubleau Impact Structure	8 km	Osagean-Meramecian Boundary
Moon et al., 2010	Weaubleau Structure	8km eccentric to 19km	Latest Osagean to earliest Meramecian
Evans et al., 2011	Weaubleau Structure	-	Latest Osagean to Earliest Meramecian
Evans et al., 2012	Weaubleau Impact Structure	8 km eccentric to 19 km fan	Latest Osagean to earliest Meramecian
Finn et al., 2012	**Weaubleau Structure**	**ring eccentric to 18km**	**-**

Table 3.1 *A bibliography traces the evolution of understanding of the structure's boundary and age, along with associated changes in naming, as reflected in descriptions in both abstracts and peer-reviewed papers published in the several decades since the structure was first observed in publication.*

3.2.5 Previous mention of round rocks

The spherical chert concretions found at Weaubleau were first mentioned by Beveridge, who described chert 'cannon balls' within his Mississippian conglomerate. Miller et al. (2008) took a closer look, associating 'Weaubleau eggs' with the same rock unit, now the informally named 'Weaubleau breccia,' an informal name that has been used to collectively refer to the breccias associated with the Weaubleau structure. They observe that the spheres uniquely originate in these breccias and describe them as chert nodules with central clasts of mudstone or dolomite. The authors propose two tentative mechanisms for formation: 1) accretion of breccia around sticky mud clasts in an immediately post-impact environment, followed by later diagenetic replacement by silica, or 2) pre-Pennsylvanian formation through localized concentration of silica around clasts of suitable chemistry. They favored the latter concretionary, diagenetic interpretation.

3.3 Methods and investigation

Several trips were made to the region south of Vista, Missouri, with the objectives of identifying the rock unit from which 'Weaubleau round rock' concretions originate, collecting samples, and identifying whether the concretions occur in rock units other than the Weaubleau breccia. Individual concretions and concretions within matrix were collected at 3 locations, along with masses of host rock. Over 50 kg of rock was sectioned in 1 to 3 cm slices on a lapidary saw in order to reveal internal structure and to locate enclosed concretions in order to enable examination of the concretion to host-rock boundary, as well as to understand changes in concretions that might have resulted from exposure to direct weathering. Fifty-seven of the Weaubleau concretions were measured to the extent possible and halved, and 17 thin sections

were prepared for evaluation. Samples for sectioning were chosen specifically to reveal the nuclei of the concretions, the boundary between the nuclei and surrounding concretion, the boundary between the concretion and surrounding host rock, and the host rock itself, the Weaubleau breccia in which the concretions occur. Nucleus material was examined with a scanning electron microscope and characterized by X-Ray diffraction. Nucleus samples were also disaggregated and picked for microfossils and larger grains beneath a dissection scope for hints to origin. Several concretions from which nucleus material had been removed were then used as molding negatives to produce latex casts of the nuclei as additional clues to the original nature of the nucleating material.

3.4 Observations

3.4.1 Observations during fieldwork

No circular structure is immediately visible in Google Earth images or readily discernible in the paths of mapped roads or streams in the area south of Vista, and topsoil badly impedes ground-level investigation on flat uplands and bottomlands. A topographic feature is present, however, as revealed by Cox and Evans (2007) and Finn et al. (2012), who identified an associated circular structure roughly corresponding to the breccia unit in high resolution DEMs, and by Miller et al. (2008), who observe an associated ring shape structure in space shuttle images. On foot, the region of disturbance can be more-or-less clearly delineated in sparse outcroppings, stream beds and bar ditches by exposures of megabreccias or by an abrupt transition to a dominant surface lithology comprised of a grainy, matrix-supported breccia containing abundant fossils, fossil fragments, and angular sub-cm to cm-scale lithoclasts of dolostone, chert, sandstone and mudstone. This rock unit is equivalent to Beveridge's

Mississippian conglomerate, and has been more recently interpreted as a resurge breccia (Miller et al., 2008)**,** meaning a crater filling breccia associated with sediment-gravity flows, crater modification, and wave action in an immediately post-impact marine environment. The region is somewhat topographically subdued compared to the surrounding erosionally dissected surface of this portion of the Ozark plateaus. A few steep hills and ravines express vertical reliefs on the order of 10 to 20 meters, and overall topographical relief across the structure ranges up to 70 meters (Finn et al., 2012).

3.4.2 Host rock - the Weaubleau breccia

The Weaubleau breccia (see Fig. 3.5) was first observed and described in Beveridge (1951) as a 'Mississippian conglomerate.' The unit was discussed at length in Miller et al. (2008). Mississippian fossils and fossil fragment, predominantly crinoid sections, are pervasive and well preserved. Abundant lithoclasts typically measure <5 cm, and show no significant rounding. In field observation with a 10x loupe, the interclast supporting matrix reveals distinct individual mineral grains within carbonate mudstone or micrite. The surface-exposed Weaubleau breccia preserves no indications of proximate clasts that appear to share pre-fracture surfaces or that otherwise appear to have originated from localized fragmentation of larger clasts. Clasts are also widely heterogenous in composition. Fine matrix-rich and coarse grain-rich layers of comminution material within the generally massive deposit suggest that the resurge breccia may either have been reworked or deposited in successive episodes of washing or debris flows from the presumed crater's ejection rim. Descriptions of variation in composition and clast size with depth, revealed during drilling and discussed in Miller et al. (2008), suggest a complete sequence of collapse and fallback breccia may be present.

Figure 3.4. *Concretion in matrix. Marker for scale. Silicified concretions are more resistant to both chemical and mechanical weathering, and are selectively preserved at the surface as surrounding carbonates erode away.*

3.4.3 The Weaubleau breccia in thin section

The resurge or uppermost facies of the Weaubleau Breccia, as represented in surface exposures, is dominantly a fossiliferous wackestone unit, with diverse (though dominantly carbonate) lithoclasts and bioclasts typically comprising significantly greater than 30% of volume. What appears macroscopically to be a homogenous matrix is revealed in thins section to be significantly composed of angular comminuted carbonate microclasts. Larger angular lithoclasts of dolostone, sandstone, shale and chert are common, as are rounded intact and fractured quartz grains. Crinoid, bryozoan and brachiopod fossils, frequently fragmented, are abundant. Quartz grains with PFs and PDFs, frequently displaying pronounced mosaicism, are abundant in the breccia. Grain sizes range from fine sand to granules. The larger grains are

likely derived from the Cambrian Lamotte Sandstone, the basal siliciclastic unit across Missouri. Though visibly shocked quartz grains (PFs or PDFs) comprise a minority of quartz grains in the unit, none of the 17 prepared thin sections were without at least several clear examples. (see Fig. 3.8b and 3.8d)

3.4.4 Concretions and host rock

One cannot do fieldwork in the area without observing samples of the Weaubleau round rock concretions preserved as free-floating cobbles in top soil, creek beds, and other erosional lows. A modest effort more specifically reveals these concretions to uniquely originate within the Weaubleau breccia (see Fig. 3.4 and Fig. 3.5). Equivalent concretions were not found in any of the surrounding undisturbed Cherokee Group Pennsylvanian sandstone or Mississippian Burlington-Keokuk Limestone exposures with the exception of two examples found within the Cherokee Group Greydon Conglomerate. We believe these were entrained in the conglomerate after weathering of nearby exposures of the Weaubleau Breccia. The findings of Miller et al. (2008) agree with these assessments.

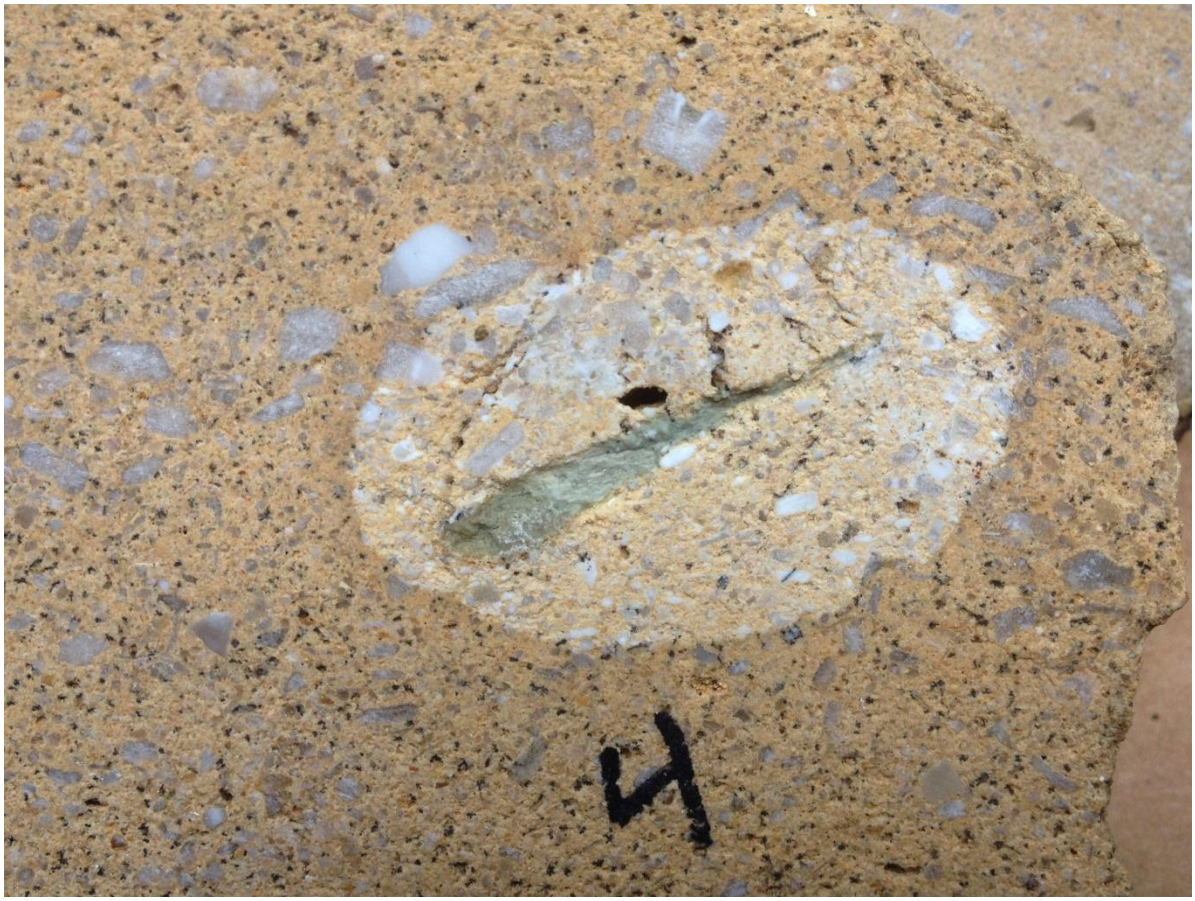

Figure 3.5. *A Weaubleau concretion revealed within its host rock. Examination in thin section reveals the lighter region forming the body of the sub-spherical concretion to be composed largely of chert, formed by silicification (replacement by silica) of the carbonate dominated surface exposure of the 'Weaubleau breccia' host rock. A crisp inner boundary surrounds the nucleating clast around which the concretion formed, while the outer boundary is revealed in thin section to be quite irregular at a microscopic scale, often capturing clasts of carbonate host rock material that were incompletely altered when growth of the concretion ceased. The largest dimension of the concretion shown is 4 cm. The '4' written on the sample is a record keeping mark.*

Fifty four samples of Weaubleau round rocks, gathered from three separate locations within the bounds of the outcropping rock unit, were halved using a lapidary saw. A significant amount of host rock was also sectioned in the hope of finding examples with an unaltered exterior boundary. This effort produced three additional examples, bringing the total studied samples to 57. A few very small examples of incompletely encircled nuclei were also exposed during sectioning of host rock. These were noted, but not further evaluated. Prior to cutting, 51

complete examples were measured in shortest and longest dimensions. Evaluated examples ranged from 3.8 to 16.3 cm in largest dimension. Both large and small examples were comparatively scarce, with most examples falling between 5 and 12 cm. Examples larger than 16 cm are particularly uncommon, with scarcity increasing rapidly with increasing size beyond this. The concretions are well-rounded to subspherical, tending to the oblate or slightly oblong. The average difference between minimum and maximum dimension of the subspherical concretions was only about 22% of the maximum dimension, with no difference exceeding 40%, and only two examples were identical to less than 0.1 cm in both dimensions, meaning most of the concretions are pretty close to spherical, but none are really spheres. Figure 3.1 illustrates a typical assortment.

All of the cut samples revealed a similar internal structure. A loosely cemented to friable nucleus of light-colored, silt-sized particles of silica filled a void with an irregular and sub-rounded shape. The nucleus material had the consistency and general appearance of packed clay. It was surrounded by a more well-rounded cherty concretion. All nuclei appeared to be of similar composition, but varied slightly in structural competence and color. Upon initial examination of hand samples, the nuclei were mistaken for clay or shale. The fine powder is loosely consolidated in some specimens, and was occasionally disaggregated and washed away during sawing. It formed a clay-like paste when wet, but with less plasticity than common sedimentary clays. Upon closer examination by SEM fitted with EDS, the nuclei were revealed to be comprised of an unconsolidated to lightly indurated microcrystalline silica powder. (see Fig. 3.6) Curiosity regarding whether this material might be related in composition and origin to coesite-bearing crushed quartz described at Barringer or Odessa, led to 3 nucleus samples being sent for XRD evaluation and interpretation by an independent lab, Corpuscular, Inc. The

resulting report showed the nuclei to contain only microcrystalline ordinary (alpha) quartz with a minor and variable montmorillonite clay component. The material shows no indication of a coesite or stishovite fraction.

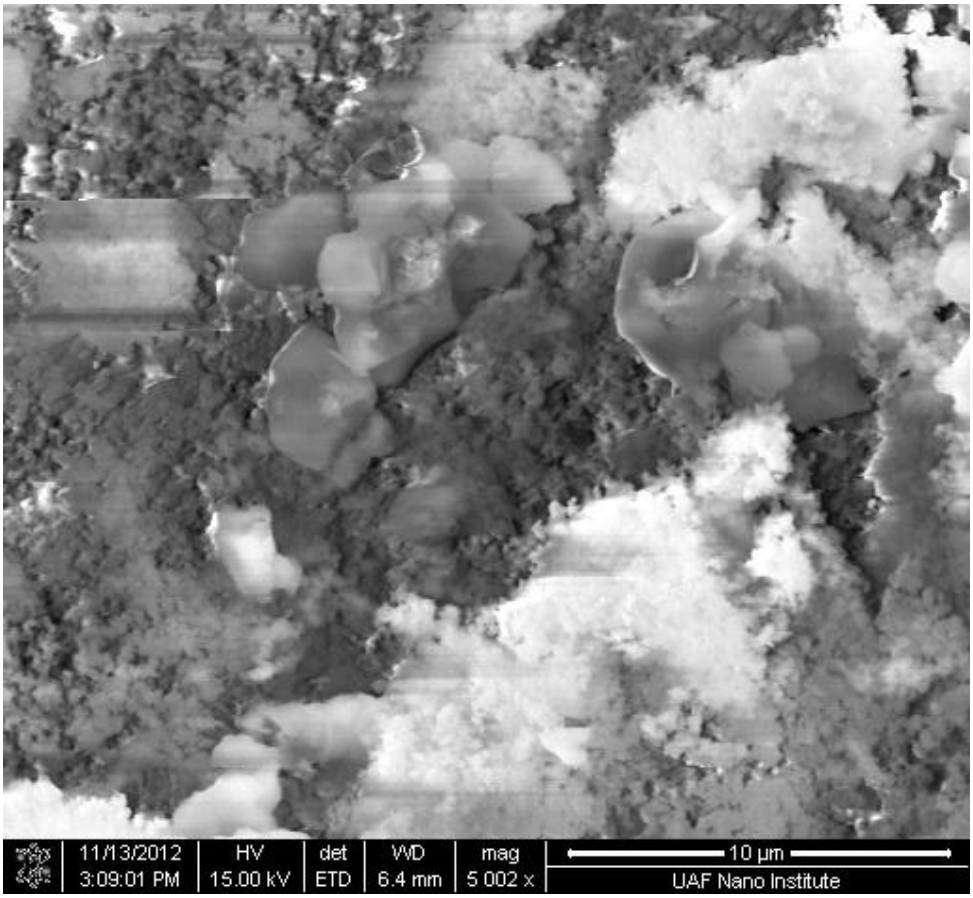

Fig. 3.6. *An SEM image of the friable silica that forms the nuclei of the concretions illustrates the extremely small grain size of the material, which gives rise to its flour or clay-like consistency when disaggregated.*

The spherical to sub-spherical concretions make up a very small percentage of the volume of the Weaubleau breccia host rock, but accumulate in great numbers on the surface due to their resistance to weathering and erosion. This is certainly the result of the differential between the vulnerability of silica versus hosting carbonates to chemical erosion. A meaningful estimate of overall volume of the Weaubleau Breccia host rock that is comprised of concretions

was not possible, and appeared to vary from point to point, but the figure is estimated to be far less than 0.1% by volume.

The host rock contains abundant angular lithoclasts, representing many different lithologies, but concretions appear to be formed around only one comparatively scarce type of clast. These were the only significantly rounded lithoclasts observed in this study, and no angular examples of these clasts were observed in surface exposed breccia or in slabbed samples. To state this more clearly; the nuclei of the concretions are the only evident rounded clasts in the breccia, and no broken or angular examples of the nucleus material are found.

3.4.5 Concretions in thin section

Nuclei in sections - When stabilized and viewed in thin section, the nuclei of the concretions revealed microcrystalline quartz containing no visible lithoclasts, fossil fragments or larger mineral grains. The presence of what appeared to be sporadic and minor FeOH mineral components in sections of some nuclei, along with variation in clay content revealed in XRD analysis (see Fig. 3.9) likely explains slight differences in color of the nuclei, ranging from light grey to yellowish, when viewed in hand samples. Beyond these minor variations, all nucleus material appeared similar or identical in composition, falling well within the range seen in the left side of figures 3.7a and 3.7c.

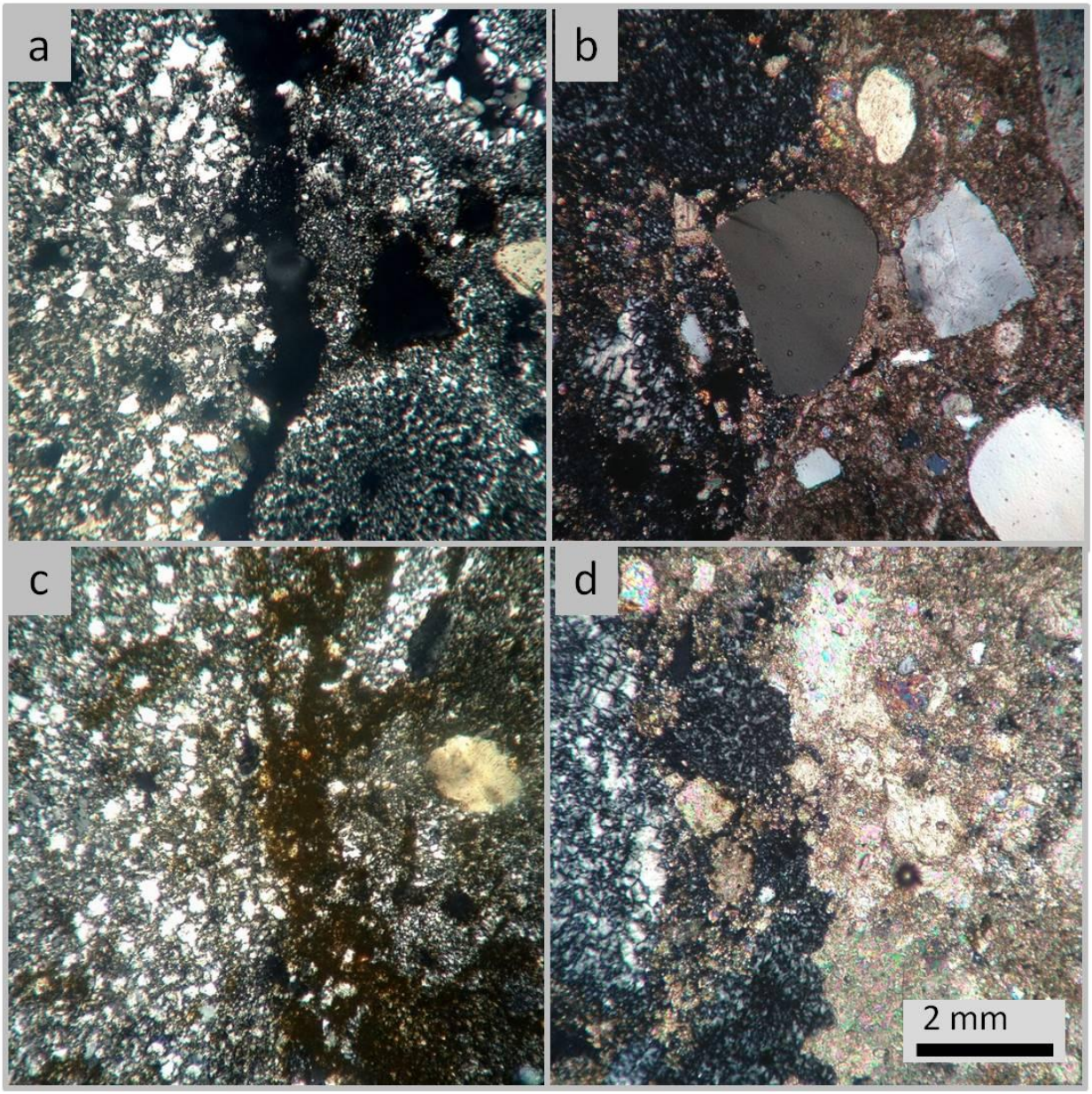

Figure 3.7. *From left to right: nucleus, body of the concretion, host rock. The images on the left show the boundary between the nucleus and concretion, and the images on the right show the boundary between the concretion and host rock. More specifically, the left sides of 3.7a and 3.7c illustrate the nucleus material and the right side of 3.7a and 3.7c illustrates the silicified mass of the concretion. The boundary between nucleus and concretion vertically bisects both images. The left side of 3.7b and 3.7d continues the silicified mass of the concretion, while the right side of 3.7b and 3.7d shows the unaltered carbonate dominated host rock. The less uniform boundary between the chert and chalcedony-replaced mass of the concretions and less altered carbonate host rock in which they occur vertically bisects 3.7b and 3.7d. Thin sections, XPL.*

The nucleus-concretion boundary marks a transition between relatively homogenous uncemented microcrystalline quartz in the nucleus versus a surrounding region of silica-replaced carbonate (chert) trapping abundant quartz grains and lithoclasts. Silicification appears to have completely replaced carbonate lithoclasts and bioclasts within the concretions, while frequently preserving the ghosts of the original structures. The boundary between the nucleus and surrounding silicified bulk of the concretion is consistently clear and distinct. It is frequently marked by a thin zone of FeOH mineralization (see left side of Fig. 3.7c), or by a narrow void (see left side of Fig. 3.7a), which may originate during cutting. No mineral grains or bioclasts span this boundary, and no bioclasts or lithoclasts occur within, impress, or intrude upon the nucleus material. The bulk of the spherical concretions is represented by a zone in which silica has nearly completely replaced originally carbonate fossils and lithoclasts (see right side of Figs 3.7a, 3.7c, left sides of Figs 3.7b, 3.7d, and all of Figs. 3.8a and 3.8c). Quartz grains are captured within this silicified zone in states ranging from unaltered to showing slight dissolution of the grain surface (see Fig. 3.3a, b, d for examples of grain surface erosion). While boundaries and detailed structures of carbonate lithoclasts and bioclasts are sometimes obscured within the silicified bulk of the concretions, general shapes are preserved, and sporadic incomplete replacement reveals original composition. A substantial percentage of quartz grains contained within the concretions and in the surrounding matrix contain PFs and PDFs or exhibit pronounced mosaicism. Concretion nuclei contain none of these.

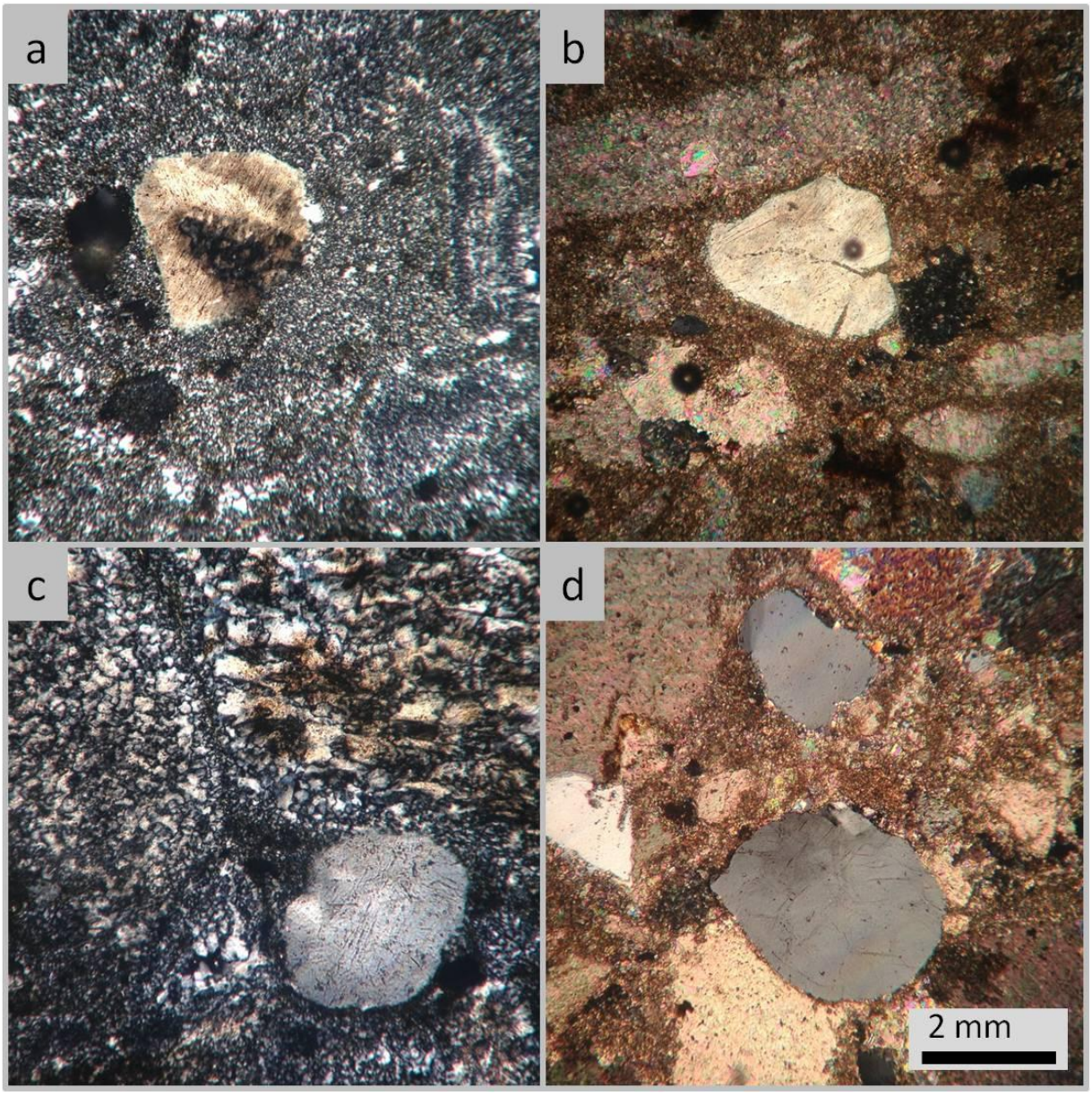

Figue 3.8. *The left side, 3.8a and 3.8c, illustrates the bulk of the concretion mass. Chert and chalcedony growths have replaced carbonate bioclasts and lithoclasts and have trapped individual quartz grains, some of which show significant evidence of shock alteration. The right side, 3.8b and 3.8d, illustrates the less altered host rock outside of the silicified boundary of the spherical concretions. The abundance of lithoclasts, bioclasts, and individual quartz grains, both shocked and unshocked, appears equivalent to what is seen as ghosts or grains within the silicified region. Thin sections, XPL.*

The boundaries between the outer rims of the concretions and the surrounding host rock are very different in character than the boundaries between nuclei and concretions. They are less regular, are often spanned by individual fossil or mineral grains, and capture half-digested

lithoclasts, in which silicification ceased prior to complete alteration. These boundaries are pronouncedly uneven, showing irregular or convoluted advance of the silicification process. Irregularities often appear to represent variations in vulnerability of particular clasts and grains to alteration and replacement (see Figs. 3.7b and 3.7d). Based on ghosts of fossils, fossil fragments, and clasts within the silicified zone, there is no apparent change in the abundance or character of lithoclasts or bioclasts across this boundary. There is, similarly, no apparent change in the abundance of quartz grains and fragments of quartz grains. It appears that the only difference between these two zones is the replacement of carbonates with silica in the form of chert and chalcedony. Within the unaltered host rock (see right side of Figs. 3.7b, 3.7d and all of figs 3.8b, 3.8d) outside of the silicified region of the concretions, dominantly carbonate lithoclasts of varied character, fossils and fossil fragments, and individual quartz grains are abundant and distinct. As in the silicified bulk of the concretions, PFs (see Figs. 3.3a, 3.3b) and PDFs (see Figs 3.3c, 3.3d) are abundant among the quartz grains in the host rock. In both cases, shocked and unshocked grains are mixed.

3.4.6 Additional investigation of the nuclei

Subsequent to sectioning, the nuclei of seven of the concretions were scraped out, gently disaggregated on a ceramic surface, and then picked for microfossils and mineral grains beneath a dissection scope. This produced only a very small number of fossil fragments and quartz grains which may have been plucked from the interior wall of the cavity during removal of the nucleus filling material. Thin sections of stabilized nucleus material supported this interpretation, revealing no lithoclasts, bioclasts or mineral grains. SEM images show the nucleus material to be composed of grains ranging to substantially smaller than 10 μm. (see Fig. 3.6)

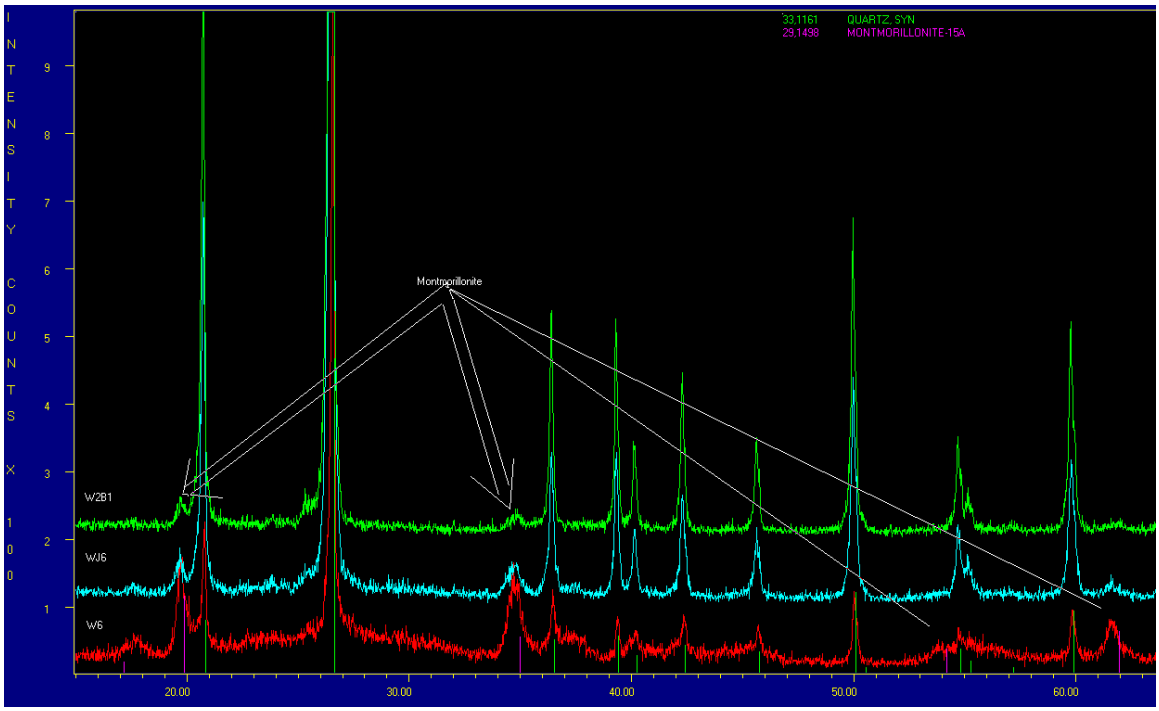

Figure 3.9. *XRD evaluation of three nucleus samples showed alpha SiO_2 silica grains with a small and variable montmorillonite component. Results for 3 samples are shown in different colors. Major peaks indicate ordinary (alpha) quartz, and arrows indicate minor peaks associated with variable montmorillonite content. No coesite or stishovite was indicated.*

The nuclei of an additional 17 concretions were then removed in preparation for reproduction of the interior cavities for morphological evaluation. The faces and interiors of the resulting 24 hollowed concretions were sprayed with a mold release agent, 33 Petrolease, and then filled with natural latex #80 to create interior molds. The halves were held together with bands for a week during drying, then were pried apart. The resulting off-white casts were trimmed and sprayed with grey and yellow acrylic paint from opposing directions to increase visibility and contrast of surface features. The resulting objects are consistently rounded and frequently flattened, showing little other consistency in shape. Orientation of flattening relative to sedimentary context was not recorded. Whether this indicates soft-sediment compaction or the emplacement of originally flattened masses is unknown, but inconsistency and a lack of

impressed lithoclasts or fossil fragments in thin section suggests the emplacement of the objects as already sub-rounded to flattened masses. (see Fig. 3.10)

Figure 3.10. *Castings of nuclei. The broad lines on the castings are trim lines from removal of excess molding material. Some surface voids result from bubbles during casting. Though of consistently similar composition, the nuclei reveal little consistency in shape. Unlike other clasts in the Weaubleau breccia units, they are rounded and often somewhat flattened. A lack of impressed lithoclasts or fossil fragments suggests that the objects were lithified when emplaced, and that their currently clay-like character could be the result of chemical change.*

3.5 Discussion and conclusions

Weaubleau round rocks are concretions nucleated around rounded, friable silica-rich clasts composed of silt-sized particles. The concretions that have formed around these nuclei are composed of chert and chalcedony that has replaced the surrounding dominantly carbonate breccia. Silicified relicts of bioclasts and lithoclasts are visible in thin section prepared from the

concretions, suggesting the bulk of the round rocks formed by diagenetic replacement of the carbonate material surrounding a nucleus. An irregular outer boundary between the concretions and surrounding stone, characterized by an irregularly advancing line of partially and completely silicified clasts, strongly supports concretion formation through silicification.

The rounded nuclei are of a common composition, suggesting that these clasts or their glass or mineral precursors prior to chemical changes, provided nucleation points for the growth of the siliceous concretions. The origin of the friable masses of finely powdered microcrystalline silica that make up the nuclei of the concretions is not certain. They are the only substantially rounded lithoclasts found in the uppermost portion, or resurge facies (Miller et al., 2008), of the Weaubleau breccia. With the possible exception of the Northview Formation (discussed later), they are distinct from exposed chert, quartzite, shale or carbonate lithologies in the area both in composition and grain size. That they did not result from the decay of such materials is further suggested by the undisturbed angular fragments of these in encompassing sediments.

Rounded structures analogous to volcanic accretionary lapilli have been reported at several impact crater locations. Accretionary lapilli are cemented aggregations of wet ash and lithic particles. Morphological details and nomenclature are reviewed in Brown et al., 2012. By definition, accretionary lapilli are significantly smaller than Weaubleau round rocks.

At Sudbury, accretionary lapilli measuring 3 to 20 mm (e.g. Fralick et al. 2012) have been recognized in ejecta deposits. The lapilli show concentric zoning by grain size, and are bounded by a distinct, fine grained exterior. Distinct nuclei occur inconsistently and are varied in composition. (Huber and Koeberl, 2013). At the Alamo Breccia, in Nevada, stratified beds and isolated examples of accretionary lapilli of carbonate composition have been reported. They

are from 1 to 30 mm in diameter, with most around 5 mm. They show concentric zoning distinguished by grain size, surround a distinct nucleus present in only a fraction of cases, and are accompanied by fragmented examples suspended in surrounding matrix (Warme et al., 2002). Lapilli and related accretionary aggregates associated with Ries crater, and from the Stac Fada impactite formation, in Scotland, are similar to those reported at Alamo or Sudbury. They are typically less than 3 cm in size, concentrically layered, bounded by a well defined exterior surface, may accompany broken fragments, and are distinct from adjacent host rock in grain size and/or composition (Graup, 1981; Branney and Brown, 2011). In each of these cases, close examination has contradicted in-situ formation through diagenetic processes.

Weaubleau round rocks share few characteristics with impact related accretionary lapilli or related plume or pyroclastically-formed aggregates. They are much larger, lack concentric layering and grain size sorting, have an irregular exterior boundary that captures partially altered clasts, have not been observed as broken fragments entrained in the hosting rock unit, and are consistently formed around a nucleus of specific composition. Relict boundaries of silicified carbonate lithoclasts and bioclasts within the concretions, along with partially silicified clasts spanning the concretion growth boundary combine to suggest that the concretions begin as material that is compositionally continuous with surrounding matrix. Evidence supports a diagenetic in-situ origin.

In contrast to the outer boundary of the concretions, the boundary between the central nucleating masses and surrounding concretions is consistently distinct. The nuclei are in no case evidently impressed or intruded by lithoclasts or bioclasts, and no grain spans this boundary. This suggests that the nuclei were solid at the time of their introduction to the soft sediment instead of the powder that we see now, and that they have subsequently undergone significant

post-impact diagenetic changes. It is possible that such chemical changes provided the impetus for nucleation and concretion growth, but this is a very general statement; initial nucleation and subsequent concretionary growth could have been initiated by any of a number of associated factors - adsorption or release of silica during clay or other mineral transformations within nuclei, localized reduction in permeability of the sediment, devitrification of an impact-related glassy component, localized changes in pH associated with mineral evolution, the dissolution of carbonates during compaction adjacent to harder masses, or the decay of organic matter.

Though we can describe and illustrate the objects in detail, we can currently only speculate regarding the ultimate origin of the nuclei. Sharp boundaries suggest that the shapes that we see now are, to some extent, indicative of the shapes of the original masses. As to the nature of these original masses, which were apparently of a common type, neither morphology nor current composition suggests a biological origin. They could be the chemically decayed remnants of glassy ejecta, rounded masses of heat-altered shale, rounded remnants of a tripolitic chert deposit entrained during resurge, or something else entirely. It is worth noting that fine-grained tripolitic silica is known and mined as a polishing agent from deposits of similar age from a nearby region about 100 to 150 km from Vista.

The most similar rock unit to the nuclei in the regional succession is the Northview formation, composed of occasionally friable shale, mudstone, and siltstone (Miller et al., 2008). It is possible that the nuclei derive from clasts of this unit entrained within the breccia. A single thin section made from a Northview sample retrieved at a nearby quarry revealed it to be locally carbonate-rich, composed largely of subhedral dolomite grains, quite distinct from the fine-grained silica compostion of the nuclei. Miller et al. (2008), however, processed nucleus material from approximately 100 broken round rocks, and recovered 4 Kinderhookian

conodonts, consistent with the age of the Northview formation. On this basis, we prefer the interpretation of nuclei as Northview clasts in the absence of a better argument.

Growth of the concretion subsequent to nucleation likely occurred in a manner consistent with the formation of more conventional chert nodules common in other regional carbonates. A substantial literature exists regarding the subjects of silicification in carbonates and chert nodule growth. Such concentric growth has been explained by the progressive dissolution of calcium carbonate at grain contacts under the physical pressure of quartz growth, and the subsequent precipitation of additional silica within a resulting micron-scale zone of dissolution and precipitation, in addition to precipitation of quartz on available unconstrained growth surfaces, with silica, in both cases, mobilized in solution in ground water. The literature offers several variations on these themes (e.g.: Maliva and Siever, 1989).

Formation by precipitation of silica on a growth surface also provides a ready explanation for the pronouncedly spherical shape of the concretions. As layers of uniform thickness are added to an asymmetric object, there is a natural and rapid mathematical progression to the lowest surface area per volume. In two dimensions, draw bands of uniform width around any irregularly shaped object, and the result will be more circular with each added layer. Along with a biased availability of reaction and precipitation surfaces on the portions of the growth that present the largest surface areas, results in the typical spherical to discoidal shape of concretions throughout geological literature. In sediment with nearly uniform permeability, ideal deposition or replacement produces a sphere regardless of nucleus shape. In an environment where factors such as bedding planes place constraints on fluid migration or concretion growth, concretions tend to be disk shaped.

3.5.1 The Weaubleau structure

That the Weaubleau Structure should be considered to be of at least probable impact origin is suggested by the presence of abundant planar fractures and apparent planar deformation features within the samples investigated here. PDFs constitute one of several widely accepted classes of unambiguous indicators of hypervelocity impact related shock**,** and are present in these deposits in sufficient numbers to make possible a credible assertion of impact origin, in a context that can be readily vetted by others. That these indicators point to a specific, localized impact structure rather than to a detrital remnant is suggested by their context within a localized unit of breccia (Beveridge, 1951; Miller et al., 2008) and by pronounced uplift of basement material, consistent with a complex impact structure of modest size, within the structure (Miller et al., 2008).

3.6 Acknowledgements

Thanks to Jerri Stevens for support and company during fieldwork, to Dr. Mourad Benamara for SEM and EDS training, and to residents of the Vista area of Missouri for generous property access and permission to collect samples.

3.7 References

Beveridge T. A. 1949. The geology of the Weaubleau quadrangle, Missouri. Ph.D. thesis, State University of Iowa, Iowa City, Iowa.

Beveridge T. R. 1951. The Geology of the Weaubleau Creek Area, Missouri. *Missouri Geological Survey and Water Resources Report, Second Series*. 32.

Branney M. J. and Brown R. J. 2011. Impactoclastic Density Current Emplacement of Terrestrial Meteorite-Impact Ejecta and the Formation of Dust Pellets and Accretionary Lapilli: Evidence from Stac Fada, Scotland. *The Journal of Geology* 119(3):275-292.

Bretz J. H. 1950. Origin of the filled sink-structures and circle deposits of Missouri. *Geological Society of America Bulletin* 61(8):789-834.

Brown R. J., Bonadonna C., and Durant A. J. 2012. A review of volcanic ash aggregation. *Physics and Chemistry of the Earth.* 45-46:65–78.

Cox M. R. 2008. Geology of the Vista 7.5 minute Quadrangle, St. Clair County, Missouri: unpublished master's thesis, Missouri State University, Springfield, Missouri.

Cox M. R., Evans K. R., Plymate T. G., and Miller J. 2006. Geologic mapping of the Weaubleau structure, west-central Missouri (abstract #21-5). Geological Society of America. Philadelphia Annual Meeting. *Abstracts with Programs* 38(7):58.

Cox M. R. and Evans K. R. 2007. Geologic map of the Vista 7.5' Quadrangle, St. Clair county, Missouri: Missouri Department of Natural Resources Division of Geology and Land Survey Open-File Report OFM-07-101-GS.

Cox M. R., Evans K. R., and Krizanich G. W. 2007. GIS-based geologic mapping of the Vista quadrangle, west-central Missouri (abstract #23-3) Geological Society of America, South-Central and North-Central Joint Section Meeting. *Abstracts with Programs* 39(3):25.

Davis G. H. 2005. The use of shallow geotechnical drilling to delineate the Weaubleau-Osceola Impact Structure, St. Clair County, Missouri (abstract). SEPM Research Conference: The Sedimentary Record of Meteorite Impacts. *Abstracts with Program*. p. 12.

Davis G. H., Evans K. R., Miller J. F., Mulvany P. S., and Rovey C. W. II. 2005. Weaubleau-Osceola, Decaturville, and Crooked Creek: New Aspects of Missouri's 38th Parallel Structures (abstract). SEPM Research Conference: The Sedimentary Record of Meteorite Impacts. *Abstracts with Program*. p. 13.

Dulin S. and Elmore R. D. 2005. Paleomagnetism of impacts in shallow-water carbonate sediments: the Weaubleau-Osceola impact and the Alamo Breccia (abstract). SEPM Research Conference: The Sedimentary Record of Meteorite Impacts. *Abstracts with Program*. p. 13.

Dulin S. A., Elmore R. D., and Gardner K. G. 2005a. Impacts in carbonate target rocks: A paleomagnetic study of the Weaubleau-Osceola and Alamo Breccia impact structures (abstract #1371). 36th Lunar and Planetary Science Conference.

Dulin S. A., Elmore R. D., Mulvany P. S., and O'Brien V. 2005b. Paleomagnetic constraints on the timing of the Decaturville impact structure, Southwest Missouri (abstract #GP33A-0105). *Eos Transactions* American Geophysical Union. Fall Meeting Supplement 86(52).

Dulin S. and Elmore R. D. 2006. Paleomagnetism of the Decaturville impact breccias and the Weaubleau-Osceola structure, southwest Missouri: Testing the serial impact hypothesis (abstract #44-15). Geological Society of America, Annual Meeting. *Abstracts with Programs* 38(7):121.

Dulin S. and Elmore R. D. 2008. Paleomagnetism of the Weaubleau structure, southwestern Missouri. In The sedimentary record of meteorite impacts, edited by Evans K. R., Horton J. W. Jr., King D. T. Jr., and Morrow J. R. *Geological Society of America Special Paper 437*. pp. 55-64.

Dulin S. A., Gardner K. G., Elmore R. D., and Totten L. A. 2004a. Post-deformational Remagnetization of the Weaubleau-Osceola Structure, SW Missouri (abstract #56-5). Geological Society of America. 2004 Annual Meeting. *Abstracts with Programs*. 36(5):145.

Dulin S. A., Gardner K. G., Elmore R. D., Totten L. A., Evans K. R., Miller J. F., and Rovey C. W. II, 2004b. Paleomagnetism of the Weaubleau-Osceola impact structure, SW Missouri (abstract #GP31A-07), *Eos Transactions American Geophysical Union. Jt. Assem. Supplement* 85(17)

Earth Impact Database, 2014. Planetary and Space Science Centre, University of New Brunswick <http://www.unb.ca/passc/ImpactDatabase/>

Elmore R. D. and Dulin S. 2007. New paleomagnetic age constraints on the Decaturville impact structure and Weaubleau structure along the 38th parallel in Missouri (North America). *Geophysical Research Letters* 34(13).

Evans K. R., Mickus K. L., Fagerlin S., Luczaj J., Mantei E., Miller J. F., Moeglin T., Pavlowsky R. T., and Thomson K. C. 2003a. New dimensions of the Weaubleau Structure: A possible meteorite impact site in southwestern Missouri (abstract #17-9). Geological Society of America, North-Central Section Annual Meeting. *Abstracts with Program*.

Evans K. R., Rovey C. W. II, Mickus K. L., Miller J. F., Plymate T., and Thomson K. C. 2003b. Weaubleau-Osceola structure, Missouri: deformation, event stratification, and shock metamorphism of a mid-Carboniferous impact site (abstract #4111). Third International Conference on Large Meteorite Impacts, Nordlingen, Germany.

Evans K. R., Mickus K. L., Rovey C. W. II, and Davis G. H. 2003c. The Weaubleau-Osceola Structure: Evidence of a Mississippian Meteorite Impact in Southwestern Missouri, in A*ssociation of Missouri Geologists Fieldtrip Guidebook*. 50th Annual Meeting. Report of Investigation No. 75. Guidebook No. 26:1-30.

Evans K. R., Rovey C. W. II, Davis G. H., Mantei E. J., Mickus K. L., Miller J. F., Moeglin T. D., and Plymate T. G. 2004. Oblique impact at Weaubleau-Osceola Structure, Missouri (abstract #110-12). Geological Society of America Annual Meeting. *Abstracts with Program* 36(5):266.

Evans K. R., Mulvany P. S., Miller J. F., Mickus K.L., and Davis G. H. 2005a. SEPM Research Conference: The Sedimentary Record of Meteorite Impacts, *Field Trips Guidebook*.

Evans K. R., Davis G. H., Mickus K. L., Miller J. F., and Rovey C. W. II. 2005b. The Weaubleau-Osceola Structure and Weaubleau Breccia–Compiling Evidence of a Marine

Impact (abstract). SEPM Research Conference: The Sedimentary Record of Meteorite Impacts. *Abstracts with Program*. p. 16.

Evans K. R., Miller J. F., Mulvany P. S., Davis G. H. 2006. Formation and emplacement of impact breccias in carbonate target rocks: Examples from southern Missouri (abstract #21-4). Geological Society of America Annual Meeting. *Abstracts with Programs* 38(7):58.

Evans K. R. 2007. A Tattered Tapestry: Interpreting Remote Sensing Imagery of the Ozark Mountains (abstract #31-7). Geological Society of America Annual Meeting. *Abstracts with Programs* 39(3):64.

Evans K. R. and Mickus K. L. 2008. Geophysical, structural, and kinematic analysis of the Weaubleau structure: Implications for an oblique impact (abstract #252-4). Joint Meeting of the Geological Society of America, Soil Science Society of America, American Society of Agronomy, Crop Science Society of America, and Gulf Coast Association of Geological Societies with the Gulf Coast Section of SEPM. *Abstracts with Programs* 40(6):379.

Evans K. Davis G. Miao X. Mickus K. Miller J. and Morrow J. 2008. Re-evaluating the 38th parallel serial impact hypothesis (abstract #P31A-1384). *Eos Transactions American Geophysical Union*. Fall Meeting Supplement 89(53).

Evans K.R., and Miller, J.F., 2010, Geology of the Decaturville and Weaubleau impact structures, west-central Missouri: 43rd Annual Meeting of the Pander Society Field Trip Guidebook, 43 p.

Evans K. R, Miller J. F., and Miao X. 2010. Origins of the 38th parallel structures (abstract #35-1). Geological Society of America North-Central/South-Central 44th Annual Joint Meeting. *Abstracts with Programs* 42(2):91.

Evans K., Miller J. F., and Ethington R. 2011. Xenoclast Biostratigraphy: Evidence for Mid-Mississippian and Late Ordovician Impacts at Weaubleau and Decaturville Structures, Missouri (abstract #117-11). Geological Society of America Annual Meeting. *Abstracts with Programs* 43(5):306.

Evans K., Mickus K. L., Miller J. F., and Davis G. H. 2012. Proximal to Distal Deformation in the Weaubleau Impact Structure, Missouri (abstract #270-13). Geological Society of America Annual Meeting. *Abstracts with Programs* 44(7):630.

Finn M. P., Krizanich G. W., Evans K. R., and Usery E. L. 2007. Contemporary high-resolution LiDAR derived DEMs could inspire developments in the study of impact structures (abstract). *Proceedings of the Association of American Geographers/ Great Plains – Rocky Mountain Section Annual Meeting*. pp. 21-22.

Finn M. P., Krizanich G. W., Evans K. R., Cox M. R., Yamamoto K. H. 2012. Visualizing Impact Structures Using High-Resolution LiDAR-Derived DEMs: A Case Study of Two Structures in Missouri. *Surveying and Land Information Science* 72(2):87-97.

Fralick P., Edgar L., and Grotzinger J. 2012. Recognition of accretionary lapilli in distal impact deposits on Mars: a facies analog provided by the 1.85 Ga Sudbury impact deposit. In *Sedimentary Geology of Mars.* (eds. Grotzinger J. P. and Milliken R. E.). Special Publication 102: SEPM (Society for Sedimentary Geology), Tulsa, OK. 211-227.

Graup G. 1981. Terrestrial chondrules, glass spherules and accretionary lapilli from the suevite, Ries crater, Germany. *Earth and Planetary Science Letters*. 55(3):407–418.

Huber M. S. and Koeberl C. 2013. Accretionary lapilli from the Sudbury impact event (abstract). *Meteoritics & Planetary Science* 48 (Suppl.):5112.pdf.

Lemons C. R. 2008. Microstructural Analysis of Calcite Within the Weaubleau Structure, West-Central Missouri (abstract #5-7). Geological Society of America South-Central Section, 42nd Annual Meeting. *Abstracts with Programs* 40(3):8.

Maliva R. G. and Siever R. 1989. Nodular chert formation in carbonate rocks. *The Journal of Geology* 97(4):421-433.

McCracken M. H. 1966. Major Structural Features of Missouri (map). Missouri Department of Natural Resources Division of Geology and Land Survey, *DNR/DGLS Fact Sheet No. 6.*

Meteoritical Bulletin Database. 2014. International Society for Meteoritics and Planetary Science. Lunar and Planetary Institute. < http://www.lpi.usra.edu/meteor/>

Miao X., Evans K. R, and Morrow J. R. 2007. Serial impacts or random alignment? Monte Carlo simulations of three 38th parallel impact structures (abstract). *Meteoritics and Planetary Science* 42 (Suppl.):5312.pdf.

Mickus K. L., Evans K. R., and Rovey C. W. II. 2005. Gravity and Magnetic Analysis of the Weaubleau-Osceola Structure, Missouri (abstract). SEPM Research Conference: The Sedimentary Record of Meteorite Impacts. *Abstracts with Program*. p. 25.

Miller J. F., Bolyard S., Evans K. R., Ausich W. I., Ethington R. L., Thompson T. L., and Waters J. A. 2005a. Implications of fossils in the ejecta breccia associated with the Weaubleau-Osceola Structure, St. Clair County, Missouri (abstract). SEPM Research Conference: The Sedimentary Record of Meteorite Impacts. *Abstracts with Program*. p. 26.

Miller J. F., Evans K. R., Bolyard S. E., Thompson T. L., Davis G. H., Ausich W. I., Waters J. A., and Ethington R. L. 2005b. Mixed-age echinoderms, conodonts, and other fossils from a mid-Mississippian impact resurge breccia, St. Clair county, Missouri (abstract #25-7). Geological Society of America Annual Meeting, *Abstracts with Programs* 37(7):62.

Miller J. F., Evans K. R., Kurtz V. R., Thompson T. L., Mulvaney P. S., Sandberg C. A., Repetski J. E., and Ethington R. L. 2006. Using conodonts and other fossils to determine the age of Missouri's 38th Parallel Structures and some "Lost Horizons" of the Ozark Dome (abstract #69-11). Geological Society of America Annual Meeting. *Abstracts with Programs* 38(7):184.

Miller J. F. and Evans K. R. 2007. The Weaubleau and Decaturville impact structures in west-central Missouri: sorting out their ages using re-deposited conodonts and crinoids in breccias: 2007 Pander Society Field Trip, 37 p.

Miller J. F., Evans K. R., Ethington R. L., Repetski J. E., Sandberg C. A., and Thompson T. L. 2007. Critical stratigraphic data from reworked conodonts in impact breccias across Missouri's Ozark Dome (abstract #30-5). Geological Society of America Annual Meeting. *Abstracts with Programs* 39(3):62.

Miller J. F., Evans K. R., Ausich W. I., Bolyard S. E., Davis G. H., Ethington R. L., Rovey C. W. II., Sandberg C. A., Thompson T. L., and Waters J. A. 2008. Mixed-age echinoderms, conodonts, and other fossils used to date a meteorite impact, and implications for missing strata in the type Osagean (Mississippian) in Missouri, USA. In *Echinoderm Paleobiology*, edited by Ausich W. I. and Webster G. D. University of Indiana Press, Bloomington. p. 246-288.

Miller J. F., Thompson T. L., Ethington R. L. 2010. Conodonts and other fossils from cores in the resurge breccia at the Weaubleau impact structure, St. Clair County, Missouri (abstract #9-12). Geological Society of America Annual Meeting. *Abstracts with Programs* 42(2):50.

Moon K. E., Evans K. R., Miller J. F., and Davis G. H. 2010. Weaubleau impact virtual core library (abstract #116-6). Geological Society of America Annual Meeting. *Abstracts with Programs* 42(5):305.

Morrow J. R. and Evans K. R. 2007. Preliminary shocked-quartz petrography, upper Weaubleau breccia, Missouri, USA (abstract #5237). *Meteoritics and Planetary Science* 42 (Suppl.):5237.pdf.

Rajmon D. 2009. Impact database 2010.1. On-line: http://impacts.rajmon.cz

Rampino M. R. and Volk T. 1996. Multiple impact event in the Paleozoic: Collision with a string of comets or asteroids? *Geophysical Research Letters* 23(1):49-52.

Rovey C. W. II, Evans K. R., Mickus K. L., Miller J. F., Plymate T. G., and Thomson K. C. 2003. Impact origin of the Weaubleau-Osceola Structure in southwestern Missouri (abstract #156-6). Geological Society of America Annual Meeting. *Abstracts with Programs* 35(6):339.

Shoberg T., Stoddard P. R. 2007. Gravity and Magnetic Surveys of the Weaubleau Quadrangle, South Central Missouri: Implications for an Impact Origin of the Weaubleau-Osceola Structure (abstract #U23A-0860). *Eos Transactions American Geophysical Union*. Fall Meeting Supplement 88(52).

Snyder F. G. and Gerdemann P. E. 1965. Explosive igneous activity along an Illinois-Missouri-Kansas axis. *American Journal of Science* 263(6):465-493.

Steadman J. A. 2007. A petrographic study of the Weaubleau-Osceola and Crooked Creek impact structures, Missouri (abstract #1-1). Geological Society of America, South-Central and North-Central Joint 41st Annual Section Meeting. *Abstracts with Programs* 39(3):1.

Stockdell R. B., Mickus K. L., Davis G. H., Evans K. R., Miller J. F., and Rovey C. W. II. 2004. Bouguer gravity and magnetic anomalies associated with the Weaubleau-Osceola impact structure, Missouri (abstract #11-3). Geological Society of America North-Central Section Annual Meeting. *Abstracts with Program* 36(3):18.

Warme J. E., Morgan M., and Kuehner H-C. 2002. Impact-generated carbonate accretionary lapilli in the Late Devonian Alamo Breccia. In *Catastrophic Events and Mass Extinctions: Impacts and Beyond* (eds. Koeberl C. and MacLeod K. G.). Boulder, Colorado, Geological Society of America Special Paper 356. 489–504.

Chapter 4 Indicators of impact origin in small terrestrial craters

4.1 Abstract

Earth's confirmed record of small, sub-kilometer impact craters, as compiled in the Earth Impact Database (2014), consists of approximately 198 explosive craters and penetration funnels from 22 different locations. The most widely accepted lines of evidence used to confirm impact origin at larger craters are only moderately useful in distinguishing sub-km impact craters from similar terrestrial structures. This systematic analysis examines the precise lines of evidence, both suggestive and unambiguous, that have allowed people to distinguish small terrestrial impact craters and penetration funnels from crater-like structure of non-impact origin. Only 7 of these 22 locations have produced unambiguous evidence of impact origin in the form of high pressure mineral polymorphs, planar deformation features, diaplectic glass, or clearly identifiable shatter cones. Nevertheless, compelling arguments for impact origins for most of these structures have been constructed and presented in the literature. In addition to the preceding lines of evidence, compelling arguments have been based upon traces of the impactor, preserved either as meteorites or iron 'shale' in proximity to crater-like structures exhibiting compelling morphological features. Internal and external indicators of shrapnel morphology in meteorites, spatial distribution of meteorite fragments, and the presence of melted materials incorporating both impactor and target rock components have each also played a role. Aggregate consideration reveals that two widely accepted crater locations probably present insufficient evidence to be reasonably considered as of impact origin, and that two more present only suggestive evidence. Unambiguous evidence of impact origin for the remainder is compiled and summarized. Commonalities among lines of suggestive and diagnostic evidence provide a predictive, generalizable description of the small impact crater population as a whole, as well as providing a

reasonable suite of specific objectives and targets for the researcher attempting to evaluate the potential impact origin of small, terrestrial crater-like structures.

4.2 Introduction

Even with close investigation, it is not always easy to distinguish between meteorite impact craters and terrestrial crater-like structures, regardless of scale. The shock pressures produced by the impacts of large meteorites, however, can exceed those produced by any naturally occurring process on Earth's surface. The impact crater science community has come to broadly recognize and use the unique and permanent changes in rocks and minerals that result from the passage of impact induced shockwaves in order to reliably distinguish impact craters from morphologically similar terrestrial structures. Such lines of evidence includes shattercones, planar deformation features (PDF) in quartz or other minerals, the evolution of diaplectic glass, or the presence of high pressure mineral polymorphs, such as coesite or stishovite. At the current state of the science, the recognition of terrestrial impact craters hinges upon the recognition and publication of unambiguous examples of such evidence or upon the presence of impactor remnants preserved either as meteorites or chemical traces in target rock. (e.g. French, 2004; French and Koeberl, 2010)

Small impact craters, less than 1 km in diameter, produce much smaller volumes of shock altered rock than larger structures. In the smallest impact craters and in the case of low velocity penetration funnels, no unambiguous grain-scale indicators of shock alteration are produced at all. This investigation finds that only 7 locations hosting examples of impact craters less than 1 km in diameter have produced examples of shatter cones, high pressure mineral polymorphs, planar deformation features, shatter cones or diaplectic glass, and that most of the known craters

less than 1 km in diameter are recognized principally upon the presence of an associated meteorite or upon nothing more than crater-like morphology or suggestive but ambiguous evidence such as planar fractures (PF). This paper originated out of frustration with being unable to clearly answer questions regarding the identification or confirmation of small impact craters and out of the author's own frustration in attempting to evaluate small structures in the field. Its purpose is to 1) clearly identify the types of evidence upon which unambiguous cases for impact origin have been constructed for terrestrial impact craters less than 1 km in diameter, 2) identify trends within the literature that might inform a generalized description of the small penetration funnel and crater population as a whole, 3) facilitate future fieldwork efforts by identifying where compelling evidence has been found in the field and what exactly has been found, 4) assess whether current widely accepted criteria for meteorite impact recognition serve the community in evaluating these structures, and finally, 5) consider the strength of the published evidence for an impact origin for each of these structures in light of these compiled observations.

The sub-km impact craters listed in the Planetary and Space Science Centre (PASSC) Earth Impact Database (EID), maintained at the University of New Brunswick, Canada, were used for this study because the list nominally represents only those known impact pits and impact craters for which a reasonably compelling argument for impact origin has been presented in the peer reviewed literature. The current body of the planet's reported record of sub-km penetration funnels and craters includes approximately 198 examples from 22 different locations. 120 of these are at Sikhote-Alin. The remaining 78 examples are distributed as single and multiple structures among the other 21 sites. Several structures not listed in the EID could have been revisited, but the purpose of this research was not to review the literature concerning small impacts, but rather to use the field reports and subsequent studies of the best evidentiated

examples of such structures to answer specific questions regarding the efficacy or failure of various classes of evidence in the evaluation of these small structures. Several of the listed sub-km impact structures used in this study have been described through fieldwork in only the sparsest detail, and thus is should be considered, throughout, that a lack of evidence in the literature may not demonstrate the lack of such evidence at the sites. Several widely accepted examples, it turns out, are questionable or poorly supported by evidence, and these have been neglected in the construction of certain generalizing statements in the report's discussion and conclusion.

4.3 Penetration Funnels vesus Impact Craters

4.3.1 Penetration funnels versus hypervelocity impact craters

The smallest impact craters, those less than a few tens of meters in diameter, are understood in terms of a distinction between low velocity 'penetration funnels' (or penetration craters, penetration pits, impact pits, plunge pits, penetration holes) and higher velocity 'explosive craters' (craters, true craters, fragmentation craters, hypervelocity impact craters). To express this distinction concisely: An explosive crater is formed when a very high velocity impactor accelerates materials away from the impact site at faster than the speed of sound in the target material producing, by definition, a shock wave. Target materials are crushed or disaggregated to a greater or lesser extent as the shock front passes, depending upon shock energy and duration and the strength of the target material, and excavation occurs within a flow field created by explosive decompression (or rarefaction) behind the shock wave (Melosh, 1989; French, 1998). The result is a characteristic explosive crater, a circular bowl with a raised rim and surrounding rubble. The impactor most often explodes in such cases, and is ejected with

rubble. The energies involved may vary over orders of magnitude, and at higher energies, depending upon intensity and duration of shock pressure (Melosh, 1989; Holsapple, 1993), melting, vaporizations or grain-scale shock metamorphism of target materials may take place.

A penetration funnel is formed when a lower velocity impactor, typically traveling at less than a few hundred meters per second (French, 1998), accelerates target materials away from the point of impact at less than the speed of sound in the target material, producing subsonic waves in the target (Melosh, 1989). A small pit or funnel is formed by compaction and/or ejection, varying in size and shape in accordance with target material strength and impactor size, speed, and angle. A penetration funnel or pit is typically no more than a few times the diameter of the impactor itself. No shock wave is produced. Impactors may or may not break up in such impacts, but typically leave much of their mass buried within the penetration funnel. Although particles are sometimes damaged by the crushing force of impact and acceleration, they are not subjected to melting or shock metamorphism at the grain scale.

Whether an explosively formed impact craters or a penetration funnel forms depends upon the speed of sound in the target material and the strength of the target material relative to the speed and properties of the impactor (Melosh, 1989). The distinction between penetration funnels and explosive craters is relevant only to craters between a few meters in diameter and something less than 20 meters or so in diameter on earth, as the planet's atmosphere prevents very small impactors from preserving the necessary pre-atmospheric speed to produce hypervelocity structures, and is at the same time insufficiently dense to slow very large impactors enough to prevent explosive hypervelocity crater formation. A generalizable function representing the relationships between initial impactor characteristics and speed and target material properties that would realiably combine to define lower limits for explosive crater

production and upper limits for simple penetration funnels has not thus far been employed in small impact crater literature due simply to the fact that the boundary is very sensitive to specifics of moisture, target soil composition and strength at the time of impact. Holsapple (1993) comments on the need for work on both small craters and low speed interactions, and Svettsov (1998) discusses some of the inherent challenges. Much work, however, has been done towards understanding the final shape and size of the craters produced by higher speed impacts as impactor properties, target strength, and gravity vary (e.g.: Melosh, 1989; Holsapple, 1993; and references therein)

4.3.2 Confusion and ambiguity - distinguishing a crater from a penetration funnel

The line between penetration funnels and craters, though it may be conceptually distinct, is somewhat ambiguous in the field. Detailed reports of the smallest structures are scarce and often cursory, motivation to investigate is low, and the structures themselves are often reduced to shallow depressions after erosion. The distinction is also ambiguous in the literature. First, both the term crater and the term funnel are used ambiguously; the terms are very often treated synonymously (e.g.: Svettsov, 1998). And when used technically, the term penetration funnel has two meanings: the pit left by a meteorite impact at a speed insufficient to produce a shock excavated crater, as well as the initial stage of penetration prior to the formation of the transient cavity in hypervelocity crater formation. Context is important in determining which use of the term is being employed by an author.

This confusion is aggravated by imprecise differentiation of the terms. The distinction between penetration funnels and explosive craters is regularly confused for its proxies: whether the impactor has been fragmented and ejected or not, whether the speed of impact is above or

below some arbitrary figure, or whether unambiguous evidence of shock metamorphism is present or not.

An explosive crater is defined by the mechanism of excavation, a flow field formed with passage of a rarefaction wave behind a shock front formed by hypervelocity impact (Melosh, 1989). Impactor presence in the final structure, speed at contact, shock metamorphism of the target, and morphology are only proxies for this distinction, and none of these factors draws a discrete line between craters and penetration funnels.

The impactor may or may not be present in a penetration funnel, due to fracturing and rebound or to weathering, though it will typically be present. And though the impactor is most often fragmented and ejected from explosive craters, this is not necessarily always the case (Vesconi et al., 2011; Svettsov, 1998). Given the very low speed of acoustic propagation of some soils (Oelze et al., 2002), the formation of an explosive crater and the disaggregation and fragmented ejection of the impactor must be treated as separate and discrete phenomena which simply co-occur in most instances. The speed of the meteoroid at the moment of impact is critical, but can serve as a predictor of crater versus penetration funnel formation only with consideration of strength and speed of sound in the target material, which may be extremely low; less than 90 meters per second in some wet soils (Oelze et al., 2002). This is approximately 60 times lower than in granite, and means that even slight remnant pre-atmospheric velocity may produce a shock wave in some weak target materials. The presence of melt or high pressure grain scale indicators of shock metamorphism are in fact diagnostic of a hypervelocity impact, but small explosive craters may be produced in soils or carbonate targets with no production of these materials (Holsapple, 1993), thus a lack of such evidence is not evidence of a lack of shock excavation in small structures. Morphology of an explosive impact crater is potentially

diagnostic, and how it changes with target strength and impactor characteristics has been much discussed in literature concerning penetration depth and crater and penetration funnel scaling (e.g.: Melosh, 1989; Holsapple, 1993; Svettsov, 1998, and references therein), but very small explosive craters and penetration funnels in a weathered state offer little in the way of revealing detail as described in many of the field reports mentioned in the present research. Further, satisfactory theoretical models constraining the lower limits of explosive crater formation and the upper limit of penetration funnel production on earth, accounting for target soil characteristics, moisture variation, impactor speed and characteristics prove to be challenging (Melosh, 1989; Holsapple, 1993; Svettsov, 1998). Explosions are poor analogs. Further, neither specific variability in penetration funnel morphology nor apparent hypbrid or transitional explosive/penetrative structures (Vesconi et al., 2011; Svettsov, 1998) have been treated in any detail.

4.3.3 Possible penetration funnels among the small crater population

It is explicitely not the purpose of this paper to examine the distinction between penetration funnels and explosive craters, but rather to examine the nature and location of evidence distinguishing crater-like structures of impact origin from morphologically similar structures originating from other terrestrial processes. Nevertheless, it may be worth observing upon the subset of these structures for which there is ambiguity regarding shock excavation, as this has potential implications for the nature of evidence likely to be found at the smallest structures by future investigators.

Haviland - After 20,000 years of erosion (Honda et al., 2002), it may not be possible to know whether Haviland struck with any remnant pre-atmospheric velocity or even whether the

structure represents the impact of a single mass or a group of smaller impactors, a theory put forth by Nininger and Figgins (1933). The multiple impactor scenario they described was based in the distribution of recovered masses, and its viability is supported by later observation of an analogous scenario at the largest crater at Sikhote Alin (Krinov, 1971; LaPaz, 1949). Nininger and Figgins (1933) postulated an explosive origin for the structure upon examination and excavation, although understanding of the dynamics was very different at the time. The associated meteorite is fragmented, with portions of the meteorite dispersed, and portion concentrated within the crater. The crater was in very poor condition at the time it was excavated, but revealed both a raised rim and substantially ellipticity.

Carancas - Brown et al. (2008) estimate an impact velocity for Carancas of 1.5 to 4 km/second. Kenkmann (2009) suggest an impact velocity of 350–600 meters/second, and Le Pichon et al. (2008) derived an impact speed of >1.5 km/second. Several other variously evidentiated estimates, summarized in Kenkmann et al. (2009), fall between or above these figures. The speed of sound in water saturated sandy soil, similar to what has been described at Carancas (Kenkmann et al. (2009), reported in Oelze et al. (2002) was found to be very low, on the order of 100 meters/second. These facts, combined with morphological consideration and the explosive ejection of the impactor, seem to argue in favor of shock driven explosive crater formation, but with only a very small volume of material experiencing shock pressures greater than 1 Gpa (Kenkmann et al. 2009), far below what is necessary to produce grain-scale shock metamorphism.

Sikhote Alin - Whether any of the small pits or craters at Sikhote Alin were excavated by shock instead of by ordinary impact mechanics is difficult to guess. Svettsov (1998) calculates impact velocities for various impactors at Sikhote Alin ranging from terminal velocity to >5

km/second or greater. It is possible that soil may have been explosively excavated, but less likely that a shock wave would have been produced in shallowly underlying rocks described in Krinov (1971), as acoustic propagation and strength are significantly higher in lithic targets. Impact energy was, however, sufficient to produce substantial fracturing and ejection of this material. The impactors associated with many of the pits were also ejected as shrapnel. Most of the smaller structures at Sikhote Alin are likely penetration funnels, as asserted in French (1998) and many other publications. The largest structure has been clearly identified to be the product of multiple impacts in close proximity, rather than a single crater (Krinov, 1971; LaPaz, 1949), thus the impact energy of individual masses may have been substantially lower than at other structures of similar size discussed in this paper. Nine hybrid or transitional structures, termed channeled funnels, ranging from 2 to 12 meters in diameter, are suggestive of a penetration funnel formed at the base of an explosive crater. These are discussed in some detail in Svettsov, 1998, who calculates impact velocities for each of these. The smaller are formed at near terminal velocity, but the larger represent minimum possible impact velocities of 1 km per second or greater, ranging up to 3 to 4 km/sec for maximum possible impact velocities. Very similar transitional or hybrid structures are seen at Campo del Cielo. For larger non-transitional craters rangin from 8 to 12 meters in diameter, Svettsov (1998) calculates impact speeds from 2.1 to greater than 5 km/second.

Henbury - Crater 13, described in Spencer and Hey (1933) is the smallest Henbury crater and the only one within which the impactor was found. It was present as large, closely associated fragments with a combined weight of approximately 200 kg. The crater is approximately 9 meters across, and the impactor penetrated to a depth of approximately 3 meters. Unlike the larger craters at Henbury, no impact glass was found in association with the

smallest structure. Morphology of the poorly preserved structure is only reported in a cursory fashion, but the crater is clearly much larger than the impactor. Evidence unambiguously constraining whether or not excavation was produced by shock is absent.

Campo del Cielo - At Campo del Cielo, it is clear that at least 4 craters were explosively produced (Vesconi et al., 2011; Cassidy and Renard, 1996), with explosive disaggregation and ejection of both the impactor and target material, but it is unclear whether additional elliptical targets with intact meteorites within or beyond them represent penetration funnels, elliptical explosive craters produced during oblique penetration by an intact impactor producing a shock wave as it penetrated, or both. Vesconi et al. (2011) and Cassidy and Renard (1996) both report excavation of multiple apparently transitional or hybrid structures, in which elliptical bowl-shaped shock excavated craters are superposed over apparent penetration funnels. The funnels, narrow channels only modestly larger than the impactors themselves, extend from the base of the broad craters. The transition is abrupt, and is interpreted by Cassidy and Renard (1996) as marking the point at which the impactor's speed becomes subsonic, and at which formation of a shock wave ceases. Similar hybrid structures have been reported at Sikhote Alin as previously described, and have been observed in experiment (Schultz et al., 2007) and possibly on the moon (Quaide and Oberbeck, 1968). In both of the latter cases, the explosive to penetrative transition was attributed to differing target material properties with depth in stratified target materials, rather than to a slowing impactor in target material of common composition as at Campo del Cielo.

For one of the hybrid Campo del Cielo structures, Crater 10, Cassidy and Renard (1996) calculated an impact speed of 3.7 to 4.5 km/second, but they point out that specific target material density was not measured, and that the speed of sound in loess was assumed to be 500

meters per second. Acoustic propagation speeds in silty soils measured in Oelze et al. (2002) varied with moisture, but were consistently less than 250 meters per second.

Odessa, Morasko, and Kaalijarv - In addition to the large crater at Odessa, Evans and Mear (2000) describe a crater that is 21 meters wide and 5 meters deep which contained substantial portions of an impactor within the crater. In addition, the authors mention at least 3 small pits of unspecified size that were associated with individual meteorites. All of these structures are greater than 60,000 years old (Holliday et al., 2005), are described only minimally, and none were exposed prior to excavations in search of meteorites. Potential for unambiguous interpretation of the mechanism of excavation is limited by a complete lack of evidence. Small pits of ambiguous origin are also listed among the craters at Morasko (20 and 25 meters and possibly smaller) (Stankowski, 2001; Classen, 1978), and Kaalijarv (down to 15 and 13 meters) (Raukas, 2002; Rasmussen et al., 2000), though neither of these were found to contain significant portions of an impactor.

4.3.4 Summary of potential penetration funnels included in this investigation

Based on the sparse evidence summarized in the preceding section, it is certainly the case that many of the smaller craters at Sikhote Alin were formed as penetration funnels, without shock driven explosive excavation, and this is likely also true for the small pits of unspecified size mentioned at Odessa. One might also consider this to be the case at Haviland, which appears to be formed by a cluster of small impactors, like the largest crater at Sikhote Alin, but it should be remembered that much of this is inference in the absence of significant data. Larger craters at Sikhote Alin were likely shock excavated. The situation at Campo del Cielo suggests a crater field in which 4 of the structures were formed by explosive shock driven disaggregation

and ejection of both the impactor and target material, and some fraction of the remainder apparently represent transitional forms in which the impactor remained intact and an explosively formed bowl yields to a narrow penetration funnel formed as the largely intact impactor decelerated to the speed of sound in loess. A very similar situation is found at Sikhote Alin. At Carancas, an explosive origin is well supported, while in the case of the smallest structures at Henbury, Odessa, Morasko, and Kaalijarv, despite published references to several structures as penetration funnels, no actual published evidence provides a footing for anything significantly better than conjecture. Unless structures are evaluated in terms of specific evidentially supported impact speed and impactor and target soil characteristics, statements regarding the mechanism of excavation may be potentially misleading.

Based on the impact remnants summarized above, it appears that a simple dichotomy between penetration funnels and explosive craters may fail to capture the diversity seen in the terrestrial cratering record. At minimum, 4 'types' of impact structures are seen: penetration funnels, explosive craters in which the impactor was also explosively ejected, explosive craters with the meteorite intact or largely present in the bottom, and transitional or hybrid structures in which a penetration funnel continues on from the base of an explosive crater.

Figure 4.1. *Approximate locations of the 22 sub-kilometer simple impact craters or crater fields examined in this study.*

4.4 Summary of impact evidence at known small craters.

4.4.1 The Carancas impact produced a single, slightly elliptical crater with a diameter of about 13.5 meters (Tancredi et al., 2008, 2009), rapidly widening to 14.2 meters subsequent to erosion (Kenkmann et al., 2009) with an original measured depth of 2.4 meters from the lowest portion of the rim (Tancredi et al., 2008,2009). A hummocky and asymmetrically raised rim, ranging up to 1 meter above original ground level, is composed of ejecta overlying up-tilted and overturned soil horizons (Tancredi et al., 2009; Kenkmann et al., 2009). The rim grades to a noticeably raised and variably stratigraphically inverted strongly asymmetric continuous ejecta blanket that is at maximum thickness at the crater edge and distinct to approximately 1 crater diameter in its greatest dimension (Tancredi et al., 2009; Kenkmann et al., 2009). These authors also point out the presence of materials not otherwise exposed at the surface amidst the ejecta blanket.

Tancredi et al. (2009) and Kenkmann et al. (2009) observe crater rays extending asymmetrically to >17 to 20 crater diameters and discontinuous ejecta to a distance of 10 to 26 crater diameters. Tancredi et al. (2009) report a notably increased abundance of PFs in quarts grains compared to controls from the surrounding area. They observe that these were found in lower layers of ejecta, 10-20 cm below the surface, and that they were found outside the crater a little less than 1/3 crater diameter down range from the impact. The results were not duplicated in similar investigation by Kenkmann et al., (2009) who found no PFs or PDFs. Tancredi et al. (2009) also describe small quantities of possible very small (1mm) glassy impactites incorporating both impactor and target material. The impactor, an H4-5 chondrite (Connoly et al., 2007; Connolly 2008) was present as grey meteorite dust and small fragments coating the interior wall of the crater and rim, and as larger fragments found around the crater, extending very asymmetrically to tens of meters (Le Pichon et al., 2008; Tancredi et al., 2009). The impact event occurred on 15 September 2007 (e.g.: Brown et al., 2008).

4.4.2 *Haviland* is a single, strongly elliptical, 10.7 m by 17 m, funnel shaped depression. At the time of its 1929 excavation, it still had a slight raised rim, and was filled with pond sediment (Nininger and Figgins, 1933). The interior was found to be heavily strewn with meteorite fragments, with the largest examples near the center. Additional fragments were found in and beyond the surrounding rim, merging with a large surrounding strewn field. Meteorite fragments within the crater were largely oxidized iron 'shale.' Location of clusters of meteorite fragments in the excavated crater walls suggests possible excavation of the crater by multiple simultaneous impacts. Primary reporting is in Nininger and Figgins (1933). The impactor, named Brenham or Hopewell Mounds, was a Pallasite, PMG-an (Buchwald, 1975). Honda et al. (2002) offer an age

of approximately 20 ± 2 ka. The crater has been largely destroyed by excavation and cultivation (Hodge, 1979).

4.4.3 Dalgaranga is a single crater with a diameter of approximately 23.5 by 24 meters and an original depth of 4.5-5 meters (Shoemaker et al., 2005; Hamacher and O'Neill, 2013). A very unevenly raised rim averages about 1.5 meters in height (Nininger and Huss, 1960, Shoemaker et al., 2005), and evidences some bilateral symmetry in wall angle and rim height (Nininger and Huss, 1960; Huss, 1962b). The rim is composed of uptilted to overturned rocks overlain by ejected rubble. A highly asymmetric continuous ejecta blanket extends beyond the rim to <3 crater diameters in its largest dimensions (Huss 1962b; Shoemaker et al., 2005). Discontinuous ejecta extends beyond this to many crater diameters (Nininger and Kelly maps shown in Hammacher and O'Neill, 2013). The crater filling sedimentation is colluvium from the crater walls and coarse grit of probable aeolian origin (McCall, 1965a; Shoemaker et al., 2005) overlying a breccia lens. Shoemaker et al. (2005) indicated an accumulation of 3 meters of fill reducing the original 5 meter depth to 2 to 3 meters. Spherules, spheroids, impact glass and fused rock were all absent despite a concerted visual and magnetic search (Nininger and Huss, 1960; Huss, 1962a). Sparse meteorite 'shale' and meteorite fragments are present. Hammacher and O'Neill (2013) show a fragment with what appears to be shrapnel morphology, and Nininger and Huss (1960) describe similar. Small, sparse meteorites are distributed strongly asymmetrically, primarily outside the crater and primarily within 2 crater diameters (Nininger and Huss, 1960; Huss, 1962a) but with sparse outliers to 300 meters (>12 crater diameters) (Hammacher and O'Neill, 2013 citing Wellard 1983:95). Oxidized 'shale' was recovered within the crater with excavation, as if small fragments had lined the crater wall (Nininger and Huss, 1960). Only fragments were found; no evident meteorite individuals have been found (McCall,

1965a). The impactor was a Mesosiderite-A (Shoemaker et al., 2005). Sparse and contradictory evidence suggest an age range from less than 3000 years to 270,000 years (best summarized in Hammacher and O'Neill, 2013).

4.4.4 The Sikhote-Alin (Sikhot-Alin) impact produced 120 penetration funnels or small craters over a span of approximately 5 km. The largest was a 26.5 meter multiple impact pit, possibly formed by a cluster of 8 or more stones (Krinov, 1971; LaPaz, 1949). Seventy-five of the pits at Sikhote Alin exceed 1.5 meters in diameter, and 17 exceed 10 meters in diameter (Svettsov, 1998). Radiating fractures, weakly resembling shatter cones, were observed in the largest examples (Krinov, 1971). Abundant microspherules, up to 2 orders of magnitude smaller than spheroids found at Barringer, were interpreted as ablation spherules (Badyukov and Raitala, 2012; Krinov, 1964; Krinov, 1971). Microscopic splinters (microshrapnel) produced by the "crushing of meteorites upon impact with the ground" were pervasive (Krinov, 1964; Krinov, 1971). The craters are located within a group of overlapping strewnfields that include many cm-scale individuals. The associated meteorite, a group IIAB iron (Buchwald, 1975), is present both as shrapnel and as regmaglypted individuals within and surrounding the pits (Krinov, 1971). Krinov (1974) and Lang and Kowalski (1973) have made sense of the strewnfield by looking closely at indications of stages of deceleration and fragmentation. The impact event occurred on 12 February 1947 (e.g.: Krinov, 1964).

4.4.5 Whitecourt is a single, very young crater with a diameter of about 36 meters and a depth of about 6 meters (Herd et al., 2008; Kofman et al., 2010). A specific search for secondary associated structures produced negative results (Herd et al., 2008). An asymmetrically uplifted rim only partially encircles the crater, and a continuous ejecta blanket, expressing weak bilateral symmetry, unevenly encircles the crater, extending to a maximum of approximately 1 crater

diameter beyond the rim, (Kofman et al., 2010). The original depth was about 8.9 meters, and the 2.9 meters of allochthonous fill is dominantly composed of sedimentary materials (Herd et al., 2008). Planar microstructures (PFs or PDFs) are present in quartz, with 1 to 3 sets present. Planar microstructure bearing quartz has been found only in grains within the transient crater surface (Kofman et al., 2010). A control study of the surrounding area showed very rare single sets of PFs in regional sediment, and these were sub planar (Kofman et al., 2010). Rare Fe/Ni spherules or spheroids were found in crater fill (Kofman et al., 2010). The impactor is present as microscopic to mm scale impactor 'dust' fragments along the buried transient crater surface (within 20 cm) (Kofman et al., 2010), as shrapnel, and as scarce regmaglypted individuals (Herd et al., 2008; Kofman et al., 2010). Impactor fragments are distributed strongly asymmetrically, primarily on the rim and outside the crater, downrange to 14+ crater diameters (which also suggests a minimum discontinuous ejecta field to at least this distance), and as very sparse fragments and weathered iron 'shale' within the crater (Kofman et al., 2010). The crater was formed by a group IIIAB Iron (Herd et al., 2008) impactor, and is about 1,100 years old (Herd et al., 2008).

4.4.6 Kamil is a single 45 meter crater with a depth of about 9-10 meters (Folco et al., 2010; Urbini et al., 2012). Secondary impact pits, likely formed by large ejecta, were observed up to approximately 5 crater diameters downrange (Urbini et al., 2012). An asymmetric rim unevenly rises to a maximum of about 3 meters. The rim is comprised of uplifted and upturned to overturned bedding (Folco et al., 2010, 2011), and is draped with and grades into a highly asymmetric continuous eject blanket which incompletely surrounds the crater, extending to a little over 1 crater diameter in its maximum dimension. Well preserved rays extend from the ejecta blanket to from <4 to >6 crater diameters. (Folco et al., 2010, 2011 (illus.); Urbini et al.,

2012). The crater is filled to a depth of about 6 m with fallback regolith overlying larger breccia from crater walls, all of which is partially superposed by up to 1 meter of aeolian sand, yielding an original transient crater depth of about 16 m (Folco et al., 2010; Urbini et al., 2012). Mosaicism, PFs and PDFs were reported in grains in ejecta and within melted material (D'Orazio et al., 2011; Urbini et al., 2012). Vesicular (pumicious or scoriaceous) cm-scale fragments of impact melt glass were found within the bowl, in proximal ejecta, and in some cases melted to meteorite fragments (Folco et al., 2010; D'Orazio et al., 2011). Impactite glass contains target rock fragments, entrained mineral grains and FeNi microspherules (D'Orazio et al., 2011). Microscopic melt particles were abundant in crater filling fallback material (Urbini et al., 2012). The later were also preferentially distributed on particular axis from the crater (Folco et al., 2010). Folco et al., 2011, illustrate melt spherules of both impactor and target material dominated composition, and ~.35 to .5 mm diameter. The impactor is present as shrapnel and as a single, regmaglypted individual (Folco et al., 2010; D'Orazio et al., 2011). Impactor fragments were predominantly located outside the crater in a highly asymmetric distribution with a maximum concentration >4 crater diameters from the rim and extending from the rim to greater than 7 crater diameters, and with outliers well beyond this, to greater than 1.5 km (Folco et al., 2011; D'Orazio et al., 2011). The impactor was an ungrouped iron ataxite (Weisberg et al., 2010; D'Orazio et al., 2011). The crater is reported as less than 5000 years old (Folco et al., 2011).

4.4.7 Sobolev (Sobolevskiy, Sobolevskii) is a single funnel-shaped crater 25 by 54 meters in diameter, with a maximum depth of 10 meters. The crater is expressed on a slope, and the maximum height (10 meters) of the strongly asymmetrically raised rim is expressed downslope. Continuous clastic ejecta is described upslope to a distance just short of one maximum crater

diameter, and discontinuous ejecta is described beyond this to an unspecified distance. Clastic material covers the rim, and an unconsolidated clastic regolith partially fills the interior of the crater. Seismic data suggest fracturing of the rock beneath and well beyond the crater rim to a distance of approximately 1 crater diameter. Possible pre-impact soil has been observed beneath ejected breccia outside the crater. Shatter cones are reported in Khryanina (1981) but photographs suggest misidentification. Sparse glassy microspherules and sub-mm particles of unspecified iron-oxide mineralogy (limonite) with nickel content of >2% were reported from clastic regolith beyond the crater rim. The age is reported as not less than 200 years old. All of the above is from Khryanina (1981).

4.4.8 *Veevers* is a single crater with a diameter of 72.5 meters between rim crests and a depth of ~7 meters (Yeates et al., 1976) or, more recently, 3 meters (Shoemaker et al., 2005). An asymmetric rim unevenly rises to an average height of about 1.5 meters (Yeates et al., 1976) and ranges up to 3 meters (Shoemaker et al., 2005). The rim is formed from uplifted, outwardly dipping bedrock slabs overlain by ejecta, which begins just below the rim and grades to an asymmetric continuous ejecta blanket extending unevenly to about 1/2 crater diameter or less in maximum dimension (Shoemaker et al., 2005). Shoemaker et al., 2005, also observes that ejecta rays/lobes correlate to high points on the crater rim. Shoemaker et al., 2005, estimates an original depth of about 15 meters, and describes the interior as partially filled with aeolian sand and colluvium from the crater walls. The impactor, a weathered group IIAB-Iron meteorite is present as fragments (Shoemaker and Shoemaker, 1985; Haines, 2005) with external and internal indicators of impact shrapnel origin (Bevan et al., 1995), and is primarily distributed strongly asymmetrically outside the crater within <1/4 crater diameter (Shoemaker et al., 2005,

Bevan et al., 1995). The age of the crater is sparsely evidentiated, and is reported as from less than 20k years to less than 4k years (Shoemaker and Shoemaker, 1988; Shoemaker et al., 2005).

4.4.9 Ilumetsa is a group of 5 depressions (Raukas et al., 2001), two or three of which, all located within a span of 900 meters, present minimal evidence of impact origin (Raukas et al., 2001; Stankowski et al., 2007). Pdrguhaud (Porguhaud), the largest, is 75-80 meters in diameter from the tops of the raised rim, and is 8 (Plado, 2012) or 12.5 (Raukas et al., 2001) meters deep. Raukas et al. (2001) cites Estonian literature suggesting that breccia below crater fill in the largest is at least 8 meters thick. The second and third largest structures are 60 and 50 m in diameter and 10 meters and 3.5 (Plado, 2012) or 4.5 (Raukas et al., 2001) meters deep, respectively. The 60 meter structure does not have a raised rim, while the 75-80 meter structure has an asymmetrically raised rim of up to 4.5 meters and the 50 meter structure has an asymmetrically raised rim of up to 1.5 meters. Raukas et al. (2001) reports that the rim of the larger crater is at least partially composed of up-tilted bedrock. All of the structures are partially filled with organic debris and pond sediment. Spherules and spheroids from microscopic to "some millimeters" in diameter were recovered and analyzed from cores ~6 km from the crater field, though no evidence connects these to the impact (Raukas et al., 2001). A suggested age for the craters is ~6000-7000 years (Raukas et al., 2001, Raukas, 2000, 2002; Stankowski et al., 2001, Plado, 2012).

4.4.10 Morasko is a group of 6 craters or penetration funnels (Stankowski, 2001) with diameters of approximately 90 (11.5 deep), 50, 30(4.3 deep), 20 by 35, 25, and 20 meters. 5 of the 6 craters are variously intermittently to permanently water filled. 2 more craters were identified in earlier research, but these have subsequently been refuted and destroyed, respectively (Classen, 1978). Classen (1978) suggests a much larger number of smaller impact funnels may have once

been present. The largest crater is slightly elliptical (Classen, 1978). The structures have unevenly raised to only partially present rims, all consistently higher on a common side throughout the group (Classen, 1978). All are partially filled with organic sediment (Stankowski, 2001). Meteorite dust, microfragments and ablation microspherules (but no larger spheroids) were found within the craters and intermittently within the strewnfield (Classen, 1978, citing Hurnik, 1977; Stankowski et al., 2002). An effort has been made at using thermoluminescence to support an impact origin for the structures (Stankowski and Bluszcz, 2012). An associated meteorite, an Iron IAB-MG (Wasson & Kallemeyn, 2002), is present as a multi-kilometer strewnfield, with the craters concentrated within an approximately 300 meter diameter area near one end (Classen, 1978). The strewnfield contains both regmaglypted individuals and fragments that, despite substantial weathering, suggest shrapnel morphology (Karwowski et al., 2011; Stankowski, 2001). Arguments for ages between about 5600 and 3500 years have been presented (Stankowski, 2001; Stankowski et al., 2002; 2007).

4.4.11 Kaalijarv (Kaali) is a group of at least 9 craters or penetration funnels clustered within a 1 square km area. The largest is water-filled, and is 105-110 meters in diameter and at least 22 meters deep (Raukas, 2002). The others are typically dry, and measure 39, 36, 33, 27, 26, 14x20, 15, and 13 meters in diameter, and range in depth from <1 to 4 meters. The largest crater is surrounded by a more-or-less evenly raised rim of 6 to 7 meters (Rasmussen et al., 2000) composed of ejecta overlying fractured and up-turned dolostone blocks (Raukas, 2002; Plado, 2012). The largest crater is filled with 5.8 meters of inorganic and organic lake sediment overlying crushed and 'burnt' dolomite to 4 to 5 meters (Raukas, 2002; Raukas et al., 2011; Rasmussen et al., 2000; Krinov, 1961). 'Rock flour' of crushed dolomite was found in the largest crater (Rasmussen et al., 2000; Krinov, 1961), and fractured target rock is present in

multiple of the structures (Plado, 2012; Krinov, 1961). Deitz (1968) shows small shatter cones found in the largest crater. Iron-rich spherules or spheroids are reported within the crater field in Russian language reports summarized in Krinov (1961). Plado (2012) summarizes a Russian language report of fractures beneath and beyond the crater rim to at least 1 crater radius. The impactor, an iron IAB-MG **(**Buchwald, 1975; Wasson & Kallemeyn, 2002**)**, is present in small quantities, as small fragments recovered within several of the smaller craters (e.g.: Krinov, 1961). Russian literature summarized in Plado (2012) and Krinov (1961) appears to suggest both morphology and internal deformation in meteorite fragments consistent with a shrapnel interpretation. Stratigraphic context of spherules found at a distance of 7 to 65 km from the crater have been presented as evidence of an age of 7600±50 years (Raukas and Stankowski, 2011), but no evidence connects these with the craters. Several alternative ages, based on palynological, radiocarbon, and other data, range to as young as 400 to 370 BCE (Russian and Estonian literature summarized in Rasmussen et al., 2000 and in Plado, 2012).

4.4.12 Campo del Cielo is a group of at least 20 small craters or penetration funnels distributed over a region extending 18 km by 3 to 4 km (Vesconi et al., 2011; Cassidy and Renard, 1996), with maximum crater dimensions ranging from 20 to 115 meters (Cassidy et al., 1965), though these dimensions reflect substantial potential enlargement due to erosion. Raised rims are only slightly expressed on some of the craters and are lacking on others (Cassidy et al., 1965; Cassidy, 1971; Vesconi et al., 2011). Craters are subrounded to elliptical and are in soil (loess), not rock (Cassidy et al., 1965; Vesconi et al., 2011). Like crater rims, continuous and discontinuous ejecta blankets are poorly and variably preserved at Campo del Cielo. An ejecta blanket is distinguishable to less than 1/2 crater diameter beyond the rim of crater 2 (Cassidy et al., 1965) before it becomes obscure, while no ejecta blanket is distinguishable at crater 9 (Cassidy, 1971).

Craters are variously partially filled to completely filled with pond and aeolian sediment and with material washed in from the crater rim (Cassidy et al., 1965; Vesconi et al., 2011). Below sedimentary fill is a rubble of unconsolidated loess, and clay target material mixed with meteorite fragments. Some loess within the excavation has been indurated by impact to form a brittle clay-stone, and a red-brown stained layer of cm-scale granular shock-indurated loess was found at the level of a suggested fall-back surface (Cassidy, 1971). Vesconi et al. (2011) observe that impactors have typically been found as large intact masses within or beneath the elevated rims of likely penetration funnels, but both Vesconi et al. (2011) and Cassidy and Renard (1996) report small, distorted fragments, typical of shrapnel, outside of the 4 larger and more rounded explosive craters, along with a lack of large impactors within these structures. Oxidized iron 'shale' is also present in some cases, both within and around craters (Cassidy et al., 1965; Cassidy 1971). The impactor was an IAB-MG Iron (Wasson & Kallemeyn, 2002). The age is ~4000 years (Cassidy and Renard, 1996).

4.4.13 Wabar is a group of at least 3 craters. The largest, 'Philby B,' is 116 m in diameter, 'Philby A' is 64 meters, and the third is 11 meters in diameter (Prescott et al., 2004; Gnos et al., 2013). The depths of all 3 are variable over time; the craters are partially filled with aeolian sand and are intermittently covered by dunes. A strongly asymmetric discontinuous ejecta blanket extends to greater than 7 crater diameters based on the largest crater (Gnos et al., 2013). A partially eroded rim, trenched and reported in (Shoemaker and Wynn, 1997) was composed of upturned bedded sand overlain by a blanket of ejecta. Inward and outward dipping thrust faults were observed beyond the initial upturned rampart, analogous to fracturing beneath and beyond the rim reported at other sites. Substantial shock evidence is present. All 3 craters show fractured quartz grains and shock lithification due to compaction and partial melting within sand

(Gnos et al., 2013; Shoemaker and Wynn, 1997). The larger two reveal PFs, PDFs, coesite and stishovite and strong mosaicism in quartz grains from ejecta, as well as poorly formed shatter cone-like structures (Gnos et al., 2013). Coesite was found in quartz trapped in ejected impact glass and in shock indurated sandstone (Chao et al., 1961; Prescott et al., 2004). Variably vesicular or vesicle-free to scoriaceous sub-cm to cm-scale melt glasses comprised of quartz sand (lechatelierite) plus impactor material are present (Gnos et al., 2013), and some examples contain FeNi metal spherules (e.g.: Spencer and Hey, 1933; Gibbons et al., 1976; Gnos et al., 2013). Glass is also found stuck to meteorite fragments and meteorite iron 'shale' amidst ejecta (Gnos et al., 2013). Sub-mm to mm-scale glassy impact spheroids are also common in ejecta, and are typically enriched in siderophile impactor components relative to target rock (Gnos et al., 2013; Mittlefehldt et al., 1992). The impactor, a group IIIAB Iron (Mittlefehldt et al., 1992), is present as regmaglypted individuals, as fragments with shrapnel morphology and as rusted iron 'shale,' located primarily outside the craters, amidst ejecta (Spencer and Hey, 1933; Gnos et al., 2013, and others). Shrapnel fragments show a twisted and bent exterior morphology and interior cracks and deformation (Spencer and Hey, 1933). The crater is very young, with a likely age of 300 years old or less. Competing proposed ages and related evidence are summarized in Gnos et al. (2013), Basurah (2003), and Prescott et al. (2004).

4.4.14 Henbury is a group of a 12 or 13 (Alderman, 1932; Milton and Michel, 1965; Milton, 1968a) to 15 (Hodge and Wright, 1971) craters, all located within a region of approximately 0.65 km^2 (Milton, 1968a). The largest 2 craters measure approximately 119 and 146 meters (Milton, 1968a), and overlap to form a single elongated basin. Two more, at about 70 and 91 meters in diameter (Milton, 1968a), share a common rim with each other and with the double impact. Additional craters range down to 8 to 9 meters rim to rim (Alderman, 1932; Hodge and Wright,

1971; Milton, 1968a). Crater rims are preserved around 10 craters (Milton, 1968a). These rims are both unevenly raised and unevenly eroded (Milton and Michel, 1965; Hodge, 1965; Milton 1968a). Preservation and exposure of bedrock vary, but where described, rims are composed of a combination of rock that is broken and displaced upward and outward, with much fracturing and folding. Strata exposed at the crater rim crest range from upturned to overturned. Rims are partially overlain by ejecta, which grades in some cases to a continuous ejecta blanket extending outward from the rim (Milton and Michel, 1965; Milton, 1968a,b). Continuous ejecta has been partially removed by erosion, but some remnants suggest assymetric distribution (Milton, 1968a). Rim height is increased between two larger adjacent craters and rims are destroyed where two craters overlap (Alderman, 1932; Milton, 1968a). Crater walls are generally composed of unconsolidated fragments of rock from powder to boulder scale, and are uneven in height in every instance. Two of the crater, numbers 3 and 4 (per the numbering of Alderman, 1932), with dimensions of around 61 and 62 meters, respectively, preserve rays extending to a maximum of nearly 1/2 crater diameter (Milton and Michel, 1965; Milton, 1968a). Milton and Michel (1965) observe that the rays are composed of specific rock types expressed at the radius of the crater from which they originate and that individual rocks within the rays are thrown a distance inversely proportional to their original distance from the point of impact. All of the structures are partially to completely filled with alluvium. Centimeter-scale masses of glass, ranging from scoriaceous to moderately vesicular, are distributed primarily outside the craters, and very asymmetrically (McColl, 1990). Some glass pieces contain entrained target rock fragments (Alderman, 1932; McColl, 1990), and some have included FeNi spheroids (Gibbons et al., 1976; Ding and Veblen, 2004). Examples of variably FeNi rich microscopic glassy spherules have also been examined from soil within and surrounding the craters (Hodge and Wright, 1971).

The impactor, a group IIIAB Iron, (Wasson et al., 1998) is present as shrapnel, as relict iron 'shale,' and as a strewnfield of regmaglypted individuals. Shrapnel fragments occur both around the craters and in crater walls, but with the significant majority of fragments distributed very asymmetrically outside the craters (Alderman, 1932; McColl, 1990). The only exception to this is the smallest crater or penetration funnel, Alderman's #13, with a diameter of about 9 meters, in which were found fractured remnants of a large meteorite and no impact glass (Spencer and Hey, 1933). Shrapnel fragments reveal cracks, internal shear surfaces, and plastic deformation evidenced in distortion of the Widmanstatten structure (Spencer and Hey, 1933; Alderman, 1932; Axon and Steele-Perkins, 1975). The structure has been dated to less than 4700 years old by Kohman and Goel (1963) and to 4.2 ± 1.9 ka by Storzer and Wagner (1977).

4.4.15 Odessa is a group of at least 5 craters (Evans and Mear, 2000), the largest of which is approximately 160 meters in diameter and 30 meters deep. The remaining 4, which may be penetration funnels, are much smaller, ranging from 5 to 21 meters in diameter and 2 to 5.2 m deep (Evans and Mear, 2000; Littlefield et al., 2007). The largest of these, designated as crater #2 by Evans and Mear (2000), is 21 meters across and 5.2 m deep. All of the smaller craters were completely filled and displayed no raised rim or depression prior to their excavation. #2 and an unspecified 3rd crater, also containing meteorite fragments, were discovered by excavation of magnetic anomalies. Crater #2 contained large meteorites in the bottom and was lined, below the fill, with meteorite fragments (Barringer, 1967). It has an off-center crater floor below fallback material and post-impact crater filling colluvium and sediment (Evans and Mear, 2000). An additional unspecified number of small funnels, up to 3 meters deep, were revealed when individual meteorites were excavated in the vicinity (Evans and Mear, 2000). Principal research is on the largest. It has an unevenly raised and heavily eroded rim composed of

upturned strata surmounted in places by remnants of ejecta (Evans and Mear, 2000; Holliday et al., 2005). Viewed in cross section, through trenching, it reveals accommodation to upward and outward motion through the general process of uptilting, but with various expressions of more complex localized deformation as rocks were "lifted, broken, folded and faulted" (Evans and Mear, 2000). Evans and Mear (2000) uniquely observe that displaced rock strata in the crater rim are uplifted as much as 15 meters above their original position, but flatten rapidly as one moves outward. A surrounding ejecta blanket is present, thinning outward. It is moderately asymmetric, and extends to approximately .25 to .75 crater diameter (Holliday et al., 2005; Evans and Mear, 2000). The primary crater is partially filled with a combination of erosional, aeolian and pond sediment to a depth of approximately 28 meters (Sellards and Evans, 1941; Holliday et al., 2005; Evans and Mear, 2000) overlying polymict breccia to a depth of approximately 5 meters, which covers a true crater floor of moderately fractured bedrock, the upper ~1.5 meters of which has been crushed to 'rock flour' (Sellards and Evans, 1941; Evans and Mear, 2000) of extremely finely crushed sand grains. Mention of an abundance of pinhead-sized fragments in Evans and Mear (2000) suggests that impact spheroids may be present. Vesicular FeNi metal-bearing glassy particles were analyzed and reported in abstract by Smith and Hodge (1997) and Nininger and Huss (1960) note that spheroids similar to those found at Barringer were found at Odessa. Evans and Mear (2000) describes a single clear shatter cone section found amidst ejecta at the crater rim. Meteorites are present both as fragments and as individual, and are distributed very asymmetrically to a distance of greater than 12 crater diameters from the largest crater (Evans and Mear, 2000; Holliday et al., 2005). Within the crater, only very small fragments were found, and these were deeply buried near the base of the fallback ejecta (Barringer, 1967; Evans and Mear, 2000). Shrapnel morphology and associated

internal characteristics have not been clearly described. An age of 63.5±4.5 ka. is supported in Holliday et al. (2005). The impactor is an IAB-MG group Iron (Holliday et al., 2005).

4.4.16 Boxhole is a single crater measuring approximately 180 (or 170x190) meters in diameter and 16 meters in depth (Shoemaker et al., 1988; 2005). The crater has an unevenly and asymmetrically raised rim, 3 to 5 meter in height (Madigan, 1937; Hodge and Wright, 1973), with asymmetry attributed at least partially to pre-impact topography (Cassidy, 1968). Rims are formed of uplifted, outwardly tilted rock overlain by ejecta exhibiting inverted stratigraphy on the crater rim (Shoemaker et al., 1988). The continuous ejecta blanket is strongly asymmetrical, and extends to a maximum of approximately 1/2 crater diameter. Discontinuous ejecta roughly corresponds to and extends the asymmetry. (Shoemaker et al., 1988; Roddy et al., 1988). Both the continuous and discontinuous ejecta are obscured by partial burial (Shoemaker et al., 1988, 2005). The crater is partially filled with colluvial, alluvial, and playa deposits (Shoemaker et al., 1988; Madigan, 1937). Very scarce spherules or spheroids were revealed only by methodical sampling (Hodge and Wright, 1973). The impactor, a group IIIAB Iron (Wasson and Kimberlin, 1967), is present as both meteorites and meteorite shale (Madigan and Alderman, 1940; Shoemaker et al., 1988; Shoemaker et al., 2005) and is present with both shrapnel morphology and as individuals (Madigan and Alderman, 1940; Bevan, 1996). Shrapnel exhibits internal evidence of impact deformation via bent and torn Widmanstatten pattern and shows evidence of rapid heating and cooling (Bevan, 1996). Meteorites are strongly asymmetrically distributed and are located outside the crater, on and beyond the rim (Madigan and Alderman, 1940; Shoemaker et al., 1990). The age of the crater may be approximately 5.4±1.5 ka (Kohman and Goel, 1963) or circa 30 ka (Shoemaker et al., 1990).

4.4.17 Macha is a group of 5 depressions measuring in diameter and depth as follows 300/40, 180/26, 90/>14, 70/>12, and 60/19.5 meters. No uplifting of the rims is reported. Possible remnants of a raised blanket of ejecta, beginning 8 to 10 meters back from the rim, and with a maximum height of 1.5 to 3 meters, are reported to occur in small sections near the largest two depressions, in both cases extending outward to significantly less than 1/4 crater diameter. The 90 meter structure is funnel shaped, with no visibly associated ejecta or raised rim. The 60 meter structure is associated with an encircling (up to) 2 meter rise extending to less than 1/4 crater diameter (Gurov and Gurova, 1998). Four of the depressions are partly filled with water and fluvial or lacustrine sediments. 1500 kg of material from rises adjacent to the larger craters produced 1 glassy spherule and 5 mm-scale metallic particles, none of which showed elevated Ni or Co. The authors report 1 to 3 (or more) sets of planar features (possible PFs) and undulose extinction in quartz from fractured rocks and fragments of breccia gathered from the crater walls (Gurov and Gurova, 1998). The authors also suggest possible detection of stishovite in samples via XRD. Spheroids are reported, but none show significant nickel (E. P. Gurov, 1996). An age of 7315±80 years is suggested (Gurov and Gurova, 1998).

4.4.18 Monturaqui is a single, slightly elliptical crater measuring approximately 350 x 370 meters in diameter and about 34 meters deep (Buchwald, 1975). It is surrounded by an unevenly and asymmetrically raised rim (Sanchez and Cassidy, 1966; Buchwald, 1975). The crater is partially filled by minor fluvial and aeolian sediments and by colluvium from the crater walls (Ugalde et al., 2007). Geophysical study by Ugalde et al. (2007) suggests this post impact sediment may overly crater-filling fractured rock over unfractured basement rock. Relict rays may be suggested by geological mapping shown in Ugalde et al. (2007) though these have not been specifically investigated. Vesicular glassy impactites, measuring up to several centimeters,

are abundantly distributed very asymmetrically on and beyond the crater rim. They are heterogeneous masses of shocked and unshocked target rock fragments and fractured and intact mineral grains entrained in glass. PFs, PDFs, FeNi spherules, diaplectic glass and coesite have been are observed in quartz and other mineral grains captured in the glassy impactites (Bunch and Cassidy, 1972, Ugalde et al., 2007). PFs, PDFs and coesite were only found in the impactites. The impactor is thus far represented only by iron 'shale' and by FeNi spherules preserved in glassy impactites, both of which are strongly asymmetrically distributed, primarily on and beyond the crater rim (Sanchez and Cassidy, 1966; Ugalde et al., 2007; Buchwald, 1975). Iron shale was predominantly found within 1 crater diameter (Sanchez and Cassidy, 1966; Ugalde et al., 2007; Buchwald, 1975), and glassy impactites have primarily been found within 1/4 crater diameter (Buchwald, 1975 and personal communication with Steve Arnold). The impactor is likely a group IAB Iron (Koeberl, 1998). The age of the crater is estimated at 0.1 Myr or greater by Buchwald (1975). Valenzuela et al. (2008) suggest an age potentially as great as 0.5 to 0.8 Ma.

4.4.19 Aouelloul is a single 390 meter crater with a depth of about 28 meters. An unevenly raised and asymmetric rim, ranging in height from 25 to less than 10 meters, is composed of variably uplifted to overturned strata (Campbell Smith and Hey, 1952; Koeberl et al., 1998; Koeberl , 1994; Fudali and Cassidy, 1972). The crater is partially filled with sandy silt and aeolian sand, which overlie a breccia lens (Koeberl, 1994; Fudali and Cassidy, 1972). The rim is also partly overlain by aeolian sediment (Fudali and Cassidy, 1972; Koeberl et al., 1998). Abundant shattered and fractured quartz grains and scarce possible PFs have been found in samples from the crater rim, but no clear PFs or PDFs were found (Koeberl et al., 1998). Abundant impact glass is distributed strongly asymmetrically, primarily outside of the crater and

within less than 1/2 crater diameter (Koeberl and Auer, 1991; Koeberl et al., 1998; O'Keefe, 1971; Fudali and Cassidy, 1972; Cressy et al., 1972; Campbell Smith and Hey, 1952). The glass ranges from dense to vesicular, and contains partially melted rock clasts, mineral grains, and zones of FeNi micro-spherules from 0.2 to 50 microns in diameter (Campbell Smith and Hey 1952; Chao et al., 1966a,b; Koeberl, 1994). Lechatelierite and Baddeleyite have been recognized as components of the glass (El Goresy 1965; El Goresy, 1968), and an impactor component has been demonstrated through observations of both elemental (Ni,Ge,Ir) and isotopic (Re-Os) changes compared to target rock composition (Morgan et al., 1975; Koeberl and Auer, 1991; Koeberl, 1998). Morgan et al. (1975) suggests a pallasite or group IIIB or IIID iron impactor, and Koeberl and Auer (1991) and Koeberl (1998) support this assessment. The age of the crater is approximately 3.25 ±0.5 Ma old per Storzer and Wagner (1977) or 3.1±0.3 Ma old per Fudali and Cressy (1976). Matsubara et al. (1991) report a less consistent potential age of 10-15Ma.

4.4.20 Amguid is a single 450 meter crater with a depth of 30 meters, surrounded by an unevenly and asymmetrically raised rim up to 50 meters high (Lambert et al., 1980; McHone et al., 1980). The rim is composed of variably upturned to overturned strata superposed by unconsolidated ejecta, which grades into an uneven but roughly symmetric continuous ejecta blanket. The outward dip of strata increases progressively upward in the wall, with material at the top nearly vertical to overturned (Lambert et al., 1980). The continuous ejecta blanket extends outward from less than 1/2 crater diameter to slightly greater than one crater diameter (Lambert et al., 1980; McHone et al., 1980). The crater is partially filled with alluvial and aeolian sediments and colluvium from the crater walls. Sparse fractured grains, consistent undulatory extinction, and scarce examples of up to 3 sets of planar elements have been observed in quartz from the exposed crater rim (Lambert et al., 1980). The authors note that the ejecta blanket is made up of

the same rocks that compose the crater walls - a somewhat unique observation employed to rule out most possible origins other than phreatic volcanism or impact. No meteorite found. Estimated age is 10,000 to 100,000 years (Lambert et al., 1980).

4.4.21 Kalkkop is a slightly oblong single structure with a diameter of approximately 600 x 680 meters (Reimold et al., 1998). It is surrounded by a raised rim of upturned and at least partly overturned strata that has accommodated upward and outward movement through complex fractures, folds and faults (Reimold et al., 1998). It is one of very few small to mid-sized structures with reported drill results (Haughton et al., 1953; Koeberl, 1994). The crater is partially filled with approximately 89 meters of limestone (Koeberl, 1994; Reimold et al., 1998; Koeberl et al., 1994), overlying approximately 70 meters of breccia, which differs in character from top to bottom, and in which at least two distinct units are observable. The upper portion of the breccia hosts impact melt (glass) fragments, and the lower section exhibits no pronouncedly shocked or melted particles and exhibits a more pronounced increase in clast size with depth (Reimold et al., 1998; Koeberl et al., 1994). Reimold et al. (1998) additionally reports a zone of fractured rock and intermittent breccia dikes in bedrock below the transient crater floor. PDFs are present in crater-filling breccia, revealed by drilling, with up to 6 sets present (Reimold and Koeberl, 2014; Koeberl et al., 1994; Reimold et al., 1998). Diaplectic quartz glass was also observed by Reimold et al. (1998). Analysis of Re and Os isotopes has been used to confirm an impactor component in the breccia, but the class of the impactor has not yet been discovered (Koeberl, 1994; Koeberl et al., 1994). Reimold et al. (1998) constrain the age of the crater to 250 ka ± 50 ka.

4.4.22 Wolfe Creek (Wolf Creek) is a single, slightly elliptical structure measuring approximately 935 x 825 meters in diameter and with a rim to floor depth of ~50-55 meters

(Hawke, 2003; Shoemaker et al., 2005; O'neille and Heine, 2005). An unevenly and asymmetrically raised crater rim, rising ~25-35 meters above the original target surface, is comprised of variably upturned to overturned rock. The rim is partially overlain by ejecta, which grades into an asymmetric continuous surrounding ejecta blanket (Guppy and Matheson, 1950; Cassidy, 1954; McCall, 1965b; Fudali, 1979; Hawke, 2003; O'neille and Heine, 2005). A possible incipient central uplift is ruled out by O'neille and Heine (2005). Strata revealed in the rim are overturned to produce inverted stratigraphy in surrounding ejecta (White et al., 1967; Hawke, 2003). The ejecta blanket external to the crater is strongly asymmetric and is partly overlapped by aeolian sediment, obscuring its extent (Shoemaker et al., 2005). Sinkholes are present in the crater floor (Guppy and Matheson, 1950; Fudali, 1979; Shoemaker et al., 2005). The crater is partially filled with aeolian sand, playa sediments and colluvium from the rim (Shoemaker et al., 2005; O'neille and Heine, 2005). Publications suggest a likely original depth from 150 meters (Hawke 2003; Fudali, 1979) to 175 meters (O'neille and Heine, 2005), or about 120 meters below the present crater floor. A gravity profile suggests that the current floor of sedimentary fill is underlain by fallback and slump breccia, and that below this is a fractured crater floor. Shoemaker et al. (2005) recovered melt glass 3 km from the crater, but it does not appear that work has been done on this material. Its presence has been confirmed in personal correspondence with Don McColl. Shatter cones are reported in the down-range rim, and PFs and PDFs have been identified and indexed in samples from the crater rim (O'neille and Heine, 2005). Heavily weathered Group IIIAB Iron meteorites (Scott et al., 1973) are present, distributed very asymmetrically downrange as iron 'shale' on the inner and outer slopes of portions of the rim and outside the crater (Reeves and Chalmers, 1949; Shoemaker et al., 2005;

Knox, 1967; White et al., 1967) and as large, heavily oxidized remnants of possible individuals (LaPaz, 1954). Shoemaker et al. (1990) report an age of approximately 300 ka.

4.5 Discussion

4.5.1 Trends in data - A summary of evidence types for small impacts

Of the 22 sub-km impact crater locations listed in the PASSC database, an impact origin is well supported by evidence for only 18, based on the evidence compiled here. This will be discussed in more detail in section 4.6.2. Meteorite fragments or their oxidized 'shale' remnants are found at only 16 of these (see Tables 4.1 and 4.2). Some of the observations collected in the preceding text are considered, below, only in the context of the 18 well evidentiated craters or the 16 craters at which meteorites have persisted. This is done in order to avoid creating a misleading impression of the ratios involved.

Table 4.1. Reported impactor classification, age, and multiple impacts among sub-km terrestrial penetration funnels and craters.

	Age	Impactor Classification	Diameter in meters (largest)	Number of craters known [1]	Directly Associated Meteorite	Additional Individual Meteorites [2]
Carancas	<0.01 ka	H4-5	13.5	1	yes	--
Haviland	~20±2 ka	PMG-an	10.7 x 17	1	yes	multiple
Dalgaranga	<~270 ka	Meso-A	24	1	yes	--
Sikhote-Alin	<0.1 ka	Iron IIAB	≤ 26.5	~120	yes	multiple
Whitecourt	~1.1 ka	Iron IIIAB	36	1	yes	multiple
Kamil	<5 ka	Iron ung.	45	1	yes	single
Sobolev	>0.2 ka	--	25 x 54	1	--	--
Veevers	≤~20 ka	Iron IIAB	72.5	1	yes	--
Ilumetsa	~6-7 ka	--	≤ 80	≤ 5	--	--
Morasko	~3.5-5.6 ka	Iron IAB-MG	≤ 90	~6	yes	multiple
Kaalijarv	~2.4-7.6 ka	Iron IAB-MG	≤ 110	≥ 9	yes	--
Campo del Cielo	~4 ka	Iron IAB-MG	≤ 115	≥ 20	yes	multiple
Wabar	<0.3 ka	Iron IIIAB	≤ 116	≥ 3	yes	multiple
Henbury	4.2±1.9 ka	Iron IIIAB	≤146	~12	yes	multiple
Odessa	63.5±4.5 ka	Iron IAB-MG	≤160	≥5	yes	multiple
Boxhole	5.4±1.5 ka	Iron IIIAB	170 x 190	1	yes	multiple
Macha	7315±80 ka	--	≤300	5	--	--
Monturaqui	>>100 ka	Iron IAB	350 x 370	1	yes	--
Aouelloul	>~3 mya	Pall, IIIB or IIID	390	1	--	--
Amguid	≤100 ka	--	450	1	--	--
Kalkkop	250±50 ka	--	600 x 680	1	--	--
Wolfe Creek	~300 ka	Iron IIIAB	935 x 825	1	yes	maybe

[1]. Number of craters known: For multiple crater sites, the total number of craters is frequently uncertain. The number listed represents a likely minimum, and includes both explosive craters and penetration funnels.

[2]. Additional Individual Meteorites: This means meteorite 'individual' in the technical sense. These are meteorites that have been been found near the crater(s) or pits(s), which are from the same fall, but which impacted the surface separately from the crater or pit forming impact, and which did not form pits or craters of their own. These are sometimes regmaglypted or fusion crusted. For a more detailed explanation, see section 4.5.4

4.5.2 Meteorite presence

Meteorite fragments have been found at 16 out of 22 sub-kilometer impact crater locations, though in two of these cases, Monturaqui and Wolfe Creek, only oxidized remnants, or iron meteorite 'shale' have been present. A tentative or positive classification of the impactor has been achieved at 17 of the total 22 locations (see Table 4.1). In the single case of Aouelloul, in which a tentative identification of the impactor was achieved in the absence of meteorites or their oxidized remnants, this was accomplished by consideration of Ni, Ge and Ir elemental ratios in glass (Morgan et al., 1975; Koeberl and Auer, 1991; Koeberl, 1998). In only 5 of 22 sub-km craters has an impactor not been identified, and 4 of these will be later discussed in regards the overall sparsity of evidence supporting their impact origin. The 5th case is Kalkkop, at which the presence of a meteoritic component has been confirmed through the study of Re and Os isotopes, but for which the class of the impactor has not been determined (Koeberl, 1994; Koeberl et al., 1994). One might consider that since meteorites have been used as a criterion for recognition of small impact craters, some portion of this high ratio of meteorite-bearing small craters may represents a circular effect. And this effect may be aggravated by the fact that other classes of evidence for small impact craters are subtle enough that motivation for a detailed search may not be adequate, in some instances, in the absence of the initial discovery of meteorites. On the other hand, only fairly young examples of small craters tend to be recognizably preserved, and these are more conducive to the preservation of meteorites, resulting in a natural bias.

The 16 sub-km craters that have produced meteorites, plus Barringer, the largest crater at which meteorite fragments have been found at greater than trace levels of abundance, represent all meteorite and explosive crater pairings currently known and listed in the PASSC database.

Larger craters do not preserve impactors, but it is not clear how much of this is the result of increase in age, and how much is due to the increase in crater size. The fact that the vast majority of larger craters are also very much older than the sub-km impact group suggests that the current record of impacts may not clearly show us where the practical upper boundary of impactor preservation in the immediate post-impact environment actually sits.

Table 4.2. Reported distribution of impactor remnants.

	Meteorite or 'Shale' Present	Large masses in crater(s)[1]	Shrapnel Morphology	Asymmetric ejection	Spherules or spheroids	Crater lining dust and fragments	External micro-frags	Metal or trace chemistry in glass
Carancas	yes	--	--	yes	maybe	yes	yes	--
Haviland	yes	yes	--	--	--	maybe	--	--
Dalgaranga	yes	--	yes	Yes	--	yes	--	--
Sikhote-Alin	yes	varies	yes		yes	yes	yes	--
Whitecourt	yes	--	yes	yes	yes	yes	--	--
Kamil	yes	--	yes	yes	yes	--	--	yes
Sobolev	--	--	--	--	maybe	--	--	--
Veevers	yes	--	yes	yes	--	--	--	--
Ilumetsa	--	--	--	--	--	--	--	--
Morasko	yes	--	yes	--	yes	--	--	--
Kaalijarv	yes	--	yes	--	yes	--	--	--
Campo del Cielo	yes	varies	yes	--	--	maybe	--	--
Wabar	yes	--	yes	yes	yes	--	--	yes
Henbury	yes	varies	yes	yes	yes	--	--	yes
Odessa	yes	varies	--	yes	yes	--	--	yes
Boxhole	yes	--	yes	yes	yes	--	--	--
Macha	--	--	--	--	--	--	--	--
Monturaqui	yes	--	--	yes	--	--	--	yes
Aouelloul	--	--	--	--	--	--	--	yes
Amguid	--	--	--	--	--	--	--	--
Kalkkop	--	--	--	--	--	--	--	yes
Wolfe Creek	yes	--	--	yes	--	--	--	--

[1]. Sikhote alin, Campo del Cielo, Henbury, and Odessa are locations with multiple impact craters. At each of these, there is at least one instance of an impactor having been ejected as shrapnel, and at least one instance of an impactor remaining within the crater. These have been indicated as 'varies' to reflect this variation at the site. See individual crater summaries and section 4.5.6.1 for more detailed explanations.

Figure 4.2. *Left: An example of shrapnel specimen from the Sikhote Alin meteorite, exhibiting characteristic torn appearance and sharp edges. Macroscopic plastic deformation of shrapnel fragments is typically accompanied, internally, by distorted crystallographic structure, the formation of shear surfaces, brittle failure on inclusion and crystal boundaries, and evidence of transient localized re-heating. Right: Individuals from the same fall, showing clear regmaglypts.*

4.5.3 Shrapnel morphology

'Shrapnel' are meteorites that have been torn apart by impact. They are sometimes termed splinter meteorites (e.g.: Gorshkov et al., 1975; Krinov, 1964), or explosion fragments (e.g.:

D'Orazio et al., 2011). They are characterized, in exterior morphology, by a twisted and torn appearance, jagged or sharp edges, an often flattened overall shape, and a lack of evident fusion of torn surfaces. Sikhote-Alin is famous for offering abundant, remarkable examples of meteorites that have been modified by impact in this manner. (see Fig. 4.2) Macroscopic plastic deformation is typically accompanied, internally, by distorted crystallographic structure, the development of shear surfaces, brittle failure and fracture on inclusion and crystal boundaries, and evidence of transient localized re-heating (e.g.: Gorshkov et al., 1975; D'Orazio et al., 2011; Bunch T. E. and Cassidy W. A. 1968; Krinov., 1964; Herd et al., 2008; Bevan et al., 1995; Buchwald., 1975).

Fragments with clear shrapnel morphology have been described in 11 out of the 14 instances of an impactor being preserved other than as oxides (meaning in those cases in which details of internal and external morphology could conceivably be preserved)(see Table 4.2). All but one of these (Dalgaranga) are relatively well preserved irons. Dalgaranga is a mesosiderite, but there are, nevertheless, indications that some samples express shrapnel morphology (Hammacher and O'Neill, 2013; Nininger and Huss, 1960). The 3 cases of relatively well preserved meteorites associated with small impact craters in which shrapnel morphology was not observed are Odessa, Haviland and Carancas. Carancas is a chondrite, Haviland is a very heavily weathered pallasite of substantially greater age than most of the remainder of the group, and Odessa is the oldest clearly dated crater directly associated with a meteorite, so may or may not have lost revealing morphology. (Older dates among this group are less well constrained.)

Jagged iron shrapnel are broadly interpreted to be a specific product of impact with the ground, but, per their abundance at Sikhote-Alin, are not necessarily indicative of substantial remnant cosmic velocity at the time of impact (Krinov, 1974). In particularly congruous cases of

association with a crater-like structure, they may be sufficiently unambiguous evidence of an impactor and impact structure pairing to constitute reasonable confirmation. If they are found in the absence of such a structure, they may indicate that one has been overlooked or has been destroyed by erosion. While it does not necessarily derive that all incidents of shrapnel morphology originate from small, crater forming impacts, it is at least reasonable to assert that the presence of shrapnel should precipitate some effort at distinguishing possible impact structures, and that the distribution of shrapnel may point to the locations of such structures.

It is further worth noting that not all small impacts produce shrapnel. Several of the impact locations mentioned above, at which shrapnel meteorites have been identified, are multiple crater locations. At several of these, some craters have produced shrapnel meteorites surrounding craters, while others have produced intact or fragmented individual found sitting within their associated impact structures. Evidence from Campo del Cielo (e.g.: Vesconi et al., 2011 and Cassidy and Renard, 1996) indicates that shrapnel-producing 'explosive' craters and impact funnels that do not produce shrapnel may be similar in size and may occur in the same impact event.

4.5.4 'Individual' meteorites and multiple impacts

A high percentage of small impact craters are multiple crater groups as opposed to single impacts. This suggests that part of the investigation of any small impact crater should include a search for additional craters, and that the ordinary evaluation of small craters should routinely involve an effort to distinguish crater ejected meteorites from associated non-crater-forming individuals.

Seven of the 16 cases in which meteorites (or iron meteorite 'shale') were found have turned out to be multiple impact crater sites. In 11 of the 16 cases in which meteorites have been located, non-crater forming individual meteorites exhibiting fusion crusted and/or regmaglypted surfaces were reported in addition to the crater-forming fall(s). These two groups do not entirely correspond. 5 single craters are associated with at least 1 non-crater forming individual, and 1 multiple impact group is associated with no additional identified individual meteorites. Cumulatively, this means that at least 12 of the 16 sub-km impact craters at which meteorite fragments or shale have been found are multiple impacts (see Table 4.1). In only one case, Wolfe Creek, is the identification of additional individuals ambiguous, and this is due to advanced weathering (LaPaz, 1954).

Though a lack of preserved meteorites at some craters and a lack or scarcity of confirming evidence at others potentially skews the conclusion, we might also more broadly observe that, among the entire set of 22 currently more-or-less accepted sub km impact craters, 14 are tentatively multiple falls, having either multiple craters or associated individuals (see Table 4.1).

It is also worth noting that the presence of non-crater-forming individual meteorites is not limited to the smaller impacts. Several of the largest are among this group, implying that the presence of nearby individuals or an immediately associated strewnfield is not evidence, in itself, that an associated crater is a terminal velocity or near-terminal velocity impact. Bland and Artemieva (2006) predict that many larger impact craters are also produced by multiple pieces of a fragmented object, but that dispersal is inadequate for these pieces to produce multiple craters in the case of larger impacts.

4.5.5 Oxidized iron 'shale'

At 10 out of 22 sub-km crater locations, entirely oxidized remnants of meteorites, commonly known as iron 'shale' have been reported. These are iron oxide and FeOH remnants of impactors, sometimes with a cortex of soil or mineral grains cemented by rust from the meteorite's decay (e.g.: Bender Kock and Buchwald, 1994; Kofman et al., 2010). The casual term 'shale' probably originated due to the material's often laminated appearance. In several instances, such as at Haviland and Wolfe Creek, traces of un-oxidized metal have been found within otherwise completely altered meteorite fragments. Oxidized shale typically makes up only a portion of the preserved meteorites within a strewnfield. In only 2 cases, Monturaqui and Wolfe Creek, have only oxidized 'shale' meteorite fragments been found, in the absence of unoxidized meteorites (see Table 4.2).

Several authors (e.g.: Madigan, 1937; Nininger and Figgins, 1933; Kofman et al., 2010) have commented on the proximity of iron shale balls to crater basins, and noted that better preserved examples of meteorites are found among individuals or among fragments located farther from the craters. While many authors have noted the role of craters as localized water catchments, and repeated submergence is a ready explanation for this effect in meteorites located within craters, the trend towards heavy oxidation of specimens found within craters continues onto crater rims and flanks, suggesting possible further considerations. Marvin Killgore, in personal communication, mentioned the possibility that this to be due to increased vulnerability of shrapnel to water penetration due to internal micro-fractures. Such internal damage is well evidenced in impact shrapnel (see discussion and related publications in the previous section on Shrapnel Morphology).

4.5.6 Meteorites - spatial distribution

Remnants of crater-forming impactors have been reported in 6 significantly distinct forms or settings in the post-impact environment: 1) large masses in-situ within the crater they formed, 2) explosively dispersed macroscopic fragments, 3) dust and small fragments lining the transient crater surface, 4) microshrapnel distributed throughout the crater area, 5) ablation spherules or impact spheroids, 6) metal spherules or dispersed impactor traces in impact glass (see Table 4.2).

4.5.6.1 Large in-situ masses

Large portions of a crater-forming impactor have been found within craters or penetration funnels at only 5 of the 22 sub-km crater localities considered here (see Table 4.2). These are Haviland, a 10.7 x 17 meter elliptical pit (Nininger and Figgins, 1933), Sikhote Alin, at which impactors were found in many of the smaller and several of the larger pits, ranging up to 26.5 meters (Krinov, 1971), the smallest of the Henbury craters, at 9 meters (Spencer and Hey, 1933), Odessa, at which a substantial portion of an impactor was found in the 21 meter crater #2 and in smaller structures (Evans and Mear, 2000), and Campo del Cielo, at which several of the craters or penetration funnels have been found to be associated with large in situ masses. The largest reported impact craters in which a significant portion of the impactor has survived are highly elliptical very low angle impact pits up to at least 26 to 28.5 meters in maximum original dimension, formed in loess at Campo del Cielo (Vesconi et al., 2011).

In nearly all other evaluable cases of confirmed impact craters, including at least 4 instances of craters less than 20 meters in diameter (Gnos et al., 2013; Spencer and Hey, 1933; Milton, 1968a; Tancredi et al., 2009), only a relatively small fraction or small fragments of

impactor material are found inside craters. To summarize clearly, the cumulative record of field investigation suggests that large masses are inconsistently preserved in craters over 10 meters in diameter, and that the dominant outcome in the case of structures larger than 20 meters or so in diameter, is that the impactor is torn apart upon contact with the ground and is explosively ejected from the crater.

4.5.6.2 Explosively dispersed macroscopic fragments

As mentioned previously, there are 16 locations at which macroscopic meteorite fragments or shrapnel have been observed to be directly associated with sub-km impact craters. In 11 of those instances, field reports have noted a substantial asymmetry in the spatial distribution of the ejected impactor fragments relative to the crater (see Table 4.2). There are no instances in which symmetrical distribution of meteorites around a crater is described. The exceptions to this trend represent a lack of data rather than converse findings, as follows: The current systematic review found no specific reference regarding shrapnel distribution relative to specific individual craters at the Sikhote-Alin multiple crater field or at the 4 Campo del Cielo craters at which the impactor is reported to have exploded. The impactor is largely located within the crater at Haviland (Nininger and Figgins, 1933), only a very small quantity of meteorite material was found at Kaalijarv (e.g.: Krinov, 1961), and no macroscopic meteorite fragments that are specifically attributable to a given crater have been reported at Morasko.

The direction of heaviest asymmetric distribution of impactor fragments is typically interpreted as ‘down range’ from the direction of the impactor’s approach (e.g.: Kofman et al., 2010; Urbini et al., 2012; Shoemaker et al., 1988). This is discussed with particular clarity in Urbini et al., 2012. The zone of maximum density of ejected impactor remnants varies

substantially between sites, and is not necessarily highest proximal to the crater and diminishing outward, but may peak at 3 to 4 or more crater diameters beyond the crater rim (e.g.: Folco et al., 2011). The maximum distance to which impactor fragments are ejected is not clearly noted in most cases, but does not seem to be definitively less than the maximum distance traveled by other macroscopic particles of discontinuously distributed ejecta.

4.5.6.3 Crater lining dust and microfragments

Small fragments, ranging from cm-scale or smaller particles to microscopic 'dust,' have been reported lining the preserved transient crater surface at Carancas (e.g.: Tancredi et al., 2009), Sikhote Alin (Krinov, 1964), Dalgaranga (Nininger and Huss, 1960) and Whitecourt (Kofman et al., 2010) and may be suggested by descriptions of field observations of rusty material or stains following the transient crater boundary or fallback surface at Haviland (Nininger and Figgins, 1933) and Campo del Cielo (Cassidy, 1971; Vesconi et al., 2011).

4.5.6.4 Proximal dust and microfragments

In addition to the very small particles of impactor material that have been observed lining the interior of small craters, similar material has been observed, in two cases, extending onto and beyond the crater rim. These are Carancas (Tancredi et al., 2009), where greyish dust draped the rim, and Sikhote-Alin (Krinov, 1964), where scattered irregular microshrapnel particles were collected throughout the crater field. A third case is suggested at Morasko, with 'meteoritic and meteoric dust' reported within the craters and throughout the strewnfield (Classen, 1978), though Stankowski et al. (2002) finds these to be rounded spherules.

It is not clear to what extent microshrapnel or sub-cm fragments of meteorites, whether lining or proximal to a crater, are a pervasive element of small, fresh impacts, especially given

their vulnerability to decomposition (Krinov, 1964), but conscious recognition of the phenomenon may facilitate future observation and capture of relevant samples.

4.5.6.5 Ablation microspherules and impact spheroids

While impact or ablative spherules or spheroids have been described in field reports from at least 9 of the 16 small impact craters at which meteorites or meteorite shale were reported, the subject is challenging to clearly summarize due to inconsistencies in terminology and degree of descriptive detail. It is at least clear, from cumulative reports, that there are two distinct classes of small, spherical objects, found at impact sites. These are ablative microspherules, typified at Sikhote Alin, where Krinov (1964) found them ranging in size from a few microns up to 0.7mm, and impact spheroids, typified at Barringer or Wabar (e.g.: Leya et al., 2002; Mittlefehldt et al., 1992) which are generally somewhat larger, ranging from substantially less than a millimeter (e.g.: Hodge and Wright, 1971) to several mm (e.g.: Mittlefehldt et al., 1992). Ablation microspherules are formed from the ablation of meteoroids during atmospheric deceleration, and impact spheroids are formed from the melting of impactor and/or target material at the moment of initial contact between the impactor and the ground. There appears to be substantial overlap in size between these two groups, but a great deal more work will be needed before reliable interpretation becomes feasible.

Among the group of sub-km impact craters, impact spheroids have been clearly described at Whitecourt (in crater fill, Kofman et al., 2010), Kamil (amidst ejecta, Folco et al., 2011), Wabar (amidst ejecta, Mittlefehldt et al., 1992) Henbury (amidst ejecta, Hodge and Wright, 1971), and Boxhole (Hodge and Wright, 1973). Impact spheroids are additionally suggested, but

less clearly described in literature describing Odessa (Evans and Mear, 2000) and Morasko (Folco et al., 2011).

Ablation microspherules, are clearly described amidst the strewnfields at Morasko (Folco et al., 2011) and Sikhote Alin (Krinov, 1964), and are suggested, but less clearly described, at Kaalijarv (Krinov, 1961).

When present, impact spheroids are typically reported distributed among ejects, within a few crater diameters of the associated crater rim. If they are unambiguously demonstrated to be composed of glass containing both impactor and target rock components, as at Wabar, Kamil or Henbury (Mittlefehldt et al., 1992; Folco et al., 2011; Hodge and Wright, 1971), impact spheroids might be considered compelling and unambiguous evidence of a crater forming impact.

Ablation microspherules, on the other hand, may be present within a strewnfield in the absence of an impact and are easily confused with cenospheres and other spherules of anthropogenic origin. Ablation microspherules are not suggestive or diagnostic of an impact event. Distinguishing between the two very similar groups of objects and clear evaluation of composition is critical to any potential utility in impact crater identification.

It is also worth noting that research at Sikhote Alin (Krinov, 1964) suggests such evidence may be subject to rapid destruction or burial within a few years after impact in some environments, though altered remnants may persist. At Morasko, Stankowski et al. (2002) found the aged remnants of microspherules to be dominantly composed of goethite, maghemite, and lepidochrosite (rust).

Figure 4.3. *Scoriaceous impact glass from the Monturaqui (left) and Henbury (right) impact craters. Impact glasses have been found at 8 of the 22 sub-km crater locations, and have proven to be an effective research target for locating unambiguous impact evidence including metal spherules, indicative elemental ratios, and formation of planar deformation features, diaplectic glass, and high pressure mineral polymorphs in trapped mineral grains.*

4.5.6.6 Impactor components in impact glass

Glassy ejecta has been clearly described at 8 of the 22 currently recognized sub-km impact crater locations examined in this paper. (see Fig. 4.3) In 7 of the 8 cases, this glass has been demonstrated to be composed of both impactor and target materials, and has captured undigested fragments and grains of target rocks. The exception is Wolfe Creek. Glass from this

location has been reported (Shoemaker et al., 2005), but the current effort produced no related record of analysis. In 6 of the 7 cases, FeNi metal spherules have been observed within samples. In the 7th case, Kalkkop, despite a lack of reported metal, both dispersed impactor components and isotopic traces of the impactor have been measured (Koeberl, 1994; Koeberl et al., 1994) (see Table 4.4). Glassy ejecta ranges from scoriaceous to vesicular, but is occasionally nearly free of bubbles, and ranges in size from millimeters to 10 cm or more (e.g.: McColl, 1990; Gnos et al., 2013; Ugalde et al., 2007). In cases where they are present, ejected impact glass fragments are found up to several crater diameters from the craters, and are frequently distributed strongly asymmetrically.

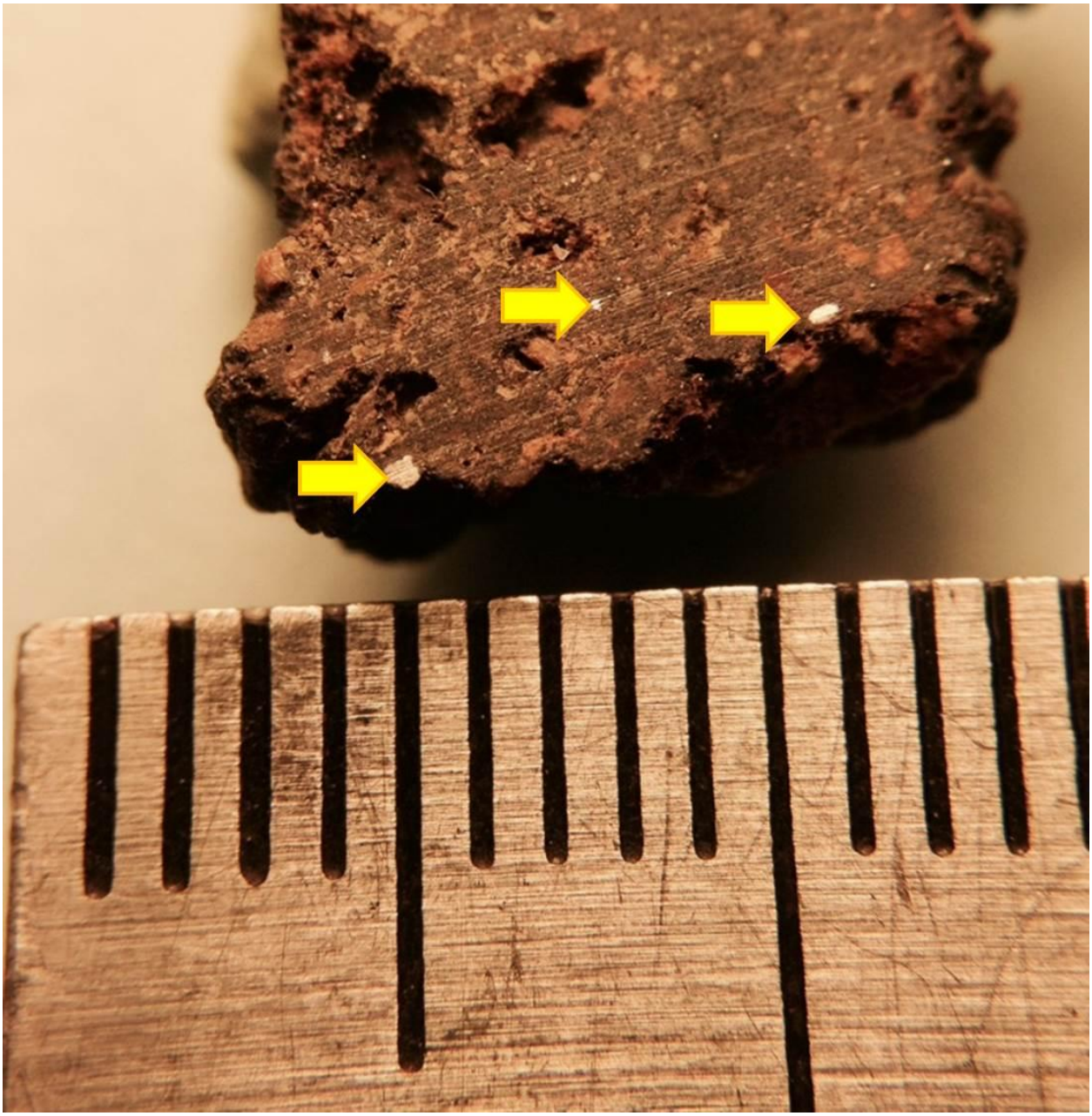

Figure 4.4. *FeNi metal spherules visible to the unaided eye in impact glass from the Monturaqui impact crater. The width of the entire sample is 11 mm. The largest spherule is significantly less than 1 mm in diameter.*

FeNi metal spherules preserved in ejected vesicular impact glass are typically spherical to subspherical, and range in size from less than a micron to greater than a millimeter, with small examples far more abundant than large (D'Orazio et al., 2011; Gibbons et al., 1976; Gnos et al.,

2013; Ding and Veblen., 2004; Bunch and Cassidy, 1972). In some cases, such as at Aouelloul, metal spherules in glass may be uniformly too small to observe with the unaided eye, and examples may be sparse (Chao et al., 1966a; El Goresy, 1968). In other cases, such as at Monturaqui (Bunch and Cassidy, 1972), a significant fraction of the spherules may be readily observed in cut specimens with the unaided eye. (see Fig. 4.4)

Gibbons et al. (1976) examined the FeNi spherules in ejected impact glass from Monturaqui, Henbury, and Wabar, and found the metal to be enriched in Ni and Co relative to Fe compared to the original impactor, and noted that enrichment scales with size of the spherules, with the largest spherules most closely matching the original composition of the impactor. Similar results were produced by Bunch and Cassidy (1972).

Even without entrained FeNi spherules, impact glasses from small craters present several possible avenues for building a suggestive or diagnostic case for the existence of an impact crater. The presence of congruously situated glassy ejecta that is clearly demonstrated to be composed of a combination of target material and meteorite components is very reasonably considered unambiguous evidence of hypervelocity terrestrial meteorite impact. Siderophile and trace element enrichment and changes in isotopic composition relative to unmelted target materials have shown potential for both crater confirmation and impactor identification (Morgan et al., 1975; Koeberl and Auer, 1991; Koeberl, 1994; Koeberl et al., 1994; Koeberl, 1998), as has study of minerals derived from precursors through high-temperature melting and quick cooling (e.g.: El Goresy, 1965; El Goresy, 1968). Beran and Koeberl (1997) observed that ejected impact glasses are dry compared to glasses of terrestrial origin, and suggested that very dry glasses may be suggestive of an impact origin. Glassy ejecta has also proven to be an effective host for widely accepted classes of grain-scale impact evidence; high pressure polymorphs,

diaplectic glass and planar deformation features have variously been found in mineral grains trapped in glassy ejecta at Wabar, Monturaqui, and Kamil (Chao et al., 1961; Gnos et al., 2013; Bunch and Cassidy, 1972; Ugalde et al., 2007; D'Orazio et al., 2011; Urbini et al., 2012). This is significant, as these 3 classes of unambiguous impact evidence have only been confidently identified at 5 sub-km craters in total (see Table 4.4). Impact glass is also potentially useful in confirming very old craters, as it may preserve crater-forming impact evidence for small craters well after crater morphology has softened and after individual meteorites have been lost to terrestrialization.

Table 4.3. Aspects of crater morphology.

	Raised Rim(s)	Asymmetric or uneven rim height	Notably hummocky rim surface	Ejecta over uplift bedding in rim	Rollover lip at all or part of perimeter	Max. continuous ejecta in crater diameters	Notably assymetric ejecta distribution. 'Bilat' = bilateral.	Rays. Poss = possible.	Max discontinuous ejecta distance in crater diameters
Carancas	yes	yes	yes	yes	yes	~1	yes	yes	~26
Haviland	yes		--	--	--	--	--	--	--
Dalgaranga	yes	yes	yes	yes	yes	<3	bilat	--	≥12
Sikhote-Alin	yes	yes	yes	--	--	--	--	--	--
Whitecourt	yes	yes	--	--	--	~1	bilat	--	≥14
Kamil	yes	yes	yes	yes	yes	~1	yes	yes	≥33
Sobolev	yes	yes	--	yes	--	≤1	--	--	≥1
Veevers	yes	yes	--	yes	--	≤0.5	yes	yes	--
Ilumetsa	yes~	yes	--	--	--	--	--	--	--
Morasko	yes	yes	--	--	--	--	--	--	--
Kaalijarv	yes	--	--	yes	--	--	--	--	--
Campo del Cielo	var.	yes	--	--	--	var. ≤0.5	--	--	--
Wabar	yes	--	yes	yes	--	--	yes	--	>7
Henbury	yes	yes	yes	yes	yes	--	yes	yes	--
Odessa	yes	yes	yes	yes	--	≤0.75	yes	--	>12
Boxhole	yes	yes	--	yes	yes	≤0.5	yes	--	--
Macha	yes	yes	--	--	--	<<0.25	--	--	--
Monturaqui	yes	yes	yes	--	--	--	--	poss.	--
Aouelloul	yes	yes	--	--	yes	--	yes	--	--
Amguid	yes	yes	--	yes	yes	≥1	--	--	--
Kalkkop	yes	yes	--	--	yes	--	--	--	--
Wolfe Creek	yes	yes	--	Yes	yes	--	yes	--	--

4.5.7 Crater morphology

All 22 known sub-km crater and penetration funnel locations reveal simple, bowl shaped structures with no trace of central uplift. Although there are a few weathered exceptions, such as some of the structures at Campo del Cielo or the buried smaller structures at Odessa, most sub-km impact craters and pits also have a raised rim. 22 of the 22 (all) listed sites show raised rims partially or completely surrounding at least some of the structures (see Table 4.3).

Among the 18 of these locations presenting clear evidence of impact origin, several additional potentially useful generalities emerge from aggregate consideration. In 15 of 18 cases, the rim is described as distinctly uneven in height. In 8 cases, it is hummocky in character, based on descriptions or images, and in 10 cases, authors specifically report the rim to be composed of two distinct components; uplifted and outwardly tilted layers of rock or soil, overlain by an unconsolidated layer of ejecta. In 8 cases, the lip of the crater is observed to be uplifted to the point of overturning at some portion of the crater perimeter, producing inverted stratigraphy on the rim. At 13 of these craters, at least some remnant of a continuous ejecta blanket is described beginning at the crater rim and thinning outward. At 11 locations, authors have described rims as unevenly surrounding the crater - either significantly asymmetric or roughly bilaterally symmetric. In 7 out of 8 cases in which it was described, the continuous ejecta blanket extended no farther than 1/2 to 1 crater diameter beyond the crater rim. In the sole remaining case, it reached to less than 3 crater diameters (see Table 4.3).

4.5.7.1 Rims

Crater rims are underpinned by rock or soil displaced outward and upward, with the cumulative movement accomplished through complex and locally varied faulting, folding and rupturing (e.g.: Shoemaker and Wynn, 1997; Evans and Mear, 2000; Reimold et al., 1998). Where folds are described, they are typically accomplished through brittle failure, with joints closely spaced in the rock (Milton, 1968a). The dip associated with uplifting of rocks beneath crater rims may increase progressively towards the upper portion of the crater wall (e.g.: Lambert et al., 1980; Milton, 1968a; Evans and Mear, 2000), though this is not uniformly the case. Shoemaker et al. (2005) observes the steepest outwardly dipping beds in the walls at Veevers to be near the bottom, and describes outward dip decreasing upward. Either way, the outward dip

frequently culminates in vertical or overturned strata near the top of crater rims. An overturned component at the top of the rim is not present in all cases, is often expressed only sporadically or in only one section around the rim, and does not appear to become increasingly likely with greater size (see Table 4.3). Several authors have observed or inferred complex fracturing associated with accommodation underlying the raised rim and extending significant distances beyond (Urbini et al., 2012; Khryanina, 1981; Plado, 2012). Evans and Mear (2000), working at Odessa, record uplift associated with such extended accommodation still present at approximately 0.25 crater diameters beyond the crater rim. This may have implications for estimations of excavated volume.

Rims are very seldom evenly raised, and are often hummocky along their crest and flanks (see Table 4.3). In addition to the internal complexity mentioned above, they also tend to vary around the circumference in angle of inner slope, dip of the uplifted strata, in height, and in depth of coverage by ejecta, and often only partially encircle structures. Authors variably attribute these irregularities to slope or other variations in topography, angle of impactor approach, pre-existing faults or fractures, or uneven erosion (e.g.: Herd et al., 2008; O'Neill and Heine, 2005; Sanchez and Cassidy, 1966; Urbini et al., 2012; Folco et al., 2011), with more than one factor often coming into play. All told, this variability may suggest that the final details of the rim of a crater formed in this size range may be strongly sensitive to variations in pre-impact target surface morphology or in target material composition.

At Henbury, it is demonstrated that rim height is increased between two adjacent craters of similar size and that no rim is formed within the craters where two simultaneously formed crater basins of similar size overlap (Alderman, 1932; Milton, 1968a).

4.5.7.2 Ejecta blanket

The upper portion of crater rims is often described as composed of a distinct layer of ejecta overlying uplifted or overturned bedrock (e.g.: Kenkmann et al., 2009; Shoemaker et al., 2005; Lambert et al., 1980). This upper layer comprises the innermost portion of a continuous blanket of ejecta that is generally thick close to the crater rim, and which thins rapidly outward, typically ending within 0.5 to 1 crater diameter (see Table 4.3). In the 9 cases in which a continuous ejecta blanket is not reported, it may be buried by aeolian sediment, removed by erosion, covered by soil and plant life, or if the structure is misidentified, may simply have never existed. A distinction between continuous and discontinuous ejecta seems to be both real and useful for craters at this scale, as several authors have communicated, either through words or illustrations, an approximate boundary between an often very asymmetrically encircling blanket of contiguous ejecta and a surrounding zone of discontinuously distributed ejecta (e.g.: Kenkmann et al., 2009; Urbini et al., 2012; Lambert et al., 1980). The first zone extends from less than 1/2 to a little over 1 crater diameter beyond the crater rim in maximum dimension, while discontinuous ejecta is distributed in a patchy and erratic field (e.g.: Urbini et al., 2012), with a dominantly downrange or bilateral trajectory, sometimes to 10 to 20 or more crater diameters.

In a few cases, a crudely inverted stratigraphic sequence has been observed in the continuous ejecta component (e.g.: Shoemaker et al., 2005; Shoemaker et al., 1988). Asymmetries in ejecta distribution are dominantly attributed to angle of impact, but causes such as inhomogeneities in target material and asymmetry of impactor have also been suggested (Urbini et al., 2012). Pre-impact soil has been identified, based on textural changes and the

presence of organic remnants, beneath the continuous ejecta blanket in rare cases (e.g.: Khryanina, 1981; Kofman et al., 2010).

4.5.7.3 Crater rays

In addition to the typical continuous ejecta blanket and discontinuous ejecta field, rays of ejecta have been reported at 4 craters, and may be discernible at a 5th (see Table 4.3). At Carancas, Tancredi et al. (2009) and Kenkmann et al. (2009) describe pristine rays of ejecta extending asymmetrically to as much as 20 crater diameters. At Kamil, easily distinguished rays (Folco et al., 2010, 2011 (illus.); Urbini et al., 2012) extend from the crater rim to a distance of <4 to >6 crater diameters. At Veevers, Shoemaker et al. (2005) notes that ejecta rays/lobes correlate to high points on the crater rim. At Henbury, craters number 3 and 4 (Alderman, 1932) preserve short remnants of rays extending to about 1/2 crater diameter (Milton and Michel, 1965; Milton, 1968a). Milton and Michel (1965) also point out that these rays are composed of specific rock types originating between the crater rim and crater center at the radius of the crater from which they orient, and that material within the rays is thrown a distance from the crater roughly inversely corresponding to its original distance from the center of the crater. Material originating closest to the center is thrown the farthest. A similar relationship, with highly shocked materials distributed farther from the crater than materials exhibiting lower levels of shock deformation, is found in ordinary ejecta at Tenoumer and Barringer (Jaret et al, 2014, and references therein), so may speak to a broad pattern. It may also be the case, per Urbini et al. (2012) that shallower target materials are thrown farther than material that originates farther below ground. A possible 5th example of relict crater rays may be indicated at Monturaqui, upon consideration of geological mapping of ejecta shown in Ugalde et al. (2007). Considered

in aggregate, the sparse record of observed and described crater rays on earth points to a comparatively ephemeral feature, potential widely expressed but poorly preserved.

4.5.7.4 Crater fill

The crater floor in all but the youngest impact structures is generally buried beneath wind-blown, organic, or water-borne sediment (e.g.: Nininger and Figgins, 1933; McCall, 1965b; Shoemaker et al., 2005; Urbini et al., 2012). At 18 out of 22 total locations, post impact sedimentary deposits cover all or a significant portion of the crater floors. In a significant number of instances, the sediment filled the crater to greater than half its estimated or measured depth, though detailed descriptions are lacking in many cases. The nature of sedimentary fill varies with target setting, but is typically described as some combination of aeolian, pond, or organic sediment mixed with erosional debris (colluvium) accumulated from mass wasting of the raised crater walls and rim. Sedimentary and erosional fill typically overlies a zone or lens of allochthonous polymict breccia (e.g.: Urbini et al., 2012; Evans and Mear, 2000; Reimold et al., 1998). The term breccia, in small impact crater litrature, is broadly used to refer to both lithified and unconsolidated crater-filling clastic material, with no distinction typically made between the two. At Kamil and Kalkkop, a detailed analysis of crater-filling breccia suggests that it may consist of at least two zones, with the lower zone possibly produced largely by collapse or slumping of the transient crater wall and the upper portion, comprised of generally smaller clasts, suggestive of fallback material (Urbini et al., 2012; Reimold et al., 1998). An equivalent distinction was inferred from gravity data at Wolfe Creek (Oneill and Heine, 2005). Below this, a fractured crater floor of parautochthonous breccia is inconsistently observed or inferred in reports, and this overlies intact basement rock or sediment. In total, these variably reported units suggest at least 4 potentially distinct zones of fill overlying intact basement rock or sediment..

From the top down: post impact sediment, fallback breccia, collapse breccia, fractured crater floor. (see Fig. 4.5)

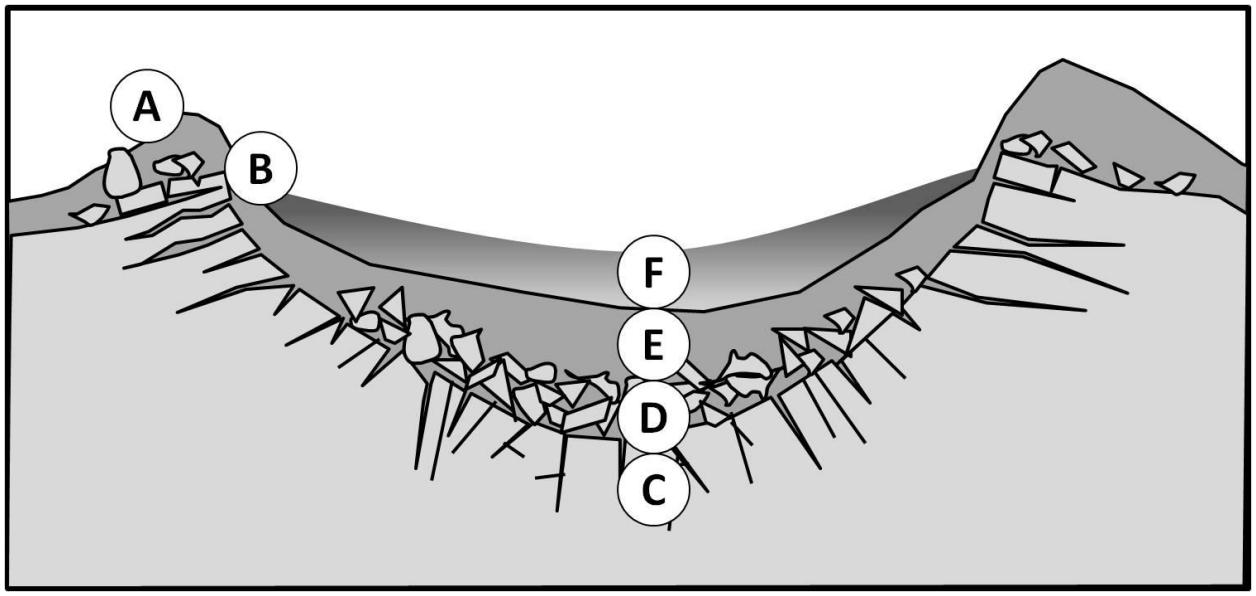

Figure 4.5. *Idealized cross section of a small, simple crater based upon compiled field reports: A hummocky, unevenly raised rim (A) comprised of ejecta overlying uptilted or overturned soil or bedrock (B) partially or completely surrounds an excavated bowl. If deep enough to reach bedrock, the floor is typically fractured (C) and overlain by coarse collapse breccia (D), with a lens of fallback breccia (E) overlying the collapse breccia. Fallback and ejection breccia also comprises the upper portion of the raised rim, and extends asymmetrically beyond the rim as a continuous ejection blanket not typically exceeding 1 crater diameter before giving way to discontinuously distributed ejecta. Within the crater, collapse and fallback breccia are typically buried beneath a lens of post-impact sediment (F).*

4.5.7.5 Erosion

Because regional erosion rates can change wildly over geologic time, and because the few known small craters vary significantly in age, size, target material, and topographic setting, discerning generalizable, predictive trends regarding the effects of erosion and age on small impact craters is challenging and imprecise at best. Nevertheless, a number of months spent in deep reading and cataloging of the relevant literature may have yielded potentially useful impressions. With age, rims diminish in height, with unconsolidated ejecta removed preferential

to uplifted bedrock. Craters typically fill with a combination of eroded colluvium from crater walls and with aeolian or pond sediments, covering and preserving collapse and fallback breccias. As craters become shallower, they also become larger in diameter. Rims may grow smoother, less hummocky, and more rounded, though this must certainly vary. Target material significantly affects the rate of loss in rim elevation and the resulting character of the remnant. Smaller craters may be completely buried, as at Odessa, may become subtle depressions as at Henbury or Haviland, or may lose their rim completely, as in some cases at Campo del Cielo. Meteorites, outside of craters, which are typically initially found within inches of the top of the soil, may be buried beneath accumulating aeolian sediment or beneath the slowly collapsing rim. And the ejecta field, as has happened at Wolfe Creek, may also be buried beneath accumulating sediment.

Table 4.4. Reported evidence supporting impact origin of structures.

	Meteorite or Shale Present	Planar fractures in quartz	Shatter Cones	Planar deformation features	Coesite (co) and/or stishovite (st)	Diaplectic Glass	Glassy ejecta	Metal in glass	Isotopic evidence in glass
Carancas	yes	maybe	--	maybe	--	--	maybe	--	--
Haviland	yes	--	--	--	--	--	--	--	--
Dalgaranga	yes	--	--	--	--	--	--	--	--
Sikhote-Alin	yes	--	--	--	--	--	--	--	--
Whitecourt	yes	yes	--	maybe	--	--	--	--	--
Kamil	yes	yes	--	yes	--	--	yes	yes	--
Sobolev	--	--	--	--	--	--	--	--	--
Veevers	yes	--	--	--	--	--	--	--	--
Ilumetsa	--	--	--	--	--	--	--	--	--
Morasko	yes	--	--	--	--	--	--	--	--
Kaalijarv	yes	--	yes	--	--	--	--	--	--
Campo del Cielo	yes	--	--	--	--	--	--	--	--
Wabar	yes	yes	--	yes	co/st	--	yes	yes	--
Henbury	yes	--	--	--	--	--	yes	yes	--
Odessa	yes	--	yes	--	--	--	yes	yes	---
Boxhole	yes	--	--	--	--	--	--	--	--
Macha	--	yes	--	maybe	st(?)	--	--	--	--
Monturaqui	yes	yes	--	yes	co	yes	yes	yes	--
Aouelloul	--	maybe	--	--	--	--	yes	yes	Re-Os
Amguid	--	yes	--	maybe	--	--	--	--	--
Kalkkop	--	yes	--	yes	--	yes	yes	--	Re-Os
Wolfe Creek	yes	yes	yes	yes	--	--	yes	--	--

4.5.8 Widely accepted impact evidence

The most widely accepted classes of impact evidence typically employed in the demonstration of impact origin for larger craters, such as shatter cones, planar deformation features, high pressure mineral polymorphs or diaplectic glass, have only been unambiguously reported at 7 sub-km impact craters, and 3 of these, Monturaqui, Kallkkop and Wolfe Creek, are among the largest of the group (see Table 4.4).

4.5.8.1 Shatter cones

Shatter cones are sparsely reported in impact craters less than 1 km in diameter (see Table 4.4). Radiating fractures, weakly resembling shatter cones, were observed in the largest craters at Sikhote-Alin (Krinov, 1971), and Khryanina (1981) reports shatter cones at Sobolev. In both of these instances, published photographs are not compelling. Images show simple fractures producing roughly conical structures only weakly resembling shatter cones. Deitz (1968) presents small but relatively well-formed shatter cones found in debris from the crater wall at the largest crater at Kaalijarv, and Gnos et al. (2013) finds radial striations in shock lithified sand at Wabar. Whether the structures at Wabar share a common origin with true shatter cones is unclear. Evans and Mear (2000) remembers a single instance of finding a shatter cone sample amidst ejecta within the Odessa crater in the 1950s, and O'neille and Heine (2005) report shatter cones in a small section of the rim at Wolfe Creek. To sum this up, the publications considered here present only 3 confident descriptions, all very brief, and a single photograph.

4.5.8.2 Coesite and stishovite

High pressure mineral phases diagnostic of a hypervelocity impact have been clearly described at only 2 sub-km impact craters. At Wabar, coesite and stishovite have been found in both shock lithified sandstone and in quartz grains trapped in ejected glass (Chao et al., 1961; Gnos et al., 2013). At Monturaqui, coesite has (only) been observed in quartz grains captured in glassy impactites (Bunch and Cassidy, 1972; Ugalde et al., 2007). In addition to the well supported coesite and stishovite occurrences at Wabar and Monturaqui, Gurov and Gurova (1998) tentatively report possible observations of stishovite at Macha.

4.5.8.3 Planar features and diaplectic glass

Planar deformation features are confidently described from only 5 of the 22 possible or confirmed sub-km impact crater localities. Planar fractures are tentatively or confidently described at an additional 5 locations (see Table 4.4).

The smallest crater at which PFs or PDFs have been tentatively reported is Carancas, at 13.5 meters. Tancredi et al. (2009) reported increased abundances of PFs in quarts grains compared to controls from the surrounding area. The hosting grains were recovered from lower layers of ejecta, about 1/3 crater diameter down-range from the impact rim. Kenkmann et al. (2009) investigated and found no similar PFs or PDFs. At Whitecourt (36 meters), likely PFs are present in quartz, with 1 to 3 sets found in grains within the transient crater surface (Kofman et al., 2010). A control study found planar microstructures to be very scarce in quartz grains in the surrounding area (Kofman et al., 2010). Sparse examples of possible PFs, present in 1 to 3 sets, have also been identified in samples collected from crater walls at Macha (Gurov and Gurova, 1998), Aouelloul (Koeberl et al., 1998), and Amguid (Lambert et al., 1980).

At Kamil, Wabar, Monturaqui, Kalkkop and Wolfe Creek, PFs and PDFs have been reported with confidence. The smallest crater at which PFs and PDFs have been clearly described is Kamil, at only 45 meters. Both categories of evidence, along with examples of pronounced mosaicism, were reported in quartz grains captured within melted material and amidst ejecta (D'Orazio et al., 2011; Urbini et al., 2012). At Wabar, PFs, PDFs and mosaicism were found, along with coesite and stishovite, in quartz grains in ejecta (Gnos et al., 2013). At Monturaqui, PFs and PDFs have been identified, along with diaplectic glass and coesite, in grains captured in the glassy impactites (Bunch and Cassidy, 1972; Ugalde et al., 2007). At

Kalkkop, up to 6 sets of PDFs were found in quartz grains revealed during drilling (Reimold and Koeberl, 2014; Koeberl et al., 1994a; Reimold et al., 1998), and PFs and PDFs have been indexed in grains from the crater rim at Wolfe Creek (O'neille and Heine, 2005).

Diaplectic glass is present in at least two cases. It was observed formed in quartz, at Kalkkop, by Reimold et al. (1998) and in quartz and feldspar, at Monturaqui, by Bunch and Cassidy (1972) and Ugalde et al. (2007).

The cumulative record of small impact crater research suggests that planar fractures and planar deformation features may be a useful tool for hypervelocity impact recognition even at relatively small craters, so long as target materials are conducive to their formation. Field reports also cumulatively suggest that optimal locations for their recovery likely include particles embedded in the buried transient crater walls, grains trapped within glassy impact ejecta, and amidst allochthonous fallback ejecta within or beyond the crater rim, with fallback ejecta providing the least productive of the 3 environments and glass ejecta providing the most.

4.5.8.4 Shock induration and shock lithification

Compaction and/or partial melting has produced indurated rock from unconsolidated sediments in at least two instances reported at small impact craters. At Wabar, sub-vitric shock lithification of quartz-rich sand was reported by Gnos et al. (2013) and Shoemaker and Wynn (1997). At Campo del Cielo, loess was compressed and/or baked to clay stone (Cassidy, 1971). Descriptions at both Wabar and Campo del Cielo appear to suggest that the boundary between coherent shock-lithified target material and unshocked sediment is not abrupt, but rather gradational, with crumbling material intermediate between fully lithified and sublithified sediment. Location of coesite in shock consolidated sandstone at Wabar suggests that shock

induration is a relatively high GPa function, at least in a quartz sand environment, and that such materials may be good targets for potential identification of diagnostic indicators of impact. It was also within shock indurated material that possible proto-shatter cones were found at Wabar (Gnos et al., 2013.) Similar materials have been previously produced in explosive experiments and observed in lunar samples (Short, 1966).

4.6 Conclusions - The identification of small impact craters

Small impact crater are among the most common geological structures on rocky planetary surfaces in the inner solar system, but are extraordinarily rare on earth, and are significantly under-represented in the terrestrial record of impact craters (Brown et al., 2002; Bland and Artemieva, 2006). Structures less than 1 km in diameter are less robust in their morphological expression, more quickly eroded, less easily distinguished from a wide variety of terrestrial structures of non-impact origin, and less likely to display clear macroscopic or microscopic indicators of shock metamorphism due to lower impact energies and smaller volumes of material subjected to extreme shock. Due to a sparsity of impact evidence, most sub-kilometer craters have been recognized on the basis of associated meteorites or meteorite remnants. It is hoped that an improved understanding of the past record of impact evidence will aid in future efforts to discriminate between small craters and similar structures of terrestrial origin.

4.6.1 Unambiguous evidence of impact origin for small craters

Considering these structures as a group, it becomes apparent that shattercones and grain scale indicators of hypervelocity impact are of substantial but limited utility in the recognition of sub-kilometer impact craters. Confident record of the occurrence of PDFs has only been put forth for 5 craters, and 3 of these are among the largest of the group, Monturaqui, Kalkkop, and

Wolfe Creek. This trio also captures both published instances of diaplectic glass, one of only three confident publications of shatter cones, and one of only two confident published observations of coesite or stishovite. Of the classes of petrologic or grain-scale evidence most often used as confirmation of impact origin for larger structures, meaning shatter cones, planar deformation features, high pressure mineral polymorphs, and diaplectic glass, only 4 craters smaller than 350 meters in diameter are associated with confidently and clearly published examples. Shatter cones have been reported at Kaalijarv and Odessa, and PDFs have been found at Kamil and Wabar (Dietz, 1968; Evans and Mear, 2000; D'Orazio et al., 2011; Urbini et al., 2012; Gnos et al., 2013). Coesite and Stishovite have been additionally reported at Wabar (Gnos et al., 2013). Among the smaller craters, Kamil and Wabar are somewhat special cases. They are exceptionally young, well preserved, located in regions with no overlying soil or ground-covering vegetation, and occur in dry quartz sandstone and sand, respectively (Urbini et al., 2012; Gnos et al., 2013); in short, optimal environments for the formation, preservation, and recovery of these well-understood and often used lines of impact evidence.

Meteorites prove to be an important class of diagnostic impact evidence among the sub-km crater population, serving as a dominant or sole class of evidence at 16 of the 22 sub-km crater locations and 16 of 18 locations at which unambiguous evidence of impact origin has been produced. The relationship between meteorites and impact craters is variously supported by proximity, specific distribution and by the presence of shrapnel morphology. Additional lines of diagnostic evidence used in building solid cases for the impact origin of sub-km craters hinge on impact related melt products containing either small preserved particles of the impactor or chemical or isotopic indicators of an impactor mixed with melted target material. These include either impact spheroids or glassy impact ejecta, which may reveal remnants of unoxidized metal,

siderophile element enrichment in glass or melt relative to pre-impact target rock, or indicative ratios of isotopes of rhenium and osmium (Koeberl, 1994; Koeberl et al., 1994).

4.6.2 Consideration of evidence supporting impact origin for this group

A detailed review of these structures in the context of their best evidentiated examples has also brought up, as mentioned several times previously, 4 structures for which unambiguous evidence of impact origin does not appear to be present in peer-reviewed publications. These are Amguid, Macha, Ilumetsa and Sobolev. There is little doubt that Amguid is an impact crater. It is entirely consistent in morphology with other well evidentiated sub-km impact craters. The site is sparsely represented by publications in the literature, however, and whether planar elements reported in Lambert et al. (1980) represent PDFs or Planar Fractures has not been clearly discerned in the portion of the literature here examined. No meteorite traces have been reported from the site, but it seems likely that a future study will provide clear confirmation. At Macha, while planar fractures (and possibly even PDFs) have been described amidst sparse publications, the descriptions suggest that the structures are morphologically inconsistent with any other known small impact craters in several regards (see Table 4.3 and Macha summary). More fieldwork is needed. At Ilumetsa and Sobolev, the reverse is the case. Publications are abundant, and the structures are somewhat similar to other impact craters in some morphological details, but unless it has been missed in this effort, no significant evidence suggestive of impact origin has been presented (see Table 4.4). These findings suggest that, until such results emerge from renewed fieldwork, these structures should only inform our general understanding of craters subject to some degree of reservation. A similar conclusion regarding Ilumetsa has previously been published in Plado (2012).

4.7 Acknowledgements

Thanks to Steve Arnold for recounting personal observations at the Haviland, White Court, Odessa, and Monteraqui craters. Thanks to Don McColl for discussion regarding Wolfe Creek. And thanks to Marvin Killgore for comments and thoughts regarding shrapnel and iron 'shale,' and for recounting observations at Imilac. Also, great thanks to Jerri Stevens for patient feedback and assistance.

4.8 References

Alderman A. R. 1932. The meteorite craters at Henbury, Central Australia, with addendum by L. J. Spencer. *Mineralogical Magazine* (London) 23:19-32.

Axon H. J. and Steele-Perkins E. M. 1975. Fracture mechanism of Henbury meteorite by separation along surfaces of shear faulting. *Nature* 256:635.

Badyukov D. D. and Raitala J. 2012. Ablation spherules in the Sikhote Alin meteorite and their genesis. *Petrology* 20(6):520-528.

Barringer B. 1967. Historical Notes on the Odessa Meteorite Crater. *Meteoritics* 3: 161–168.

Basurah H. M. 2003. Estimating a new date for the Wabar meteorite impact. *Meteoritics & Planetary Science* 38:A155–A156.

Bender Koch C. and Buchwald V. F. 1994. Weathering of Iron Meteorites from Monturaqui, Chile. *Meteoritics* 29:4,443.

Beran A. and Koeberl C. 1997. Water in tektites and impact glasses by fourier-transformed infrared spectrometry. *Meteoritics & Planetary Science* 32:211–216.

Bevan A. W. R., Shoemaker E. M., and Shoemaker C. S. 1995. Metallography and thermo-mechanical treatment of the Veevers (IIAB) crater-forming meteorite. *Records of the Western Australian Museum* 17:51-59.

Bevan A. W. R. 1996. Australian crater-forming meteorites. *AGSO Journal of Australian Geology & Geophysics* 16:421-429.

Bland P. A. and Artemieva N. A. 2006. The rate of small impacts on Earth. *Meteoritics & Planetary Science* 41:607–631.

Brown P., ReVelle D. O., Silber E. A., Edwards W. N., Arrowsmith S., Jackson Jr L. E., Tancredi G., and Eaton D. 2008. Analysis of a crater-forming meteorite impact in Peru. *Journal of Geophysical Research* 113:E09007.

Brown P., Spalding R. E., ReVelle D. O., Tagliaferri E., and Worden S. P. 2002. The flux of small near-Earth objects colliding with the Earth. *Nature* 420:294–296.

Buchwald V. F. 1975. *Handbook of iron meteorites: Their history, distribution, composition, and structure*. Berkeley: University of California Press.

Bunch T. E. and Cassidy W. A. 1968. Impact-induced deformation in Campo del Cielo meteorite. French, B.M. and Short, N.M., eds., *Shock Metamorphism of Natural Materials*, Mono Book Corp., Baltimore, MD, 601-612.

Bunch T. E. and Cassidy W. A. 1972. Petrographic and electron microprobe study of the Monturaqui impactite. *Contributions to Mineralogy and Petrology* 36:95–112.

Campbell Smith W. and Hey M. H. 1952. The silica-glass from the crater of Aouelloul Adrar, western Sahara. *Bulletin de l'Institut Francais d'Afrique Noire* 14(3):762-776.

Cassidy W. A. 1968. Descriptions and topographic maps of the Wolf Creek and Boxhole craters, Australia (abstract). French, B.M. and Short, N.M., eds., *Shock Metamorphism of Natural Materials*, Mono Book Corp., Baltimore, MD, p. 623.

Cassidy W. A. 1954. The Wolf Creek, Western Australia, meteorite crater (CN =– 1278,192). *Meteoritics* 1:197–199.

Cassidy W. A. 1971. A small meteorite crater: Structural details. *Journal of Geophysical Resources* 76(17):3896–3912.

Cassidy W. A. and Renard M. L. 1996. Discovering research value in the Campo del Cielo, Argentina, meteorite craters. *Meteoritics & Planetary Science* 31:433–448.

Cassidy W. A., Villar L. M., Bunch T. E., Kohman T. P., and Milton D. J. 1965. Meteorites and craters of Campo del Cielo, Argentina. *Science* 149:1055–1064.

Chao E. C. T., Fahey J. J., and Littler J. 1961. Coesite from the Wabar crater, near Al Hadida, Arabia. *Science* 133:882-883.

Chao E. C. T., Dwornik E. J., and Merrill C. W. 1966a. Nickel-iron spherules from Aouelloul glass. *Science* 154:759-765.

Chao E. C. T., Merrill C. W., Cuttitta F., and Annell C. 1966b. The Aouelloul crater and the Aouelloul glass of Mauritania. Africa. *EOS Transactions of the American Geophysical Union* 47:144.

Classen J. 1978. The meteorite craters of Morasko in Poland. *Meteoritics* 13: 245–255.

Connolly H. C., Smith C., Benedix G., Folco L., Righter K., Zipfel J., Yamaguchi A., and Chennaoui Aoudjehane H. 2007. The Meteoritical Bulletin, No. 93, 2008 March. *Meteoritics & Planetary Science* 43:571–632.

Cressy P. J., Schnetzler C. C., and French B. M. 1972. Aouelloul Glass: AI-26 limit and some geochemical comparisons with Zli sandstone. *Journal of Geophysical Research* 77:3043-3051.

Dietz R. S. 1968. Shatter cones in cryptoexplosion structures. In *Shock Metamorphism of Natural Materials* (eds. B. M. French and N. M. Short). Mono book corp., Baltimore, Maryland, USA. 267-285.

Ding Y. and Veblen D. R. 2004. Impactite from Henbury, Australia. *American Mineralogist* 89(7):961-968.

D'Orazio M., Folco L., Zeoli A., and Cordier C. 2011. Gebel Kamil: The iron meteorite that formed the Kamil crater (Egypt). *Meteoritics & Planetary Science* 46:1179–1196.

El Goresy A. 1965. Baddeleyite and its significance in impact glasses. *Journal of Geophysical Research* 70:3453-3456.

El Goresy A. 1968. "The opaque minerals in impactite glasses." In *Shock metamorphism of natural materials*: 531-554. (eds. B. M. French and N. M. Short), Mono Book Co., Baltimore, Maryland, USA. 531-553.

Evans G. L. and Mear C. E. 2000. The Odessa meteor craters and their geological implications: Waco, Texas, Baylor University. *Occasional Papers of the Strecker Museum* 5.

Folco L., Di Martino M., El Barkooky A., D'Orazio M., Lethy A., Urbini S., Nicolosi I., Hafez M., Cordier C., van Ginneken M., Zeoli A., Radwan A. M., El Khrepy S., El Gabry M., Gomaa M., Barakat A. A., Serra R., and El Sharkawi M. 2010. The Kamil Crater in Egypt. *Science* 329(5993):804 and supporting online material.

Folco L., Di Martino M., El Barkooky A., D'Orazio M., Lethy A., Urbini S., Nicolosi I., Hafez M., Cordier C., van Ginneken M., Zeoli A., Radwan A. M., El Khrepy S., El Gabry M., Gomaa M., Barakat A. A., Serra R., and El Sharkawi M. 2011. Kamil Crater (Egypt): Ground truth for small-scale meteorite impacts on Earth. *Geology* 39:179-182.

French B. M. 1998. *Traces of Catastrophe: A Handbook of Shock-Metamorphic Effects in Terrestrial Meteorite Impact Structures*. LPI Contributions No. 954, Lunar and Planetary Institute, Houston. 120 pp.

French B. M. 2004. The importance of being cratered: The new role of meteorite impact as a normal geological process. *Meteoritics & Planetary Science* 39(2):169–197.

French B. M. and Koeberl C. 2010. The convincing identification of terrestrial meteorite impact structures: What works, what doesn't, and why. *Earth-Science Reviews* 98(1–2):123-170.

Fudali R. F. 1979. Gravity investigation of Wolf Creek crater, Western Australia. *Journal of Geology* 87:55-67.

Fudali R. F. and Cassidy W. A. 1972. Gravity reconnaissance at three Mauritanian craters of explosive origin. *Meteoritics* 7:51-70.

Fudali R. F. and Cressy P. J. 1976. Investigation of a new stony meteorite from Mauritania with some additional data on its find site: Aouelloul crater. *Earth and Planetary Science Letters* 30(2):262-268

Gibbons R. V., Hörz F., Thompson T. D., and Brownlee D. E. 1976. Metal spherules in Wabar, Monturaqui, and Henbury impactites. *Proceedings of the 7th Lunar Science Conference* 863–880.

Gnos E., Hofmann B. A., Halawani M. A., Tarabulsi Y., Hakeem M., Al Shanti M., Greber N. D., Holm S., Alwmark C., Greenwood R. C., and Ramseyer K. 2013. The Wabar impact craters, Saudi Arabia, revisited. *Meteoritics & Planetary Science* 48:2000-2014.

Gorshkov E. S., Gus'kova E. G., and Pochtare V. I. 1975. The magnetic investigation of the Sikhote-Alin iron meteorite shower at the site of the fall. *Meteoritics* 10:9-19.

Guppy J. D. and Matheson R. S. 1950. Wolf Creek, Western Australia. *Journal of Geology* 58:30-36.

Gurov E. P. 1996. The group of Macha craters in western Yakutia (abstract). *Lunar and Planetary Science* (27):473-474.

Gurov E. P. and Gurova E. P. 1998. The group of Macha crater in western Yakutia. *Planetary Space Science* 46(2-3):323-328.

Haines P. W. 2005. Impact Cratering and Distal Ejecta: The Australian Record. *Australian Journal of Earth Sciences* 52:481-507.

Hamacher D. W. and O'Neill C. 2013. The Discovery and history of the Dalgaranga meteorite crater, Western Australia. *Australian Journal of Earth Sciences* 60(5)

Haughton S. H., Blignault J. J. G., Rossouw P. J., Spies J. J., and Zagt S. 1953. Results of an investigation into the possible presence of oil in karoo rocks in parts of the Union of South Africa. In: *Geological Survey Memoir* Department of Mines, Pretoria 45:90-92.

Hawke P. J. 2003. Geophysical Investigation of the Wolfe Creek Meteorite Crater. *Geological Survey of Western Australia Record* 10:1-9.

Herd C. D., Froese D. G., Walton E. L., Kofman R. S., Herd E. P., and Duke M. J. 2008. Anatomy of a young impact event in central Alberta: Prospects for the ‘‘missing’’ Holocene impact record. *Geology* 36:955–958.

Hodge P. W. and Wright F. W. 1971. Meteoritic particles in the soil surrounding the Henbury Meteorite Craters. *Journal of Geophysical Research* 76(17):3880-3895.

Hodge P. W. and Wright F. W. 1973. Particles around Boxhole meteorite crater. *Meteoritics* 8(4):315-320.

Hodge P. W. 1979. The location of the Haviland meteorite crater. *Meteoritics & Planetary Science* 14:233–234.

Hodge P. W. 1965. The Henbury meteorite craters. *Smithsonian Contributions, Astrophysics* 8:199-201.

Holliday V. T., Kring D. A., Mayer J. H., and Goble R. J. 2005. Age and effects of the Odessa meteorite impact, western Texas, USA. *Geology* 33:945-948.

Holsapple K. A. 1993. The scaling of impact processes in planetary sciences. *Annual Review of Earth and Planetary Sciences* 21(333-373).

Honda M., Caffee M. W., Miura Y. N., Nagai H., Nagao K., and Nishiizumi K. 2002. Cosmogenic nuclides in the Brenham pallasite. *Meteoritics & Planetary Science* 37:1711-1728.

Hurnik H. 1977. Meteorite "Morasko" and the region of the fall of the meteorite. In Meteorite Morasko and Region of Its Fall. Uniw. *Adama Mickiewicza Poznan, Ser. Astronomia* 2:3-6. (Polish)

Huss G. I. 1962a. Australia's Dalgaranga crater, Part I. *The Mineralogist* 30(9/10):4-7.

Huss G. I. 1962b. Australia's Dalgaranga crater, Part II. *The Mineralogist* 30(11/12):12-14,16.

Jaret, S. J., Kah, L. C. and Harris, R. S. (2014), Progressive deformation of feldspar recording low-barometry impact processes, Tenoumer impact structure, Mauritania. Meteoritics & Planetary Science, 49: 1007–1022.

Karwowski Ł., Pilski A. S., Muszynski A., Arnold S., Notkin G., Gurdziel A. 2011. New finds in the Morasko Meteorite Preserve, Poland. *Meteorites* 1(1):21–28.

Kenkmann T., Artemieva N. A., Wünnemann K., Poelchau M. H., Elbeshausen D., and Prado H. N. d. 2009. The Carancas meteorite impact crater, Peru: Geologic surveying and modeling of crater formation and atmospheric passage. *Meteoritics & Planetary Science* 44:985-1000.

Khryanina L. P. 1981. Sobolevskiy meteorite crater (Sikhote-Alin' Range). *International Geology Review* 23(1).

Knox R. 1967. Surviving Metal in Meteoritic Iron Oxide from the Wolf Creek, Western Australia, Meteorite Crater. *Meteoritics* 3:235-238.

Koeberl C. 1994. African meteorite impact craters: Characteristics and geological importance. *Journal of African Sciences* 18:263-295.

Koeberl C., Reimold W. U., and Shirey S. B. 1998. The Aouelloul crater, Mauritania: On the problem of confirming the impact origin of a small crater. *Meteoritics & Planetary Science* 33:513-517.

Koeberl C. and Auer P. 1991. Geochemistry of impact glass from the Aouelloul crater, Mauritania. *Abstracts of the Lunar and Planetary Science Conference* 22:731.

Koeberl C. 1998. Identification of meteoritic components in impactites. In: Grady, M., Hutchison, R., McCAll, G., Rothery, D. (Eds.), *Meteorites: Flux with Time and Impact Effects*. Geological Society, London. 133–153.

Koeberl C., Reimold W. U., Shirey S. B., and Le Roux F. G. 1994. Kalkkop crater, Cape Province, South Africa: Confirmation of impact origin using osmium isotope systematics. *Geochimica et Cosmochimica Acta* 58:1229-1234.

Kofman R. S., Herd C. D. K., and Froese D. G. 2010. The Whitecourt meteorite impact crater, Alberta, Canada. *Meteoritics & Planetary Science* 45:1429-1445.

Kohman T. P. and Goel P. S. 1963. Terrestrial ages of meteorites from cosmogenic C14. *International Atomic Energy Agency Report* 395-411.

Krinov E. L. 1961. The Kaalijarv meteorite craters on Saarema Island, Estonian SSR. *American Journal of Science* 259:430-440.

Krinov E. L. 1964. Scattered meteoritic matter in the area of the fall of the Sikhote-Alin iron meteorite. *Annals of the New York Academy of Sciences* 119:224-234.

Krinov E. L. 1971. New studies of the Sikhote-Alin iron meteorite shower. *Meteoritics* 6:127-138.

Krinov E. L. 1974. Fragmentation of the Sikhote-Alin meteoritic body. *Meteoritics* 9:255–262.

LaPaz L. 1949. The Reported Crater-Producing Meteoritic Fall of 1947 February 12 in Eastern Siberia. *Contributions of the Meteoritical Society* 4:179–183.

LaPaz L. 1954. Meteoritic material from the Wolf Creek, Western Australia, crater (CN =– 1278, 192). *Meteoritics* 1:200-203.

Lambert P., McHone J. F., Dietz R. S., and Houfani M. 1980. Impact and impact-like structures in Algeria part 1 four bowl-shaped depressions. *Meteoritics* 15:157-179.

Lang B. and Kowalski M. 1973. Sikhote-Alin meteoroid: A contribution to the story of its fragmentation and fragment scattering. *Earth and Planetary Science Letters* 21:85–90.

Le Pichon A., Antier K., Cansi Y., Hernandez B., Minaya E., Burgoa B., Drob D., Evers L. G., and Vaubaillon J. 2008. Evidence of a meteoritic origin of the September 15, 2007, Carancas crater. *Meteoritics & Planetary Science* 43:1797–1809.

Leya I., Wieler R., Ma P., Schnabel C., and Herzog G. F. 2002. Preatmospheric depths and thermal histories of Canyon Diablo spheroids. *Meteoritics & Planetary Science* 37:1015–1025.

Littlefield D. L., Bauman P. T., and Molineux A. 2007. Analysis of formation of the Odessa crater. *International Journal of Impact Engineering* 34:1953-1961.

Madigan C. T. 1937. The Boxhole crater and the Huckitta meteorite (central Australia). *Royal Society South Australia Transactions and Proceedings* 61:187-190.

Madigan C. T. and Alderman A. R. 1940. The Boxhole Meteoritic Iron, Central Australia. *Mineralogical Magazine* 25(168):481-486.

Matsubara K., Matsuda J., and Koeberl C. 1991. Noble gases and K-Ar ages in Aouelloul, Zhamanshin, and Libyan Desert impact glasses. *Geochimica et Cosmochimica Acta* 55(10):2951-2955.

McCall G. J. H. 1965a. New material from, and a reconsideration of, the Dalgaranga meteorite and crater, Western Australia. *Mineralogical Magazine* 35:476-487.

McCall G. J. H. 1965b. Possible meteorite craters Wolf Creek, Australia and analogs. *Annals of the New York Academy of Sciences* 123:970-998.

McColl D. 1990. Distribution and sculpturing of iron meteorites from the major craters at Henbury (abstract). *Meteoritics* 25:384.

McHone J. F. Jr., Lambert P., Dietz R. S., and Briedj M. 1980. Impact structures in Algeria (abstract). *Meteoritics* 15:331.

Melosh H. 1989. *Impact Cratering a Geologic Process.* Oxford University Press, New York, New York. 245 pp.

Milton D. J. 1968a. Structural geology of the Henbury meteorite craters, Northern Territory, Australia. *U.S. Geological Survey Professional Paper 599-C* C1-C17.

Milton D. J. 1968b. Structure of the Henbury meteorite craters, Australia. In: *Shock Metamorphism of Natural Materials*, French, B.M. and Short, N.M., editors. Mono Book Corp., Baltimore, MD. 115-116.

Milton D. J. and Michel F. C. 1965. Structure of a ray crater at Henbury, Northern Territory, Australia. In: *Geological Survey research 1965: U.S. Geol. Survey Professional Paper 525-C*.

Mittlefehldt D. W., See T. H., and H€orz F. 1992. Dissemination and fractionation of projectile materials in the impact melts from Wabar Crater, Saudi Arabia. *Meteoritics* 27:361-370.

Morgan J. W., Higuchi H., Ganapathy R., and Anders E. 1975. Meteoritic material in four terrestrial meteorite craters. In: *Lunar Science Conference Proceedings, 6th, Houston, TX*. New York, Pergamon Press, Inc. Volume 2:1609-1623.

Nininger H. H. and Figgins J. D. 1933. The Excavation of a Meteorite Crater Near Haviland, Kiowa County, Kansas. *Proceedings of the Colorado Museum of Natural History* 12(3)9-16.

Nininger H. H. and Huss G. I. 1960. The unique meteorite crater at Dalgaranga, western Australia. *Mineralogical Magazine* 32:619-639.

O'Keefe J. A. 1971. Physical chemistry of the Aouelloul glass. *Journal of Geophysical Research* 76(26):6428–6439.

O'Neill C. and Heine C. 2005. Reconstructing the Wolfe Creek meteorite impact: deep structure of the crater and effects on target rock. *Australian Journal of Earth Sciences* 52(4-5).

Oelze M. L., O'Brien W. D. Jr., and Darmody R. G. 2002. Measurement of attenuation and speed of sound in soils. *Soil Science Society of America Journal* 66(788–796).

Plado J. 2012. Meteorite impact craters and possibly impact-related structures in Estonia. *Meteoritics & Planetary Science* 47:1590–1605.

Prescott J. R., Robertson G. B., Shoemaker C., Shoemaker E. M., and Wynn J. 2004. Luminescence dating of the Wabar meteorite craters, Saudi Arabia. *Journal of Geophysical Research* 109:1-8.

Quaide W. L. and Oberbeck V. R. 1968. Thickness determinations of the lunar surface layer from lunar impact craters. *Journal of Geophysical Research* 73(16):5247–5270.

Rasmussen K. L., Aaby B., and Gwozdz R. 2000. The age of the Kaalijärv meteorite craters. *Meteoritics & Planetary Science* 35:1067-1071.

Raukas A. 2000. Study of meteoritic matter for precise regional stratigraphy. *Geologos* 5: 77-86.

Raukas A. 2002. Postglacial impact events in Estonia and their influence on people and the environment. In: Koeberl C., MacLeod K. G. (eds) Catastrophic events and mass extinctions: impacts and beyond. *Geological Society of America Special Paper* 356:563–569.

Raukas A. and Stankowski W. 2011**.** On the age of the Kaali craters, Island of Saaremaa, Estonia. *Baltica* 24(1):37-44.

Raukas A., Tiirmaa R., Kaup E., and Kimmel K. 2001. The age of the Ilumetsa meteorite craters in southeast Estonia. *Meteoritics & Planetary Science* 36:1507-1514.

Reeves F. and Chalmers R. O. 1949. The Wolf Creek Crater. *Australian Journal of Science* 11:154-156.

Reimold W. U. and Koeberl C. 2014. Impact structures in Africa: A review. *Journal of African Earth Sciences* 93:57-175.

Reimold W. U., Koeberl C., and Reddering J. S. V. 1998. The 1992 drill core from the Kalkkop impact crater, Eastern Cape Province, South Africa: stratigraphy, petrography, geochemistry and age. *Journal of African Earth Sciences* 26(4):573-592.

Roddy D. J., Shoemaker E. M., Shoemaker C. S., and Roddy J. K. 1988. Aerial photography and geologic studies of impact structures in Australia (abstract). 19th Lunar and Planetary Science Conference.

Sanchez J. and Cassidy W. 1966. A previously undescribed meteorite crater in Chile. *Journal of Geophysical Research* 71(20):4891-4895.

Schultz P. H., Eberhardy C. A.., Ernst C. M., A'Hearn M. F., Sunshine J. M., Lisse C. M. 2007. The Deep Impact oblique impact cratering experiment. *Icarus* 190:295-333.

Scott E. R. D., Wasson J. T., and Buchwald V. F. 1973. The chemical classification of iron meteorites, VII: A re-investigation of irons with Ge concentrations between 25 and 80 ppm. *Geochimica et Cosmochimica Acta* 37(8):1957–1976.

Sellards E. H. and Evans G. L. 1941. Statement of progress at Odessa meteor craters: Austin, University of Texas at Austin, Bureau of Economic Geology, 13 p.

Shoemaker E. M., Roddy D. J., Shoemaker C. S., and Roddy J. K. 1988. The Boxhole Meteorite Crater, Northern Territory, Australia (abstract). 19th Lunar and Planetary Institute Science Conference.

Shoemaker E. M. and Shoemaker C. S. 1985. Impact structures of Western Australia. *Meteoritics* 20:754-756.

Shoemaker E. M. and Shoemaker C. S. 1988. Impact structures of Australia (1987) (abstract). 19th Lunar and Planetary Science Conference.

Shoemaker E. M., Shoemaker C. S., Nishiizomi K., Kohl C. P., Arnold J. R., Klein J., Fink D., Middleton R., Kubik P. W., and Sharma P. 1990. Ages of Australian meteorite craters - A preliminary report (abstract). *Meteoritics* 25:409.

Shoemaker E. M., Macdonald F. A., and Shoemaker C. S. 2005. Geology of five small Australian impact craters. *Australian Journal of Earth Sciences* 52:529-544.

Shoemaker E. M. and Wynn J. C. 1997. Geology of the Wabar meteorite craters (abstract #1313). 28th Lunar and Planetary Science Letters.

Short N. M. 1966. Shock-lithification of unconsolidated rock materials. Science 154:382-384.

Smith T. R. and Hodge P. W. 1997. Discovery of impactite at the Odessa meteorite crater (abstract #5039). Meteoritics and Planetary Science 32:A122.

Spencer L. J. and Hey M. H. 1933. Meteoritic iron and silica glass from the meteorite craters of Henbury central Australia and Wabar Arabia. Mineralogical Magazine 23:387-404.

Stankowski W. T. 2001. The geology and morphology of the natural reserve ‘‘Meteoryt Morasko.’’ *Planetary and Space Science* 49:749–753.

Stankowski W. T. J. and Bluszcz A. 2012. Luminescence Dating as Comparative Data to Radiocarbon Age Estimation of Morasko Spherical Depressions. In *Radiometric Dating*, edited by Nawrocka D. M. InTech, publisher.

Stankowski W., Muszynski A., Klimm K., and Schliestedt M. 2002. Mineralogy of Morasko Meteorite and the structure of the craters. *Proceedings of the Estonian Academy of Sciences, Geology* 51(4):227-240.

Stankowski W., Raukas A., Bluszcz A., and Fedorowicz S. 2007. Luminescence dating of the Morasko (Poland), Kaali, Ilumetsa and Tsõõrikmäe (Estonia) meteorite craters. *Geochronometria* 28:25-29.

Storzer D. and Wagner G. A. 1977. Fission track dating of meteorite impacts. *Meteoritics* 12:368-369.

Tancredi G., Ishitsuka J., Rosales D., Vidal E., Dalmau A., Pavel D., Benavente S., Miranda P., Pereira G., Vallejos V., Varela M. E., Brandstätter F., Schultz P. H., Harris R. S., and Sánchez L. 2008. What do we know about the “Carancas-Desaguadero” fireball, meteorite and impact crater? (abstract #1216). 39th Lunar and Planetary Science Conference.

Tancredi G., Ishitsuka J., Schultz P. H., Harris R. S., Brown P., Revelle D. O., Antier K., Pichon A. L., Rosales D., Vidal E., Varela M. E., Sánchez L., Benavente S., Bojorquez J., Cabezas D., and Dalmau A. 2009. A meteorite crater on Earth formed on September 15, 2007: The Carancas hypervelocity impact. *Meteoritics & Planetary Science* 44:1967-1984.

Ugalde H., Valenzuela M., and Milkereit B. 2007. An Integrated Geophysical and Geological Study of the Monturaqui Impact Crater, Chile. *Meteoritics & Planetary Science* 42,2153-2163.

Urbini S., Nicolosi I., Zeoli A., El Khrepy S., Lethy A., Hafez M., El Gabry M., El Barkooky A., Barakat A., Gomaa M., Radwan A. M., El Sharkawi M., D’orazio M., Folco L. 2012. Geological and geophysical investigation of Kamil crater, Egypt. *Meteoritics & Planetary Science* 47(11):1842-1868.

Valenzuela M., Bourles D. L., Braucher R., Faestermann T., Finkel R. C., Gattacceca J., Korschinek G., Merchel S., Morata D., Poutivtsev M., Rochette P., Rugel G., Suavet C. 2008. New Age Estimation of the Monturaqui Impact Crater. 2008 Annual Report of the Tandem Accelerator Facility, University of Munich, Germany, 27.

Vesconi M. A., Wright S. P., Spagnuolo M., Jacob R., Cerrutti C., Garcia L., Fernandez E., and Cassidy W. A. 2011. Comparison of four meteorite penetration funnels in the Campo del Cielo crater field, Argentina. *Meteoritics & Planetary Science* 46:935–949.

Wasson J. T., Choi B-G., Jerde E. A., and Ulff-Møller F. 1998. Chemical classification of iron meteorites: XII. New members of the magmatic groups. *Geochimica et Cosmochimica Acta* 62:715-724.

Wasson J. T. and Kallemeyn G. W. 2002. The IAB iron-meteorite complex: A group, five subgroups, numerous grouplets, closely related, mainly formed by crystal segregation in rapidly cooling melts. *Geochimica et Cosmochimica Acta* 66:2445–2473.

Wasson J. T. and Kimberlin J. 1967. The chemical classification of iron meteorites - II. Irons and pallasites with germanium concentrations between 8 and 100 ppm. *Geochimica et Cosmochimica Acta* 31:2065- 2093.

Weisberg M. K., Smith C., Herd C., Haack H., Yamaguchi A., Chennaoui Aoudjehane H., Welzenbach L., and Grossman J. N. 2010. The Meteoritical Bulletin, No. 98. *Meteoritics & Planetary Science* 45(9):1530–1551.

Wellard G. E. P. 1983. *Bushlore, or, this and that from here and there*. Perth: Artlook Books.

White J., Henderson E., and Mason B. 1967. Secondary Minerals Produced by Weathering of the Wolf Creek Meteorite. US National Museum. *American Mineralogist* 52.

Yeates A. N., Crowe R. W. A. and Towner R. R. 1976. The Veevers Crater; a possible meteoritic feature. *BMR Journal of Australian Geology & Geophysics* 1:77-78.

Chapter 5 Conclusion and Ongoing Work

5.1 Conclusion

The studies reported in this dissertation address the nature of impact altered materials in the early and modern solar system through the examination of the impacted surface of an asteroid as recorded in the macrostructure of the Sutter's Mill CM chondrite, a polymict regolithic breccia formed from an assemblage of clasts produced and aggregated by generations of impacts, through examination of the petrographic evidence constraining the origin of an unusual class of sub-spherical concretions found at the Weaubleau, Missouri, probable impact crater, and through a systematic examination of fieldwork and materials analysis from terrestrial sub-kilometer impact pits and craters, addressing the precise manner in which compelling arguments for impact origin have been constructed.

Each of these three efforts examines the physical record of impact altered materials from a unique perspective and in a different moment in the solar system's history. First, in one of the most primitive and oldest known objects in the solar system, the CM chondrite regolith, we find that an impact breccia preserves remnants of the materials that precede the impact event, as well as indications of processual timing. By examining the components that make up this impact altered meteorite, we are provided a glimpse across time, at the environment that preceded the impact, and are able to tease apart aspects of the timing and nature of changes that subsequently occurred. A similar effort is undertaken in interpreting the origin of concretions in the much younger, but much more altered environment of the marine resurge breccia associated with the Weaubleau structure. The resurge breccia, now exposed as a continental regolith, is again teased apart, revealing the history of chemical change that occurred in a violently mixed assemblage of crushed and mixed micritic sediment and lithic clasts. Finally, the earth's youngest impact

environments are examined. The complex assemblages of impactor and target materials reported from 22 terrestrial sites are considered in an effort to establish exactly which components of the impact environment best reveal the specific impact event, allowing these structures to be distinguished from morphologically similar terrestrial sites.

In each case, ranging from some of the oldest to the youngest in the solar system, grain - scale and macroscopic clues illuminate the story of how impacts mix and alter target materials, both obscuring and preserving components of the preceding landscape, while permanently recording the moment of impactor-target interaction in a 3 dimensional assemblage of altered materials. And in each case, these stories are obscured by subsequent and ongoing processes, each leaving their own physical and chemical trace in the impactite record. Cumulatively, they contribute to our ability to interpret such environments through microscopic and macroscopic physical traces and relationships, allowing us to better tell the story of previous impact environments as well as to anticipate what we might find in those not yet explored.

5.2 Directions for future work

Work on the Sutter's Mill impact breccia was begun as a result of fortuitous opportunity. The fall occurred during the course of doctoral work, and the meteorite turned out to be a regolith breccia, a three dimensional record of impact processes. While further work on this material would require access to further scarce samples and to relevant analytic instruments, work on the Sutter's Mill meteorite was part of a longer term work flow centered on the investigation of impact evidence preserved in meteorites. Unless circumstances lend themselves to further work that is specifically centered on Sutter's Mill samples, the next step in this overall

path of investigation will involve the petrographic examination of a significant collection of shatter cones preserved in ordinary chondrites.

The in-depth compilation and analysis of previous field investigations of small, confirmed impact craters that is reported here began during an attempt to confirm or refute impact origin for a small structure in New Mexico. During literature review, it became apparent that the path to the unambiguous evidentiation of a sub-km impact pit or crater was obscure at best, and that it might lean on impossible criteria in some instances. This 'small impact problem' has been addressed in the current work, but this is only the first half of an intended two part investigation. The second part is to follow up with an investigation of the characteristics of pseudo-impacts and crater like objects that have been or could be mistaken for terrestrial meteorite impact craters within the same size range. It is hoped that, within a few years, the combination of these two efforts will act as key references for discrimination of impact craters in this size range and as a useful tool for investigators attempting the identification of such structures.

The work presented here regarding the Weaubleau probable impact structure is also only part of an ongoing project of larger scope. Discussion regarding next research steps, in cooperation with personnel at Missouri State University, includes the publication of more detailed descriptions of cores, the indexing of planar deformation features in order to unequivocally demonstrate impact origin, and the mapping of surface exposures at the site in order to better define the extent of the structure and associated disturbance. Work is also underway on a project examining how regionally specific circumstances may contribute to the Ozark Plateaus acting as an ideal impact crater preservations surface and further work is upcoming at the nearby Belton possible impact structure.